Combining induced pluripotent stem cells and fibrin matrices for spinal cord injury repair

by

Amy Montgomery
BSc. Mechanical Engineering, University of Calgary, 2009

A Thesis Submitted in Partial Fulfillment
of the Requirements for the Degree of

MASTER OF APPLIED SCIENCE

in the Department of Mechanical Engineering

Supervisory Committee

Combining induced pluripotent stem cells and fibrin matrices for spinal cord injury repair

by

Amy Montgomery
BSc. Mechanical Engineering, University of Calgary, 2009

Supervisory Committee

Dr. Stephanie Willerth, Department of Mechanical Engineering
Supervisor

Dr. Rustom Bhiladvala, Department of Mechanical Engineering
Departmental Member

Abstract

Supervisory Committee
Dr. Stephanie Willerth, Department of Mechanical Engineering
Supervisor
Dr. Rustom Bhiladvala, Department of Mechanical Engineering
Departmental Member

Spinal cord injuries result in permanent loss of motor function, leaving those affected with long term physical and financial burdens. Strategies for spinal cord injury repair must overcome unique challenges due to scar tissue that seals off the injury site, preventing regeneration. Tissue engineering can address these challenges with scaffolds that serve as cell- and drug-delivery tools, replacing damaged tissue while simultaneously addressing the inhibitory environment on a biochemical level. To advance this approach, the choice of cells, biomaterial matrix, and drug delivery system must be investigated and evaluated. This research seeks to evaluate (1) the behaviour of murine induced pluripotent stem cells in previously characterized 3D fibrin matrices; (2) the 3D fibrin matrix as a platform to support the differentiation of human induced pluripotent stem cells; and (3) the ability of an affinity-based drug delivery system to control the release of emerging spinal cord injury therapeutic, heat shock protein 70 from fibrin scaffolds.

Acknowledgements

I would like to extend my sincere thanks to Dr. Stephanie Willerth for her guidance and support. My appreciation also to Dr. Rustom Bhiladvala and Dr. Bob Chow for valuable feedback and advice.

I also owe much to all of the members of the Willerth Lab group for their hard work and willing collaboration over the last two years. Especially to Nicole Gabers, Alixandra Wong, Meghan Robinson, and Craig King for their assistance with the mouse stem cell and fibrin work; to Lin Sun for sharing her biochemistry expertise and knowledge of cell culture techniques; to Andrew Agbay for advice on running ELISAs; to Alexandra Shapka and Aliya Mitchell for assistance with culturing human stem cells; to John Edgar, Rishi Vasandani, Nathan Muller, and David Rattray for asking great questions and helping out around the lab; to Nima Khadem Mohtaram and Jose Gomez for their support as fellow graduate students.

Table of Contents

List of Tables

List of Figures

Abbreviations

General Abbreviations

ABDS	*affinity-based delivery system*
bFGF	*basic fibroblast growth factor*
BSA	*bovine serum albumin*
CNS	*central nervous system*
EB	*embryoid body*
ELISA	*enzyme linked immunosorbance assay*
ESC	*embryonic stem cell*
Eth-D	*ethidium homodimer*
FDA	*Food and Drug Administration*
GFP	*green fluorescent protein*
HBDS	*heparin-binding delivery system*
hESC	*human embryonic stem cell*
hiPS	*human induced pluripotent stem cell*
HSP	*heat shock protein*
iPSC	*induced pluripotent stem cell*
KS	*Kolmogorov-Smirnov*
KW	*Kruskal Wallis*
MEF	*mouse embryonic fibroblast*
mESC	*mouse embryonic stem cell*
miPS	*mouse induced pluripotent stem cell*
NGS	*normal goat serum*
NIM	*neural induction media*
NPC	*neural progenitor cell*
NPM	*neural progenitor media*
NRSA	*neural rosette selection agent*
NSC	*neural stem cell*
NT-ESC	*nuclear transfer embryonic stem cells*
PBS	*phosphate buffered saline*
PDGF	*platelet derived neurotrophic factor*
PLO	*poly-L-ornithine*
PNS	*peripheral nervous system*
RA	*retinoic acid*
SCI	*spinal cord injury*
SCNT	*somatic cell nuclear transfer*
SEM	*standard error of the mean*
SD	*standard deviation*
TBS	*tris buffered saline*

Common Transcription Factors and Signalling Pathway Components in Stem Cells

BMP4 *bone morphogenetic protein 4*
→ A ligand (with TGFβs and activins) of the TGFβ signalling pathway. A protein implicated in proliferation, differentiation, and other functions in cells. Activated BMP4 signalling is required for the maintenance of pluripotency in murine stem cells.

c-Myc *c-Myc*
→ One of the 4 "Yamanaka" transcription factors implicated in the maintenance of stem cell pluripotency. Forced expression of Oct3/4, Sox2, c-Myc and Klf4 is used to induce somatic cells into pluripotency.

FGF *Fibroblast growth factor*
→ Ligands of the FGF Receptors, part of the Receptor Tyrosine Kinase family of receptors and downstream Mitogen Activated Protein Kinase signalling pathway. Activated FGF signalling is required for the maintenance of pluripotency in human stem cells.

JAK/STAT *Janus Kinase / Signal Transducer and Activator of Transcription*
→ A signalling pathway that typically binds cytokine ligands at receptors, activating the autophosphorylation of the receptor-associated Janus Kinases and downstream activation of STAT transcription factors. LIF target genes are activated through the JAK/STAT pathway.

Klf4 *Kruppel-like factor 4*
→ One of the 4 "Yamanaka" transcription factors implicated in the maintenance of stem cell pluripotency. Forced expression of Oct3/4, Sox2, c-Myc and Klf4 is used to induce somatic cells into pluripotency.

LIF *leukemia inhibitory factor*
→ A ligand of the LIF Receptors which activate the downstream JAK/STAT pathway. Activated LIF signalling is required for the maintenance of pluripotency in murine stem cells.

Lin28 *Lin28*
→ An alternative transcription factor implicated in the maintenance of stem cell pluripotency. Forced expression of Oct3/4, Sox2, Lin28, and Nanog is used to induce somatic cells into pluripotency.

MAPK *mitogen activated protein kinase*
→ A group of membrane receptor protein kinases, including serine, threonine, and tyrosine protein kinases. FGF target genes are activated through MAPK signalling.

Nanog *Nanog*
→ An alternative transcription factor implicated in the maintenance of stem cell pluripotency. Forced expression of Oct3/4, Sox2, Lin28, and Nanog is used to induce somatic cells into pluripotency. Nanog is commonly used as a marker for pluripotent stem cell, with high levels of expression indicating pluripotency.

Oct3/4 *octamer-binding transcription factor 4*
→ One of the 4 "Yamanaka" transcription factors implicated in the maintenance of stem cell pluripotency. Forced expression of Oct3/4, Sox2, c-Myc and Klf4 is used to induce somatic cells into pluripotency. Oct3/4 is commonly used as a marker for pluripotent stem cell, with high levels of expression indicating pluripotency.

Shh *sonic hedgehog*
→ Ligand of the sonic hedgehog signalling pathway. Binds to transmembrane receptor Patched-1 and targets downstream Gli protein transcriptional regulators.

Sox2 *(sex determining region Y)-box2*
→ One of the 4 "Yamanaka" transcription factors implicated in the maintenance of stem cell pluripotency. Forced expression of Oct3/4, Sox2, c-Myc and Klf4 is used to induce somatic cells into pluripotency. Sox2 is commonly used as a marker for pluripotent stem cell, with high levels of expression indicating pluripotency. However, Sox2 expression is also implicated in stages of differentiation.

SSEA1 *stage specific embryonic antigen 1*
→ A cell-surface protein that is commonly used as a marker for murine pluripotent stem cells, with high levels of expression indicating pluripotency.

SSEA4 *stage specific embryonic antigen 4*
→ A cell-surface protein that is commonly used as a marker for human pluripotent stem cells, with high levels of expression indicating pluripotency.

TCF3 *T-cell factor 3*
→ A transcription factor that participates in the regulation of OCT3/4, Sox2, and Nanog, for the maintenance of stem cell pluripotency.

TGFβ *Transforming growth factor β*
→ A ligand (with BMPs and activins) of the TGFβ signalling pathway. A protein implicated in proliferation, differentiation, and other functions in cells. Activated TGFβ/Activin signalling is required for the maintenance of pluripotency in human stem cells.

Wnt *Wnt*
→ A ligand that binds to the transmembrane receptor Frizzled, ultimately resulting in the accumulation of β-catenin, which acts with TCF as a transcriptional regulator for Wnt-target genes. Activated Wnt signalling is required for the maintenance of pluripotency in murine and human stem cells.

Common Neurotrophic Factors

BDNF *brain derived neurotrophic factor*
GDNF *glial cell line derived neurotrophic factor*
NGF *nerve growth factor*
NT-3 *neurotrophin-3*

Common Markers of Pluripotency

Nanog — *Nanog*
→ Nanog is commonly used as a marker for pluripotent stem cell, with high levels of expression indicating pluripotency.

OCT3/4 — *octamer-binding transcription factor 4*
→ Oct3/4 is commonly used as a marker for pluripotent stem cells, with high levels of expression indicating pluripotency.

Sox2 — *(sex determining region Y)-box2*
→ Sox2 is commonly used as a marker for pluripotent stem cell, with high levels of expression indicating pluripotency. However, Sox2 expression is also implicated in stages of differentiation.

SSEA1 — *stage specific embryonic antigen 1*
→ A cell-surface protein that is commonly used as a marker for murine pluripotent stem cells, with high levels of expression indicating pluripotency.

SSEA4 — *stage specific embryonic antigen 4*
→ A cell-surface protein that is commonly used as a marker for human pluripotent stem cells, with high levels of expression indicating pluripotency.

Common Markers of Neural Progenitor Cells and Neurons

Nestin — *Nestin*
→ An intermediate filament protein primarily (although not exclusively) expressed in neural progenitor cells

TUJ1 — *β-III-tubulin*
→ A specific isoform of β-tubulin that is found exclusively in neurons. TUJ1 expression is a common marker of neurons.

Chapter 1 Introduction

Spinal cord injuries (SCI) currently affect or 85,000 of Canadians with over 4,000 new cases new cases per year. [1] Traumatic SCI, typically caused by car collisions, falls, and sporting accidents, can lead to partial or full loss of motor function. The lifetime cost of care for a patient with SCI can reach up to $25 million depending on the severity of the injury. Given both physical and financial burdens, the development of effective treatments for SCI remains a priority.[1]

Therapies for SCI and other conditions of the central nervous system face unique challenges. The blood-brain barrier separates the central nervous system from the circulating immune system, preventing access of the typical wound-healing response to the brain and spinal cord. Instead, the injury site is sealed off with a scar which isolates the damage and spares healthy tissue. Although serving a protective function, this scarring creates an inhibitory environment that prevents the future regeneration of neural tissue, the underlying reason that spinal cord injuries can become permanently debilitating.[2 3]

SCI treatments are often described in the context of their neuroregenerative and neuroprotective roles. The term neuroregenerative refers to the regeneration of neural tissue, whether by growth of existing neurons, sprouting of new axons from existing neurons, remyelination, or plasticity among surviving connections. The term neuroprotective refers to the ability of a therapy to increase the sparing of neurons and decreasing the size and extent of scarring. The path to functional recovery should therefore involve both strategies: direct enhancement of neuron growth and indirect enhancement by targeting the inhibitory environment of the injury site.

Tissue engineering has emerged as a promising therapeutic approach for SCI.[4-8] The field of tissue engineering is based on the concept of replacing lost or damaged tissue with a designed solution. Each application has its own specific set of design parameters and constraints. In general, cells are combined with an appropriate biomaterial construct and implanted *in vivo* to perform, augment, or replace a normal cellular function. Drug delivery systems may also be incorporated to further enhance the effect of the engineered tissue construct.

Cell sources may be from a different site on the same subject, from a different subject of the same species, or even from a different species. Cells may be specialized adult somatic cells or unspecialized multipotent or pluripotent cells which have the potential to differentiate into various specific cell types. Pluripotent stem cells have the advantage that they offer a continuous source of cells, overcoming issues related to a limited donor cell supply. Furthermore, induced pluripotent stem cells (iPSCs) are of interest because they can used to develop patient-specific tissue and thereby avoid immune rejection.

Various biomaterials are used to support and influence the cells with which they are combined. In general, biomaterials are materials which are used in conjunction with biological systems. They may be natural biomolecules such as proteins and polysaccharides or synthetic materials such as polymers, metals, and ceramics. Of the candidate biomaterials, fibrin is one example of a protein that has been extensively characterized in combination with stem cells as a scaffold for SCI treatment.

Fibrin matrices have the ability to sequester and release therapeutic factors in a controlled manner over time. Various methods may be used to control the release kinetics, including the addition of fibrin-binding peptides that also have an affinity for the

loaded drug. Building on the fibrin-based drug delivery systems developed for growth factors commonly associated with neuroprotection and neuroregeneration, there is growing interest in other factors such as heat shock proteins as potential SCI therapeutics.

The research presented in the following thesis supports the development of tissue engineering strategies for spinal cord injury repair. It addresses three active areas of investigation including (1) the evaluation of protocols for the differentiation of induced pluripotent stem cells into neurons, (2) the translation of the existing fibrin cell-delivery platform for the differentiation of human stem cells, and (3) the incorporation of controlled drug delivery from biomaterial matrices.

Chapter 2 Review

Tissue engineered therapies for spinal cord injury

The brain and spinal cord, which collectively make up the central nervous system (CNS), are primarily comprised of three neural cell types: neurons, oligodendrocytes, and astrocytes. Neurons are excitable cells which transmit electrical and chemical signals through interconnected networks. In a main supporting role, oligodendrocytes insulate neuronal axons with sheaths of myelin to block the leakage of ions and facilitate the saltatory conduction of action potentials. This is analogous to the role played by Schwann cells in the peripheral nervous system (PNS). Astrocytes serve supporting functions, including provision of nutrients and maintenance of the blood-brain barrier which controls the diffusion of molecules between the blood circulatory system and the CNS. This organization of neurons, oligodendrocytes, and astrocytes in the brain and spinal cord is responsible for the sensing of stimuli and actuating of responses that must be coordinated to produce movement[9].

When spinal cord injury (SCI) occurs, the physical trauma itself causes immediate damage to neurons and oligodendrocytes which can manifest in the loss of motor control. The resulting cell death and inflammation from the primary injury creates a hypoxic environment, driving adjacent neural cells towards apoptosis. To prevent the damage from spreading to the surrounding tissue, astrocytes migrate to the injury and deposit proteoglycans and glycoproteins, creating a scar that effectively seals off the site[10]. While the formation of this scar tissue is a protective mechanism that preserves healthy tissue, it creates an inhibitory environment that discourages other cells from migrating to the injury site, thus preventing any attempts by the spared tissue to regenerate. In addition to the scar, other inhibitory molecules are present after SCI. These molecules include cytokines present as part of the inflammatory response to the injury, as well as myelin-associated inhibitory molecules

released by damaged oligodendrocytes and cytotoxic neurotransmitters released by damaged neurons.[3] The path to functional recovery should therefore involve both strategies: direct enhancement of neuron growth and indirect enhancement by targeting the inhibitory environment of the injury site.

To address the loss of functional neurons and glia that occurs as a result of SCI, the implantation of stem cells and stem cell-derived progenitor cells within biomaterial cell-delivery scaffolds has emerged as a promising regenerative therapy.[4] A key milestone in this type of regenerative SCI therapy was achieved in 2009 when the US Food and Drug Administration (FDA) approved clinical trials for biotechnology company Geron to conduct a stem cell-based spinal cord injury treatment[11]. This trial used human embryonic stem cell-derived oligodendrocyte progenitor cells developed by Keirstead et al.[12] to support the regeneration of neurons *in vivo*. Unfortunately, though the company continues to follow the four existing participants, financial difficulties have reportedly halted further trials[13]. However, it is an important case study in the development of clinically relevant stem cell-based tissue engineering strategies which remains an active area of biomedical research.

Stem cells and the promise of pluripotency[1]

Pluripotent stem cells are cells which have two key properties: the ability to continuously self-renew and the ability to differentiate into all somatic cell types, known as pluripotency. These are the cells from which all tissues are derived during early development. Following their discovery in the 1980s[14 15], embryonic stem cells have been

[1] For a list of abbreviations and short definitions related to common transcription factors and signalling pathway components for stem cells, see Abbreviations on page ix through page xii of the front matter.

investigated for their therapeutic potential, particularly as a possible mechanism for generating replacement tissues and organs.

While many of the underlying biochemical mechanisms of stem cell renewal and differentiation are yet to be elucidated, several key pathways are known to be necessary for maintaining "stemness". It is important to understand this regulation when working with pluripotent stem cells because the factors needed for the maintenance of pluripotency as well as the various pathways for differentiation rely on this regulation.

For human pluripotent stem cells, active Wnt signalling, as well as Transforming Growth Factor-β (TGFβ)/Activin pathway activation, and Fibroblast Growth Factor (FGF) activated signalling through the Mitogen Activated Protein Kinase (MAPK) pathway components, are all required to maintain cells in a pluripotent state, as summarized in Figure 1A.

For mouse pluripotent stem cells, active Wnt signalling is also necessary. However, in place of TFGβ/Activin is a member of the same family of ligands, Bone Morphogenetic Protein-4 (BMP4), as well as Leukemia Inhibitory Factor (LIF) signalling with downstream JAK/STAT activation replacing the FGF/MAPK activation, as summarized in Figure 1B.

In both species, these pathways converge upon a limited number of transcription factors, the most essential of which have been identified as OCT4, SOX2, Nanog, and TCF3[16]. The factors OCT4, SOX2, Nanog, bind to each other's promoter regions, creating an autoregulatory network that allows them to enhance their own expression; TCF3, a target of Wnt signalling, binds to the promoter regions of the other three factors but is not regulated by them[17].

The standard criteria by which "stemness" is judged consider both key stem cell properties: the ability to continuously self-renew and the ability to differentiate into all cell types. The ability to continuously self-renew is judged by high levels of telomerase expression – enzymes that add DNA sequence to the ends of chromosome telomeres and thereby prevent DNA loss through repeated division – and the ability of the cells to maintain a stable karyotype after extensive cell division.

The ability to differentiate into all cell types is judged by a number of factors. First, high levels of expression of key pluripotency factors including Oct4, Sox2, and Nanog (discussed in the previous section) demonstrate that the biomolecular signalling regulating pluripotency is active.

Second, when induced under the appropriate conditions, pluripotent stem cells should demonstrate the ability to spontaneously differentiate and form tumor-like structures containing tissue of all three germ layers. Germ layers are the first tissue specification that occurs in embryonic development. The developing organism is first divided into three germ layers: the ectoderm or outside layer which forms the brain, spinal cord, and skin; the mesoderm or middle layer which forms tissue such as muscle and blood; and the endoderm or inside layer which forms internal organs such as the lungs, thyroid, and pancreas. Thus, if it can be determined that a cell is able to give rise to cells of all three germ layers, it follows that the cell must be able to generate all cell types.

Another key property by which pluripotency can be judged is the ability of cells to contribute to a functional organism when introduced into a host blastocyst.[18] The resulting organism, known as a chimera, contains a mixture of both the host cells and the implanted stem cells. Successful chimera formation in animal models is considered to be

an indication that the implanted cells are free of defects that would hamper normal development. However, for ethical reasons, human cells lines are not verified through generation of chimera.

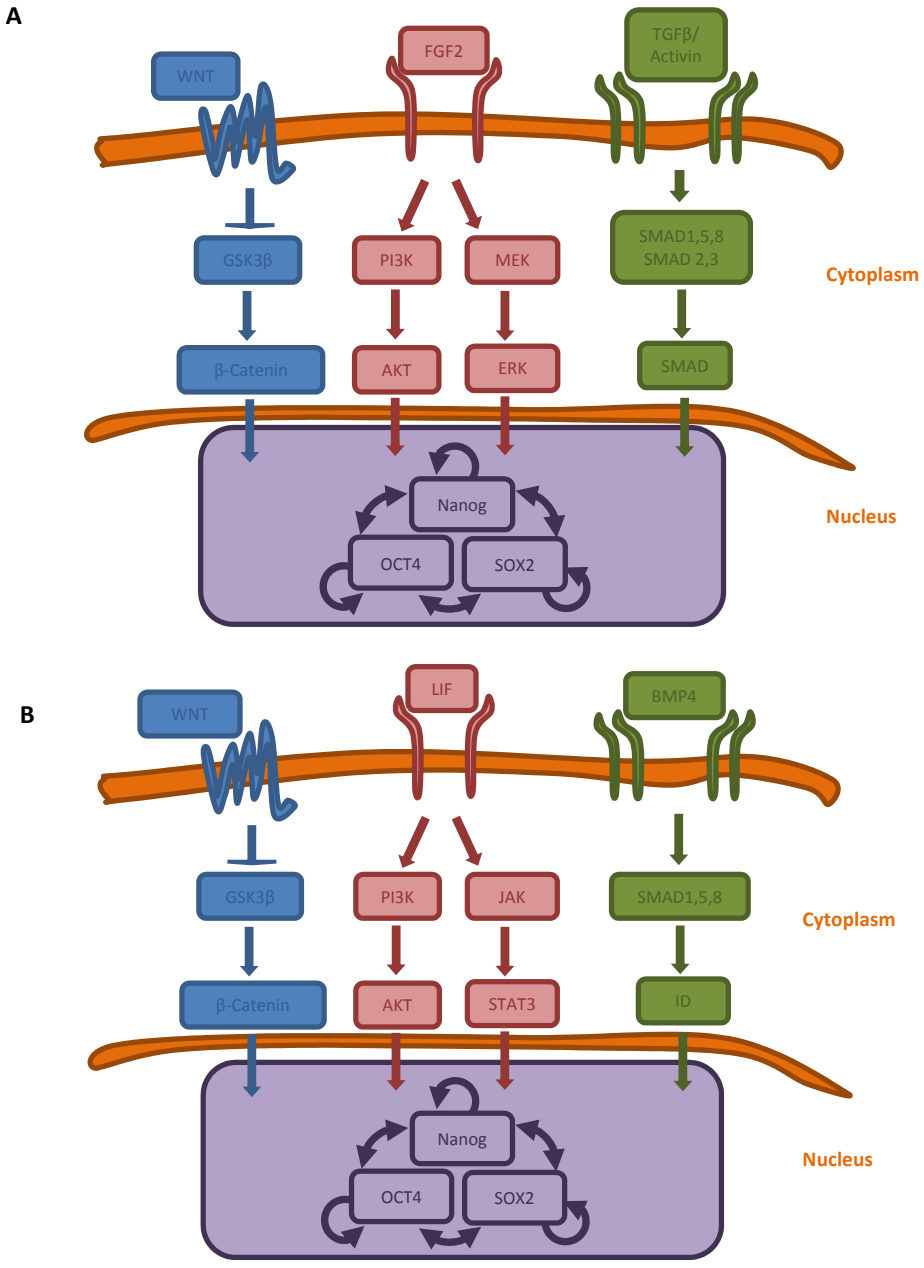

Figure 1 Major signalling pathways regulating stem cell pluripotency. (A) Human Wnt signalling through the G-protein-coupled receptor Frz inhibits GSK3β which allows for accumulation of β-catenin and regulation of TCF/LEF. FGF2 signalling operates on parallel pathways: PI3K/AKT and MAPK. TGFβ activates SMADS. **(B) Mouse** LIF replaces FGF, with downstream JAK/STAT signalling instead of MAPK siganlling, and BMP4 replaces TGFβ/Activin. Adapted from Bieberich and Wang.[19]

Embryonic stem cells (ESCs)

What is often considered the first published work on stem cells emerged in the early 1960s from the research of Till and McCulloch, republished in 2011,[20] who observed that bone marrow cells implanted into irradiated mice formed small donor cell colonies in host spleens. They further demonstrated the property of self-renewal in the implanted donor cells whereby a single cell was seen to give rise to multiple colonies.[21] This discovery of multipotent adult cells was the first to support the concept of "stem" cells which might be able to regenerate in an unspecialized state while also giving rise to specialized cells.

In concurrent research involving mouse embryonic development from the late 1950s and into the 1970s, it was found that murine germ cell tumors containing pluripotent cells could be maintained and subsequently differentiated in culture, leading to the development of embryonal carcinoma cell lines.[22] It was using these cells that an effective cocktail of signalling factors and many of the protocols for the isolation, culture, and differentiation of pluripotent stem cells would be developed.[23]

In 1981, both Martin[14] as well as Evans and Kauffman[15] independently reported the successful establishment of murine embryonic stem cell (ESC) lines isolated from the inner cell mass of mouse blastocysts. These cells were distinct from the previously developed embryonal carcinoma lines which are now understood to be the malignant counterpart of stem cells.[24] Nearly two decades later, Thomson et al.[25] first reported the successful establishment of human ESC lines derived from the inner cell mass of donated excess pre-implantation embryos produced by *in vitro* fertilization. These cell lines fulfilled the criteria of stemness including the ability to undergo long periods of

undifferentiated proliferation with a stable karyotype, the expression of pluripotency markers, and the ability to differentiate into all three germ layers.

Induced pluripotent stem cells (iPSCs)

Other milestones include the discovery of murine induced pluripotent stem cells (iPSCs) by Yamanaka and Takahashi[26] in 2006 and human iPSC by both the Yamanaka lab[27] and the Thomson lab[28] in 2007. With an understanding of the underlying regulation gained from ESC culture, they introduced 24 different genes encoding key factors into somatic cells to determine which were necessary for maintaining pluripotency. The result was that the transfection of genes encoding only four factors, Oct3/4, Sox2, c-Myc, and Klf4 in the Yamanaka lab, and Oct3/4, Sox2, Nanog, and Lin28 in the Thomson lab, could induce somatic cells to become pluripotent. After inducing the expression of these key pluripotency factors in somatic cells through retroviral transfection, the resulting iPSCs demonstrated the ability to continuously self-renew and the ability to differentiate into cells of all three germ layers. The importance of their discovery – the ability to derive a stem cell population from adult somatic cells – means the potential to generate patient-specific cells and tissues for implantation exists.

The field of iPSC generation is quickly evolving. The first studies in 2007 reported less than 1% of transfected somatic cells becoming stem cells,[29] with the low efficiencies being attributed to epigenetic factors such as residual DNA methylation.[30] A recent study achieved a near 100% efficiency by regulating the epigenetic state through inhibition of a key protein implicated in blocking the transcription of transfected genes.[31] In another recent approach targeting epigenetic regulation, micropatterned culture substrates were

shown to upregulate the expression of histone modifying proteins, with aligned topologies resulting in greater reprogramming efficiency[32].

In terms of safety, concerns have been raised over the use of retroviral vectors for the transfection of somatic cells for iPSC generation as they introduce the risk of insertional mutagenesis or may provoke an immune response. Methods of non-integrating transfection have been introduced, using high concentrations of notably plasmids to reprogram,[33] however, these methods have not yet demonstrated induction efficiencies to match those of retroviral transfection. Another concern is the potential risks related to the sustained proliferation of implanted cells. To address this, a protocol for evaluating non-tumor forming "safe" iPSC lines has been developed for therapeutic applications.[34 35] Screened and selected in this way, iPSCs should have a lower risk of tumour formation compared to ESCs. As many laboratories continue to tackle the challenges associated with iPSC generation, it is critical that the tissue engineering field concurrently investigate the downstream differentiation protocols and applications for iPSC-derived cells in order to incorporate the advancing iPSC technology effectively.

Other stem cells

The term stem cells is also used to describe multipotent cells. In contrast to pluripotent stem cells which have the ability to differentiate into all cells types, multipotent stem cells are only able to differentiate into cells of a particular lineage. Multipotent stem cells have been discovered within specialized niches in many adult tissues; upon isolation, these cells can be cultured as primary cells and differentiated into specialized phenotypes. For example, multipotent neural stem cells (NSCs) were first described by Temple[36] and characterized by their ability to develop into the primary cells of the CNS. In another

pioneering work, Reynolds and Weiss[37 38] successfully demonstrated that multipotent neural stem cells isolated from the adult mouse striatum could be induced to differentiate into both neurons and astrocytes using epidermal growth factor. While the behaviour of primary multipotent stem cells is an active area of investgation in terms of differentiation, growth, and survival, when considering clinical applications, these cells suffer from the same problems as therapies that rely on donor tissues and organs: donor scarcity and immunogenicity.

Recently, stem cells have been derived from embryos generated by somatic cell nuclear transfer (SCNT), and termed nuclear transfer embryonic stem cells (NT-ESCs). In this technique, the nucleus of a donor oocyte is replaced with the nucleus of a somatic cell and grown *in vitro* to the blastocyst stage, at which point ESCs may be isolated.[39] While these cells represent an emerging area of stem cell sourcing, the technique is technically difficult to establish and thus has not been taken up to the same extent as traditional ESCs and iPSCs. Furthermore, rather than simplifying the regulatory conditions surrounding cell generation, this technique would introduce additional concerns related to cloning.

From stem cells to neural cells[2]

The power of pluripotent cells can only be harnessed for tissue engineering if they can be differentiated into the desired cell populations using efficient, reproducible, and clinically relevant techniques. One active area of research in the field involves the development of biochemically- and biophysically-mediated methods to differentiate pluripotent cells into desired phenotypes.

---

[2] The following section contains excerpts from: **Combining protein-based biomaterials with stem cells for spinal cord injury repair,** Montgomery et al.*,* 2014 OA Stem Cells Review, Jan 18;2(1):1.

For SCI treatment, stem cells should be differentiated into neural cells and neural progenitor cells (NPCs) to overcome the inhibitory environment of the glial scarring which seals off the injury site. The isolation of a pure population of neural cells and NPCs is necessary to prevent the uncontrolled differentiation of undesired cell types following implantation. It has been shown that stem cell-derived NPCs transplanted in a non-inhibitory environment survive and differentiate into neurons and oligodendrocytes, leading to regeneration,[8] whereas the environment of an injured spinal cord inhibits NPC survival and promotes differentiation into astrocytes and glial scarring.[40] Therefore, many stem cell-based therapies seek to promote the generation of neurons and oligodendrocytes while reducing the differentiation of astrocytes. However, as astrocytes are also implicated in a number of positive roles following SCI, another therapeutic approach is based on supporting the protective function of astrocytes.[41] In either case, differentiation protocols should ideally be tailored to achieve high yields of pure populations containing specific cell types. Although sorting of partially differentiated cells can be performed using techniques such as fluorescence-activated cell sorting or bacterial resistance, the introduction of markers or bacterial resistance genes may cause inadvertent genomic manipulation through selection and thus increase the associated tumorigenic risks.[42]

Neural differentiation protocols for murine stem cells

As early as the first studies in the 1980s, murine stem cells have been directed to differentiate *in vitro* through removal from media conditioned for maintenance of pluripotency and subsequent culture in suspension on non-adhesive plates. The result of this process is the formation of suspended cell aggregates called embryoid bodies (EBs) which contain multipotent progenitor cell types of all three germ layers.[14] The standard

protocol for EB formation was tailored in 1995 by Bain et al.[43] to include treatment with 500 nM retinoic acid (RA) during the last 4 days of an 8 day induction period; it is commonly known as the 4-/4+ protocol in neural tissue engineering applications. The introduction of RA was informed by previous work on teratocarcinoma lines and a growing body of evidence in the field of developmental biology that implicated this retinol derivative in the development of the brain and spinal cord.[44 45] Based on these studies and others, RA has been well characterized as an important signalling factor in neural differentiation. However, some of the underlying mechanisms of RA-mediated patterning – in particular its action as a potential morphogen across a concentration gradient – are not fully understood. Experiments involving the exposure of cultured cells to RA are known to be complicated by the concentration-, stage-, or duration-dependent effects[44] and, as such, protocols for the differentiation of pluripotent stem cells which involve RA remain relevant for the continued elucidation of its mechanistic action.

After the establishment of the 4-/4+ RA-based differentiation protocol, other factors emerged as potential targets for *in vitro* neural differentiation protocols. For instance, in the developing mammalian neural tube, ventrally expressed sonic hedgehog (Shh), dorsally expressed BMPs, and FGF expressed at the posterior end of the neural tube, together with RA generated in the somites of the adjacent mesoderm, are all known to direct the patterning of the spinal cord.[45] In particular, Shh signalling plays a key role in neural development.[46] The pathway is activated upon the binding of the Shh ligand to the transmembrane receptor Patched (Ptc), which relieves the inhibition of a second transmembrane receptor, Smoothened (Smo), and downstream intracellular signalling that converts the Gli transcription factors to an active form. In the absence of the bound

Shh ligand, Gli transcription factors are converted to a repressor form where they block the transcription of Shh target genes.[47] In the developing vertebrate, Shh is expressed ventral to the neural tube and a gradient of signalling from ventral to dorsal is responsible for the patterning and specification of five ventral neural progenitor sub-types in a manner inversely proportional to the distance from this source.[48] The neural progenitor sub-types then differentiate into distinct neuronal sub-types, including commissural neurons, association neurons, motor neurons, and ventral interneurons.[46] This morphogenic effect can be substantiated *in vitro*, as the differentiation of motor neuron and interneuron cell types which are found closer to the source of Shh *in vivo* requires a higher dose of Shh compared to the sensory neuron subtypes found dorsally.[46]

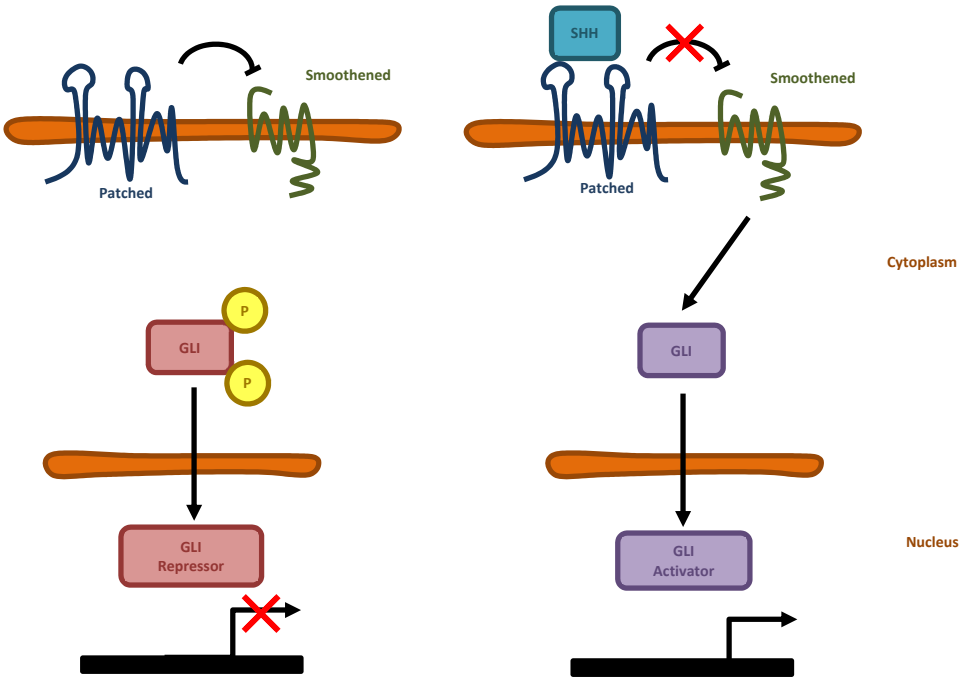

Figure 2 Sonic Hedgehog (Shh) Signalling Pathway. (A) In the absence of Shh, the receptor Patched (Ptc) inhibits Smoothened (Smo) and Gli transcription factors are processed to a repressor form where they prevent transcription of Shh target genes. **(B)** When Shh binds to Ptch, it relieves the inhibition of Smo, and the downstream signal converges on Gli transcription factors, which are processed to an activator form and enable transcription of Shh target genes. Figure adapted from Crompton et al.[49]

The application of both RA and Shh during embryoid body formation in mouse ESCs was investigated by Wichterle et al.[50] and in human ESCs by Li et al.,[51] among others. Interestingly, Wichterle et al. further reported that while together RA and Shh increased the number of post mitotic neurons generated from EBs, Shh alone did not appear to have an effect on neural induction, suggesting interdependent regulation of the two factors.[50]

Following the report of the small synthetic molecule purmorphamine acting on the Shh pathway directly through the receptor Smo (in contrast to the traditional pathway where Shh targets the receptor Ptc and upon ligand binding relieves the inhibition of Smo), the substitution of purmorphamine for Shh was suggested.[52] A key advantage of the commercially produced synthetic molecule purmorphamine is its stability and affordability compared with Shh.[53]

A modified version of the 4-/4+ differentiation protocol has emerged, known as the 2-/4+ protocol, and involves treatment with 500 nM RA and 1 μM purmorphamine in the last 4 days of a 6 day induction period.[54] Although it is understood that the use of Shh agonist purmorphamine in this protocol should yield a higher proportion of neurons than the 4-/4+ protocol and has been used in recent studies, [55] this comparison has not been explicitly explored.

Neural differentiation protocols for human stem cells

EB-mediated protocols which give rise to the non-specific differentiation into cells of all three germ layers have also been developed for human stem cells.[56] [57] Many directed differentiation protocols have been refined using optimized media formulations and soluble chemical factors which selectively enhance or inhibit lineage specification.[58] For neural lineage-specific differentiation, protocols for the generation of NPCs from

pluripotent stem cells involve ectodermal induction through the inhibition of BMP4, TGFβ/Activin, and/or Wnt pathways.[59] Following ectodermal commitment, the induction of neural lineage cells *in vitro* culminates in the formation of morphologically distinct structures containing repeated clusters of radially oriented NPCs, known as neural rosettes, which are understood to be an *in vitro* recapitulation of neural tube formation in the developing vertebrate embryo.[60] Neural rosettes express many proteins in common with the neural tube, including Pax6, Sox1, ZO-1, and nestin,[61] and have demonstrated the capacity to differentiate into neural and glial sub-types.[59 62] Generation of rosettes is the basis of most published methods for neural induction of pluripotent stem cells,[63] after which, cells are typically dissociated and re-plated for downstream differentiation into specific neural cell types. Currently, the induction of neural rosettes and NPCs have been reported for adherent culture on 2D laminin-coated tissue culture surfaces. Laminin is a glycoprotein found in basement membranes, such as those lining blood vessels and nerves, but is also known to occur in the extracellular matrix (ECM) at early stages of embryonic development where it interacts with cell surface receptors and regulates adhesion, migration, and neurite outgrowth.[64] Although laminin-coated surfaces provide clear advantages for the support of *in vitro* neuronal growth, this approach faces the same challenges of 2D culture techniques, in particular, the inability to generate cells which remain viable upon transplantation into the 3D *in vivo* environment.[65] Given the demonstrated effect of the 3D culture environment on the growth and differentiation of stem cells, it remains of interest how these well characterized stages of neural differentiation in 2D may also be achieved in 3D.

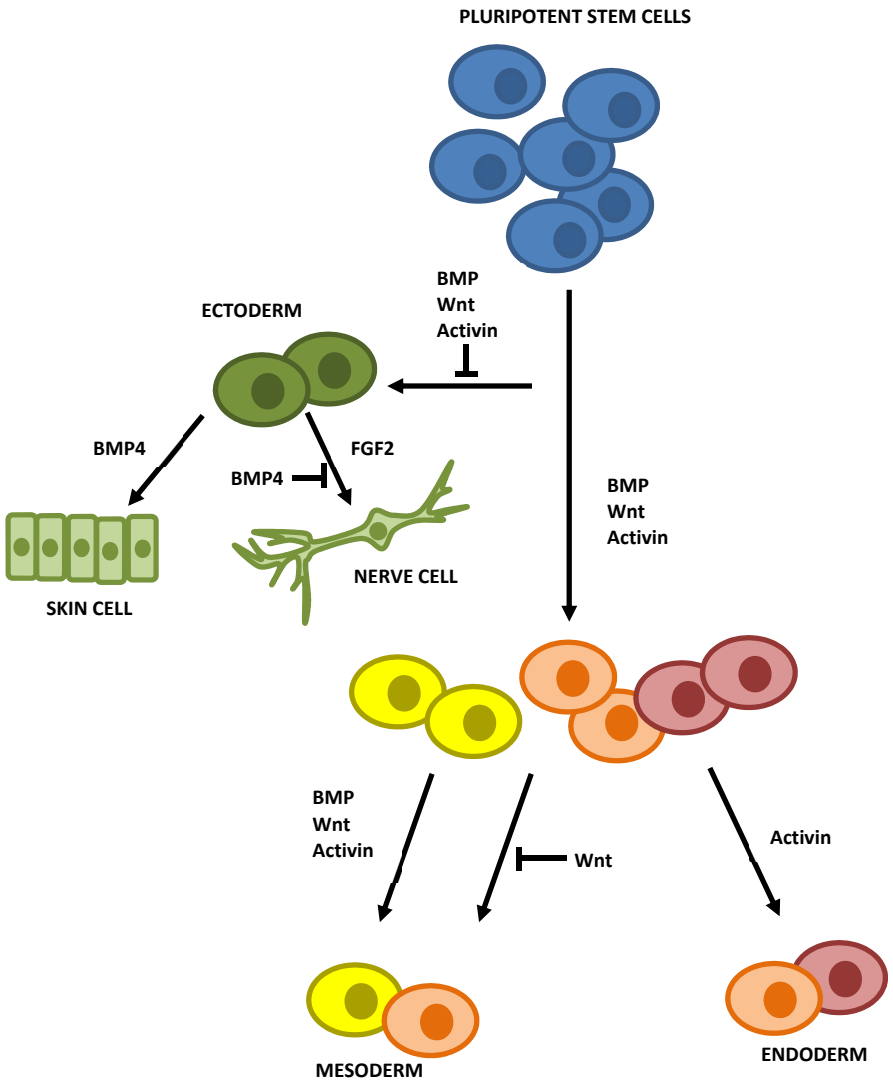

Figure 3 Proposed model of lineage specification of human pluripotent stem cells. Although the mechanisms of signalling that govern the specification of pluripotent stem cells to ectodermal, mesodermal, and endodermal lineages have not been definitively determined, several key factors have been implicated: members of the bone morphogenetic protein (BMP) family of growth factors, as well as the transforming growth factor-β (TGFβ)/Activin, and Wnt. There is evidence that BMPs, TGFβ/Activin, and Wnt prevent cells from following a "default" pathway to ectodermal fate; relief of this inhibition is required for ectodermal specification. The ectoderm can give rise to both epidermal cells as well as neural cells, with reactivation of BMP4 signalling resulting in epidermal differentiation and continued inhibition of the BMP4 signalling resulting in neural differentiation. There is also a proposed role for FGF2 in specifying neural fate.[59] Figure adapted from Murry and Keller.[66]

Biomaterial scaffolds for neural differentiation[3]

A related consideration that has arisen simultaneously from several inter-related fields is the physical microenvironment in which cells reside and the effect that the properties of this environment have on the cell behaviour. Thus, we have a thrust of research that is dedicated to the design and fabrication of biomaterial scaffolds that promote desired cell behaviours. This research has been applied to the field of neural tissue engineering with a variety of scaffolds that have been shown to support the differentiation and survival of neurons and neural progenitors derived from induced pluripotent stem cells.

Naturally-derived biomaterials for neural differentiation

As the name suggests, natural biomaterials are those which originate from nature and include the proteins and polysaccharides that perform essential functions in living organisms. In tissue engineering applications, these materials can closely mimic the ECM of native tissue which contains a complex 3D environment of polysaccharides and embedded fibrous proteins, providing adhesion sites as well as important chemical and mechanical signals to the cells. These similarities shared with the ECM confer a high degree of biocompatibility and biodegradability to natural polymers when implanted *in vivo*. However, despite these key advantages, natural biomaterials cannot be tuned to the same high degree that is available with synthetic polymers in terms of properties such as molecular weight or chain length. Nor can the extraction and purification from natural sources across different species be as consistent as those which are synthesized commercially.

---

[3] The following section contains excerpts from: **Neural Tissue Engineering Applications**, Nima Khadem Mohtaram, Amy Montgomery, Jose Carlos Gomez, Andrew Agbay, and Stephanie Willerth. Encyclopedia of Biomedical Polymers and Polymeric Biomaterials, 2014, *In Press*.

Among the natural polymers used in tissue engineering applications, fibrin has emerged as a promising cell- and drug-delivery platform for SCI treatment. Fibrin is a blood plasma protein, activated from its zymogen form fibrinogen in response to injury via the coagulation cascade, and forms the fibrous component of a blood clot. It was one of the first natural polymer biomaterials to be used in clinical applications and has been well characterized in terms of its biocompatibility and mechanical properties.[67] [68]

A key advantage of fibrin is that there are existing FDA-approved commercially available products currently being used to treat peripheral and central nerve injuries. These products form an established base upon which modifications and novel techniques can be more easily developed and translated to clinical practice.

Another advantage of fibrin is that it can be modified with proteins and peptide sequences to alter the release kinetics of loaded therapeutic drugs. Unlike synthetic polymers where changes in the drug delivery system are often linked to changes in mechanical and structural properties, drug release from fibrin can be modified through different binding affinities or number of binding site, leaving other properties unchanged.

Another important property of fibrin is the ability to polymerize hydrated gels *in situ*, opening up the potential for the future development of injectable drug delivery and cell-based therapies for neural tissue engineering, such as those described by King et al.[69].

Neural differentiation in fibrin matrices

Fibrin has been combined with stem cells for various neural tissue engineering applications, including peripheral nerve injury repair. A nerve conduit developed by Pettersson et al.[70] made from commercially available fibrin sealant demonstrated the ability to support greater distances of nerve regeneration and also permitted more

Schwann Cell intrusion after four weeks in a rodent sciatic nerve injury model compared to a control conduit. Intrusion of endogenous Schwann Cells into the conduit is a desirable outcome because these cells provide support for the newly regenerated neurons. Using a similar conduit design and injury model, another study by Pettersson et al.[71] showed that the fibrin conduit was comparable to an autograft in functional recovery, as assessed by lower limb muscle size in short nerve gap cases. Furthermore, in a 16 week sciatic nerve injury model, their group showed that 50% to 60% of neurons were regenerated in a fibrin conduit compared to the autograft control. [70]

The Sakiyama-Elbert lab has developed a fibrin scaffold for repair of spinal cord injuries. Among these studies, Willerth et al.[72] focused on optimizing fibrin seeding conditions to support the neural differentiation of ESC-derived EBs. In various *in vitro* studies, the optimal concentrations of fibrin (10mg/mL or 12.8mg/mL), thrombin (2 NIH U/mL), and aprotinin (5 ug/mL) were found. These optimized scaffolds supported the differentiation of ESC-derived neural progenitors into neurons and astrocytes, with intact EBs demonstrating more robust growth and survival in 3D culture than dissociated EBs. A later study by Kolehmainen and Willerth[73] demonstrated that 3D fibrin scaffolds are also an effective platform to support the neural differentiation of EBs derived from mouse iPSCs.

Delivery of therapeutic factors from fibrin matrices[4]

Drug delivery systems

Controlled drug delivery of therapeutic factors has been used to address the loss of cells in various neurological disease and disorders.[74-76] To-date, however, clinical trials

[4] The following section contains excerpts from: **Biomaterial-based drug delivery systems for the controlled release of neurotrophic factors**, Nima Khadem Mohtaram, Amy Montgomery, and Stephanie M. Willerth, 2013 Biomed. Mater. 8 022001

utilizing such therapies have obtained unsatisfactory results, largely due to an inability to deliver sufficient doses. [77] Several barriers preventing the delivery of drugs to the CNS have been identified, including failure to cross the blood-brain barrier, poor stability in the spinal fluid, limited diffusion, and an inability to precisely control dosing.[78]

Affinity-based drug delivery systems (ABDS) are a subset of controlled release approaches that show promise for controlling release of bioactive agents for neural tissue engineering applications, including spinal cord injury.[79-87] ABDS function on the basis of non-covalent interactions between the target drug and the device material. [88] These systems are easily incorporated into protein-based biomaterial platforms by mimicking the various transient binding interactions that occur in the ECM.[81] Delivery of bioactive agents from ABDS can be regulated in several ways including tailoring the affinity of the device materials for the loaded drug, the number of binding sites, and the degradation rate of the selected material. In one of the most well-known examples of ABDS, Edelman et al.[89] pioneered a heparin-binding delivery system (HBDS) for the controlled release of basic fibroblast growth factor (bFGF) for wound healing and tissue repair applications. This system took advantage of heparin's ability to bind and stabilize bFGF in order to control the release. This approach has since been adapted in many other controlled release applications.

Neurotrophic factors

Neurotrophic factors are proteins that are known to promote the development, survival, and regeneration of neurons. Examples include nerve growth factor (NGF), glial cell line-derived neurotrophic factor (GDNF), brain-derived neurotrophic factor (BDNF) and neurotrophin-3 (NT-3) and each factor targets specific populations of neural cells. NGF

plays a prominent role in sensory neurons by stimulating neurite outgrowth and increasing the survival of sympathetic neurons during inflammation.[90] It also promotes axonal regeneration in central and peripheral nervous system after injuries.[91] GDNF enhances nerve regeneration in a rat nerve injury models and promotes survival of motor neurons.[92] It has exhibited both neuroregenerative and neuroprotective effects for the dopaminergic neurons present in Parkinsonian animal models.[93] NT-3 promotes the differentiation of new neurons and enhances corticospinal tract formation during development.[88] For neural tissue engineering applications, these factors can be used with biomaterial scaffolds to enhance the survival and regeneration of host cells and also in conjunction with cell therapies to enhance the differentiation of stem cells or progenitor cells into neurons, oligodendrocytes, and astrocytes.

Controlled delivery of neurotrophic factors from fibrin

Enhancing host cell survival and regeneration

In a study by Moore et al.,[92] nerve guide conduits functionalized with a neurotrophic factor ABDS implanted 12 weeks post-operative in rat sciatic nerve injury models showed and enhancement of functional recovery compared to the same conduits without ABDS. These results were echoed those obtained by Lee et al., [94] who polymerized a fibrin scaffold containing HBDS and NGF inside a silicone tube that was tested in the same injury model. Histomorphological analysis revealed that the nerve guide conduits loaded with fibrin scaffolds containing an NGF ABDS enhanced peripheral nerve regeneration compared to conduits with fibrin and NGF without a delivery system.

A fibrin sealant matrix loaded with NGF was compared to plain fibrin sealant in a rat sciatic nerve transection by Zeng et al.;[95] this study reported that the NGF-loaded sealant exhibited a burst release during the first 18 hours with slower release for subsequent two

weeks and contributed to enhanced functional recovery after nine weeks. Fibrin glue loaded with NGF was used by Chunzheng et al.[96] at the suture site in rat sciatic nerve transections to enhance functional recovery 12 weeks postoperative compared to fibrin glue alone.

Enhancing neural differentiation of stem cells

Building on earlier work involving the optimization of fibrin matrices for neural differentiation, Willerth et al.[88] showed that murine ESC-derived NPCs responded to soluble growth factors when seeded inside fibrin matrices for 14 days. In this study, NT-3 and sonic hedgehog (Shh) were found to increase the yield of neurons and oligodendrocytes while platelet derived growth factor (PDGF) and basic fibroblast growth factor (bFGF) were shown to increase cell viability compared to untreated cells. Fibrin scaffolds incorporating an affinity-based drug delivery system were then used to deliver these neurotrophic factors in a controlled manner over time.[86] It was found that the simultaneous controlled release of NT-3 and PDGF successfully promoted the proportion of murine ESC-derived EBs that differentiated into NPCs, neurons, and oligodendrocytes while reducing the proportion of astrocytes as compared to untreated cells. This work was translated for *in vivo* studies by Johnson et al.[80 97] who transplanted mouse ESC-derived NPCs encapsulated in fibrin into a rat model of SCI. The fibrin scaffolds protected the cells from the inhibitory environment of the injury site *in vivo*, as indicated by increased cell survival compared to transplanted cells without fibrin. Growth factors NT-3 and PDGF added to the fibrin scaffold, with and without an affinity-based heparin binding drug delivery system, increased proliferation of the transplanted cells and differentiation into neurons.

Lu et al.[98] investigated the ability of NSC-derived neurons to regenerate axons *in vivo* after neural injury. Both rat and human fetal spinal cord-derived NSCs were embedded into growth factor-containing fibrin matrices and grafted into rat SCI lesion sites two week post-transection. Grafted cells differentiated into neurons with a large number of long axons, which formed synapses with host cells. Transplanted cells were also observed to be myelinated by host oligodendrocytes. Functional recovery was enhanced in NSC grown in growth factor-containing fibrin matrices three weeks post-grafting compared to the non-treated control. Furthermore, human ESC-derived NPCs combined with fibrin and growth factors in an anatomical study of rat SCI were shown to express neural markers *in vivo*, demonstrating that ESC-derived cells could also differentiate into neurons and extend axons in the inhibitory injury site.

Enhancing neural differentiation of primary neural cells

Wood et al.[87] showed that the controlled release of GDNF from fibrin matrices increased the outgrowth of nerve fibers from dorsal root ganglia compared to fibrin alone. In a different approach, Maxwell et al.[81] tailored the interaction between a fibrin scaffold and the loaded drug by screening different peptide functional binding sites to find sequences with varying degrees of affinity for heparin, which in turn could bind NGF. Peptide affinity was investigated, along with the ratio of binding sites, binding kinetics, and the rate of enzymatic degradation to determine the effect on the drug delivery profile. In vitro assays using dorsal root ganglia showed that fibrin scaffolds with NGF delivery systems using heparin and peptides of various heparin-binding affinity showed increased neurite extension compared to scaffolds with only diffusion-based delivery of NGF.

Heat shock proteins: a new therapeutic target for SCI

Heat shock proteins (HSPs) are a class of proteins which are known to act as molecular chaperones for protein folding within the cell.[99] These proteins, which are numbered according to molecular weight, are both constitutive and inducible, being upregulated as part of the stress response in the cell where they act to stabilize other proteins, preventing them from unfolding due to fluctuations such as increased heat or pressure.[100] HSPs have also been implicated in roles outside of the cell, notably in the regulation of the immune response, which has aroused interest in their therapeutic potential[101-103].

Unlike most cells, neurons have not been shown to upregulate HSPs in response to stress; instead, it has been shown that glial cells secrete HSPs into the extracellular environment for the neurons to uptake, thereby increasing neuronal survival rate after injury.[104-107] Additionally, HSPs have been shown to inhibit glial scarring the CNS, allowing for a more permissible environment to support the regeneration of neurons.[108] Therefore, the exogenous application HSPs seems a logical therapeutic intervention for neurological diseases and disorders. Recent studies, such as those reviewed by Reddy et al.,[109] have shown that delivery of HSP as a therapeutic can preserve nerve function and promote regeneration after SCI.

Particular interest in specific families such as the HSP70s have emerged based on findings that elucidate the critical role of HSP70 in motor neuron survival in the spinal cord.[106 110] In another study, Tidwell et al.[105] showed that HSP70 has a concentration dependent effect on the sparing of motor and sensory neurons after injury. Lai et al.[111] applied HSP70 modified with a peptide uptake sequence to *in vitro* culture of neurons, demonstrating the ability of this modified HSP70-peptide to prevent the degradation of

neurons in response to stress. These studies support the further investigation of HSP70 as a therapeutic target for treating SCI.

HSPs in neuronal differentiation

In addition to the reported neuroprotective effects of HSPs, these proteins have also been shown to have an effect on the differentiation of stem cells into neural lineage cells.[112 113] The upregulation of HSPs in response to stress has been shown to promote neurogenesis *in vivo*, as seen in the formation of the neural plate during embryogenesis. [114 115] Interestingly, pluripotent and multipotent stem cells initially express high levels of HSP, but these levels decline when the cells are terminally differentiated into neurons.[116] Given the reported neuroprotecive role of HSP70, these results also demonstrate the potential for HSPs to be further investigated for tissue engineering applications in SCI treatment, such as those developed using more typical neurotrophic factors.

HSPs in drug delivery applications

HSPs have been previously characterized in controlled drug delivery applications. One study[117] presented the release of an HSP60-derived peptide sequence from polymer microspheres in order to delay the immune response in a skin transplantation application. Injected into the nasal mucosa, the microspheres were intended to degrade from the surface, releasing the peptide over time in a diffusion-based manner. After 5 days, the inflammatory response of grafted mice was seen to be less severe in the group with treated with the HSP60-derived peptide microspheres compared to the control. In a different study,[118] HSP27 was encapsulated in polymer microspheres which were seeded in an alginate hydrogel to further slow the diffusion-based release profile. This system

was demonstrated release of bioactive HSP27 over 3 weeks and was intended as an anti-apoptotic therapy to promote cadiomyoblast survival following myocardial infarction.

HSPs in affinity-based drug delivery

Previous work on ABDS in fibrin has shown that rationally designed peptide sequences can be chosen to achieve controlled drug release.[85] Such peptides should contain a fibrin-binding domain consisting of a transglutaminase substrate (amino acid sequence NQEQVSPKA) at the N terminus for it to be covalently incorporated in a fibrin clot via the activity of cross-linking Factor XIIIa.[119] To facilitate non-covalent binding with the target, it is known that HSPs require a domain of 7 or more amino acids. Furthermore, these 7 amino acids should contain residues which are hydrophobic and aromatic.[120] A series of peptides with demonstrated binding affinities include: PLSQETFSGLWKLLPPEDG, derived from p53[121]; GCEVFGLGWRSYKH, derived from CD40 receptor[122]; AKVKGDGTISAITE, derived from GABA transporter 4[123]; FIKEEERPLPEKEYQRQV, derived from potassium voltage-gated ion channel[123]; and TMVYLLPLGPKGSGNREQDK, derived from coagulation factor V[123]. Any of these sequences synthesized on the C terminus of the fibrin-binding domain would be candidate peptides for fibrin-based HSP70 ABDS.

Review conclusion: state of the art

The use of biomaterials in tissue engineering applications has been an active area of research for over two decades,[124] with more recent efforts focussing on scaffolds which support and direct stem cell differentiation.[125] The protein-based biomaterial fibrin has been well characterized for the differentiation of murine ESCs into neural lineage cells for SCI treatment[72 84 86 88 92], but there remains a need to extend this work to include iPSCs. In addition, the two specific differentiation protocols typically used to prime

murine pluripotent stem cells towards neurons[43 54] prior to combination with fibrin scaffolds have yet to be assessed in terms of comparative neuronal differentiation efficiency.

The existing body of work involving fibrin-based scaffolds as a platform for the differentiation of pluripotent stem cells into neurons should also be adapted appropriately to include human cells. As a first step, there is a need for initial proof-of-concept work to confirm the ability of fibrin to support the viability and differentiation of NPCs derived from human iPSCs. This will establish opportunities for future investigation, including systematic optimization of fibrin scaffolds for the differentiation of human iPSCs using the same approach reported for murine ESCs.[72]

To further enhance the effectiveness of a fibrin-based tissue engineering therapy for SCI, scaffolds can be functionalized with drug delivery capacity. While many neurotrophic factors such as NGF, GDNF, BDNF, and NT-3 have been investigated,[126] the heat shock protein HSP70 is an emerging therapeutic factor with demonstrated neuroprotective potential[105 106] which has yet to be investigated along with the appropriate drug delivery system.

Chapter 3 Research Plan

Problem Statements

In general, tissue engineering strategies for spinal cord injury must optimize the choice of cells, biomaterial matrix, and delivery system for therapeutic factors. Working within this general problem statement, three specific gaps in knowledge are identified in the specific problem statements below.

Problem statement 1

There are multiple differentiation protocols reported for the generation of neurons from murine embryonic stem cells. These protocols have not yet been compared in terms of their capacity to generate neurons and, furthermore, the capacity to generate neurons has been shown to vary between types of stem cells. As such, the existing protocols that were developed and optimized for murine embryonic stem cells needs to be evaluated in applications using murine induced pluripotent stem cells.

Problem statement 2

Of the biomaterial matrices for tissue engineering, naturally-derived protein-based fibrin matrices have been extensively characterized for neural differentiation using murine embryonic stem cells. However, to increase the clinical relevance of this approach, the existing fibrin-based cell delivery tools must be adapted for human cells, in particular, human induced pluripotent stem cells.

Problem statement 3

Drug-releasing fibrin matrices have been developed with various therapeutic factors using affinity-based drug delivery systems; however, this has not yet been investigated for heat shock proteins. Heat shock proteins have been shown to play an important role in

the regeneration of neurons after spinal cord injury and the exogenous application of heat shock proteins has been shown to have a neuroprotective effect on neural cells in culture. Given the emerging evidence supporting heat shock proteins as a promising spinal cord injury therapeutic, there is an opportunity to develop a new affinity-based drug delivery system for the controlled release of these proteins from fibrin matrices.

Research Aims

Three specific research aims directly address the gaps in knowledge identified in the specific problem statements above.

Specific research aim 1

This research aim seeks to evaluate the differentiation efficiency of the 6-day 2-/4+ neural differentiation protocol using retinoic acid and purmorphamine compared to the traditional 8-day 4-/4+ retinoic acid-based protocol using murine induced pluripotent stem cells. Differentiation efficiency is defined as the quantity of neurons – i.e. cells expressing neuronal marker β-III-tubulin (TUJ1) – generated as a proportion of the total cell population. Cells generated from both differentiation protocols will be seeded in 3D fibrin matrices for 14 days.

➔ It is hypothesized that the 2-/4+ differentiation protocol has the ability to produce neurons from murine induced pluripotent stem cells with higher efficiency than the 4-/4+ protocol when cells are seeded inside 3D fibrin matrices for 14 days.

Specific research aim 2

This research aim seeks to evaluate the ability of fibrin-based matrices to provide functional support of neural progenitor cells derived from human induced pluripotent stem cells in terms of viability and differentiation efficiency. Viability is defined as the proportion of viable cells out of the total cell population. Differentiation efficiency is defined as the proportion of neurons – i.e. cells expressing neuronal marker β-III-tubulin (TUJ1) – generated as a proportion of the total cell population. This proof-of-concept

work will include seeding of neural progenitor cells inside fibrin matrices of varying concentrations and at different time points in the differentiation program for 14 days.

- ➔ It is hypothesized that neural progenitor cells derived from human induced pluripotent stem cells will exhibit high levels of viability when seeded inside 3D fibrin scaffolds for 14 days.

- ➔ It is hypothesized that neural progenitor cells derived from human induced pluripotent stem cells will differentiate into neurons when seeded inside 3D fibrin scaffolds for 14 days.

Specific research aim 3

This specific research aim seeks to develop an affinity-based drug delivery system for the controlled release of HSP70 from fibrin matrices. In this work, the ability of fibrin matrices modified with HSP70-binding peptide to sequester HSP70 will be compared to unmodified fibrin matrices. The ability of fibrin to sequester HSP70 will be evaluated based on the concentrations of HSP70 retained after an equilibrium release study.

- ➔ It is hypothesized that under equilibrium conditions, fibrin matrices modified with a covalently bound HSP70-affinity peptide will retain more of the loaded HSP70 than unmodified fibrin matrices.

Chapter 4 Experimental Methods – Aim 1

Cell culture protocols

Maintenance of pluripotent cells

Murine iPSCs (System Bioscience) and ESCs (R1 line from the Nagy Lab[127], University of Toronto) were cultured on a feeder layer of mouse embryonic fibroblasts (MEF; Cedarlane) and 0.1% gelatin (Millipore) in the presence of stem cell media with 1000 U/mL leukemia inhibitory factor (LIF; Millipore). The stem cell media used contains Dulbecco's Modified Eagle Medium (DMEM) High Glucose No Glutamine (Life Technologies), 15% ES-cell qualified fetal bovine serum (FBS) (Life Technologies), 0.1 mM MEM Non-Essential Amino Acids (Life Technologies), 2 mM GlutaMAX^{TM} Supplement (Life Technologies), 0.055mM β-mercaptoethanol, 0.1 mM nucleosides (Millipore),100 μg/mL Penicillin-Streptomycin (Life Technologies). Cells were passaged enzymatically with trypsin (0.25% Trypsin-EDTA, Invitrogen) approximately every 2 days at a ratio of 1:5. Cells were maintained at 37˚C and 5% CO_2 throughout routine culture and differentiation protocols.

Differentiation protocols

To begin EB formation, pluripotent stem cells at a concentration of approximately $5x10^4$ cells/mL were suspended in stem cell media without LIF and were cultured on non-adherent 0.1% agar(Sigma)-coated polystyrene cell culture dishes. For the 8-day 4-/4+ protocol, EBs were formed for 4 days without treatment followed by 4 days in the presence of 500 nM RA[43]. For the 6-day 2-/4+ protocol, EBs formed for 2 days without treatment followed by 4 days in the presence of 500 nM RA and 1 mM purmorphamine[54]. Media was changed every 2 days.

Seeding EBS inside 3D fibrin scaffolds

Preparation of fibrinogen solution

Fibrinogen solution was prepared, as previously described[128], from lyophilized fibrinogen (Calbiochem, Switzerland) reconstituted in tris buffered saline (TBS), pH 7.4, and dialyzed in 10,000 molecular weight cut-off dialysis tubing (Thermo) for 24 hours to remove large impurities. The fibrinogen solution was sterile filtered using a 0.2 μm pore cellulose acetate syringe filter and diluted to the appropriate concentration in sterile TBS.

Cell seeding

EBs were seeded inside 3D fibrin scaffolds as previously described [72 86 88 128]and as shown schematically in Figure 4. Briefly, 10 mg/mL sterile fibrinogen was polymerized in the presence of 40 U/mL thrombin (Sigma) and 50 mM $CaCl_2$ in the wells of a 24-well polystyrene cell culture plate; single EBs were seeded on the surface of a 300 μL fibrin gel with another 100 μL fibrin gel subsequently polymerized on top. Following seeding, gels were incubated for 1 hour at 37 ˚C to allow for full polymerization, after which 1 mL of stem cell media was added to each well. Media was changed to NeuralBasal Media (Invitrogen) with B27 Supplement (Invitrogen) after 3 days. EBs were maintained for 2 weeks before harvesting for flow cytometric analysis or fixed for immunocytochemistry. An image of a typical fibrin scaffold is shown in Figure 5.

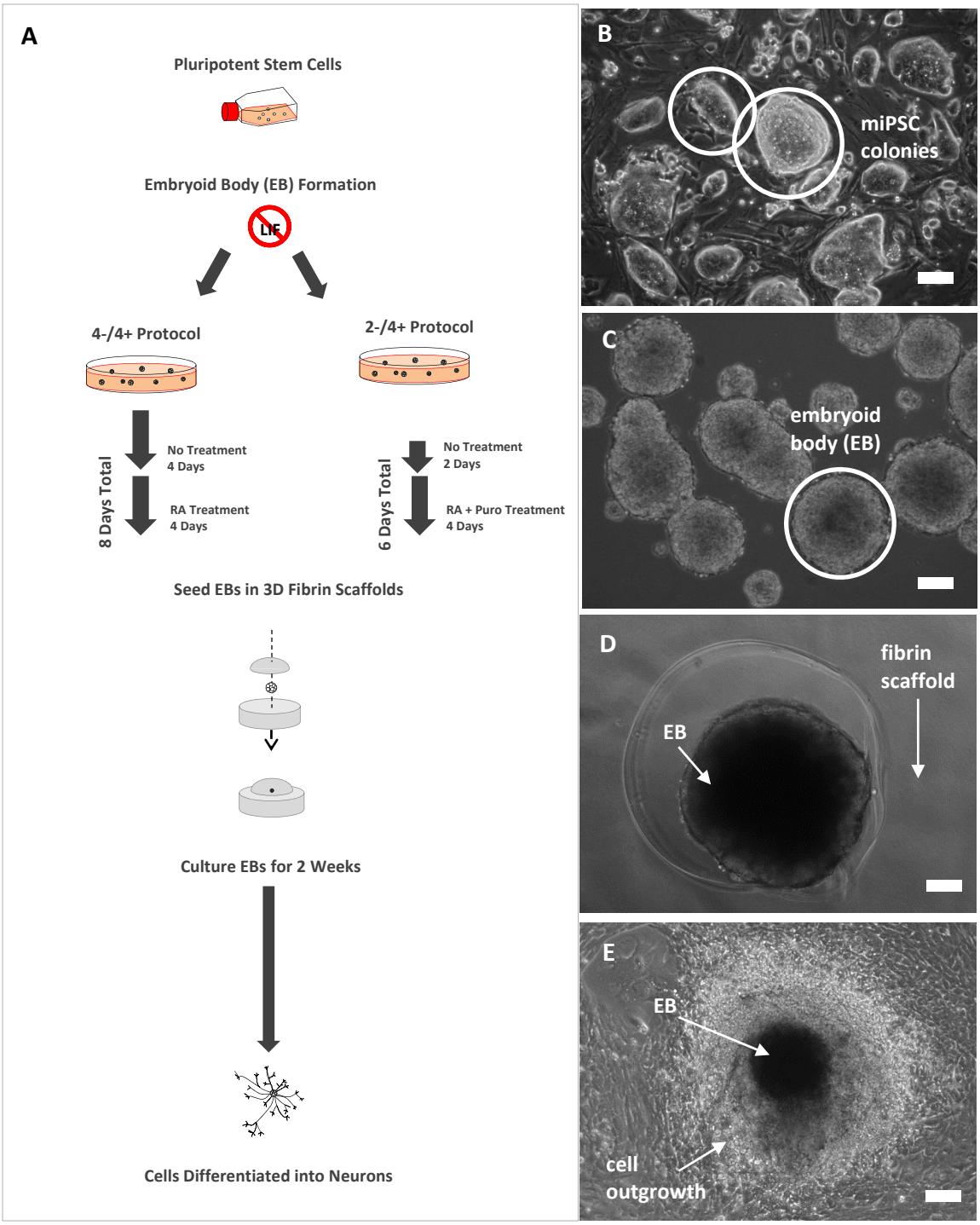

Figure 4 Embryoid body (EB) formation and seeding inside 3D fibrin scaffolds. (A) Schematic outline of EB formation and seeding in 3D fibrin scaffolds. Pluripotent murine stem cell colonies (B) are removed from routine culture and induced to form embryoid bodies (EBs) (C) using either the 8-day 4-/4+ protocol with retinoic acid (RA) treatment in the last 4 days or the 6-day 2-/4+ protocol with RA and purmorphamine (Puro) treatment in the last 4 days. EBs are then seeded inside 3D fibrin scaffolds (D) and cultured for 2 weeks to support differentiation into neurons (E). Scale bars are 100 μm.

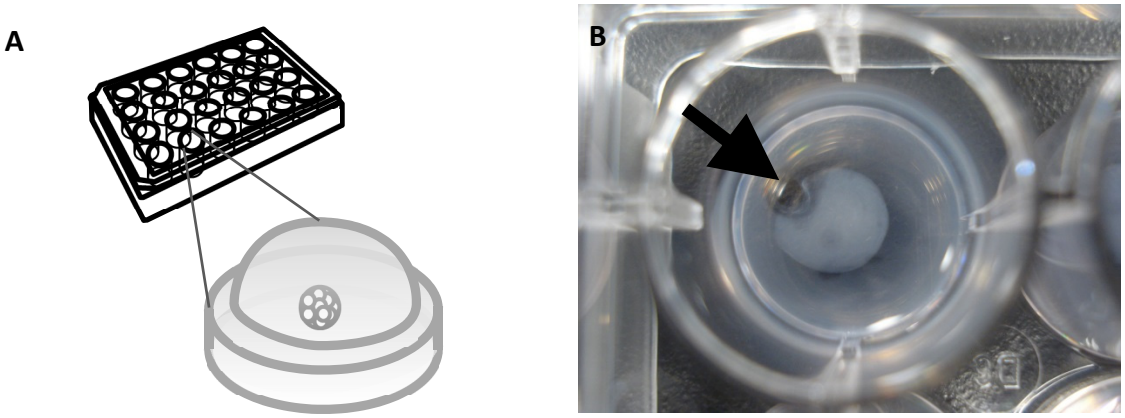

Figure 5 Typical images of a fibrin scaffold (A)A schematic of a 400 µL fibrin scaffold encapsulating a single EB. **(B)** A 400 µL fibrin scaffold polymerized in the well of a 24-well tissue culture plate. **Arrow** indicates voids showing degradation by cell-secreted proteases after 14 days of culture.

Cell viability

Viacount sample preparation

Whole EBs were dissociated enzymatically by incubating with trypsin at room temperature for 20 minutes. Samples were triturated to break up any remaining cell clumps and passed through a 60 µm pore strainer. The resulting single cell suspensions were diluted 1:10 in Viacount reagent (Millipore) and incubated at room temperature, protected from light, for 5 minutes. The Viacount reagent includes two DNA intercalating dyes. The first dye is able to permeate the intact cell membrane, entering and staining nucleated cells. The second dye is only able to permeate compromised cell membranes, entering and staining dead or apoptotic cells. Samples were then analysed using GuavaSoft Viacount Software on a Guava EasyCyte HT (Millipore) flow cytometer.

LIVE/DEAD® Sample preparation

Cells were stained for viability using the LIVE/DEAD® Viability/Cytotoxicity Kit (Invitrogen). Samples were incubated in PBS containing 2 µM calcein-AM and 4 µM ethidium homodimer (EthD-1). In live cells, the calcein-AM passes through the cell membrane where it is cleaved into fluorescent calcein by intracellular esterase activity.

Thus, live cells can be identified by green fluorescence. EthD-1 is excluded from live cells due to its size; however, it penetrates the ruptured membranes of dead cells and binds to nucleic acids which then causes an amplification of its fluorescence. Thus, dead cells can be identified by red fluorescence.

LIVE/DEAD® Imaging

Fluorescent images were obtained on a Leica DMI 3000B microscope with a QImaging RETIGA 2000R camera at a magnification of 100X. Leica supplied GFP and CY3 filters were used to obtain green and red fluorescent channels, respectively. QCapture software (QImaging) was used for image capture. Phase contrast and fluorescent images were captured for each sample. Green and red channel images were merged using Adobe PhotoShop software with the opacity of the layers at 50%.

Flow cytometry

Flow cytometry sample preparation

To assess expression of undifferentiated stem cell marker Stage specific embryonic antigen-1 (SSEA-1), pluripotent stem cells from adherent colonies were first dissociated enzymatically by incubating with trypsin at 37 ˚C for 5 minutes. Samples were quenched and collected in stem cell media, triturated to break up cell clumps, washed with PBS, and passed through a 60 μm strainer to ensure a single cell suspension. Samples were then prepared according to the directions of the Human/Mouse Pluripotent Stem Cell 4 Color Flow Cytometry Kit (R&D Systems). Briefly, single cell suspensions of approximately 500 cells/mL were washed and incubated in a Fixation/Permeabilization Buffer (containing 1% formaldehyde and 0.05% sodium azide) for 30 minutes at 2 – 8 ˚C. Samples were washed and incubated in Permeabilization Buffer (containing 0.05% sodium azide) with stains at a dilution of 1:100 for 30 minutes at 2 to 8 ˚C; stains

included directly conjugated antibodies SSEA1-PerCP and matched IgM-PerCP isotype control. Samples were washed and resuspended in PBS prior to analysis.

To assess neural progenitor marker nestin and early neuronal marker β-III-tubulin (TUJ1), whole EBs and associated cell outgrowth were first isolated from within fibrin scaffolds by incubating with trypsin at 37 ˚C for 20 minutes. Samples were quenched and collected in stem cell media, triturated to break up cell clumps, washed with PBS, and passed through a 60 μm strainer to ensure a single cell suspension. Samples of differentiated cells were then prepared according to the directions of the FlowCellect Rodent NSC Characterization Kit (Millipore). Briefly, single cell suspensions of approximately 500 cells/mL were incubated in the Fixation Buffer for 20 minutes at room temperature, washed and incubated in Permeabilization Buffer with fluorescent stains for 1 hour on ice; each sample was subdivided and treated with a single target marker or isotype control at a dilution of 1:100. Stains included directly conjugated TUJ1-PE-CY5, IgG2a-PE-CY3 isotype control, nestin-PE, IgG1-PE isotype control, SOX2-FITC, and IgG2A-FITC isotype control. Samples were washed and resuspended in Assay Buffer for analysis.

Flow cytometric analysis

Data was collected using a Guava EasyCyte HT flow cytometer. Standard gating was performed to exclude debris and doublet cells. Gain controls were set for each isotype control such that fluorescence intensity above 10^1 was minimized. Each sample was collected up to a maximum of 5000 gated events. Data analysis was performed using GuavaSoft InCyte software. Positive populations for each marker were defined as being

greater in fluorescent intensity than a threshold excluding approximately 99% of the isotype control population representing non-specific binding.

Immunocytochemistry

Immunocytochemistry sample preparation

Cells inside 3D fibrin were washed with PBS and fixed with 10% formalin for 1 hour at room temperature and then permeabilized with 0.1% Triton-X (Sigma) for 45 minutes at 2 – 8 ˚C. Wells were blocked with 5% normal goat serum (NGS) for 2 hours at 2 to 8 ˚C. Primary antibody TUJ1 (Millipore) was added at a dilution of 1:500 and incubated at 2 to 8 ˚C overnight. Cells were washed 3 times with PBS including a 15 minute incubation at 2 to 8 ˚C between each wash. The secondary antibody was added at a dilution of 1:200 and incubated for 4 hours at room temperature. Cells were again washed 3 times with PBS including a 15 minute incubation at 2 to 8 ˚C between each wash. Additional PBS was added to each well to prevent drying of the samples for imaging.

Immunocytochemistry imaging

Fluorescent images were obtained on a Leica DMI 3000B microscope with a QImaging RETIGA 2000R camera at a magnification of 100X; a GFP filter was used for fluorescent green channel. QCapture software (QImaging) was used for image capture. Both phase contrast and fluorescent images were captured for each sample.

Statistical analysis

Sample sets for data analysis represented the 4 experimental conditions (miPSC 4-/4+, miPSC 2-/4+, mESC 4-/4+, and mESC 2-/4+) at 2 separate time points. Overall, this included data from 8 separate 24-well plates, with each plate containing 6 wells prepared for each experimental condition. Cells from the 6 wells were pooled into one sample in

order to obtain sufficient cells for analysis. Of the 8 plates prepared, 4 plates were analyzed after 7 days and 4 plates were analyzed after 14 days.

Sample sets were first tested for normality using the one sample Kolmogorov-Smirnov (K-S) test in order to determine the applicable tools for statistical analysis. Results were determined to a 5% significance level. It was determined that the data were not normally distributed and therefore significant differences between sample sets were tested using both the two sample K-S test and the Kruskal-Wallis (K-W) one-way analysis of variance test, both of which are applicable to data without an underlying distribution. Tests were carried out in MATLAB. Results were determined to a 5% significance level for both tests. Standard deviation (SD) and standard error of the mean (SEM) are reported. The p-values determined for all tests are reported in Supplementary Data Tables 2, 3, and 5 to 7.

Chapter 5 Results and Discussion – Aim 1

Viability assessment

Cell viability is high at completion of EB formation and prior to seeding. Both differentiation protocols in both cell lines yield EBs with a high proportion of viable cells. As shown in Figure 6, no qualitative differences in viability were evident between differentiation protocols or cell lines based on LIVE/DEAD® images.

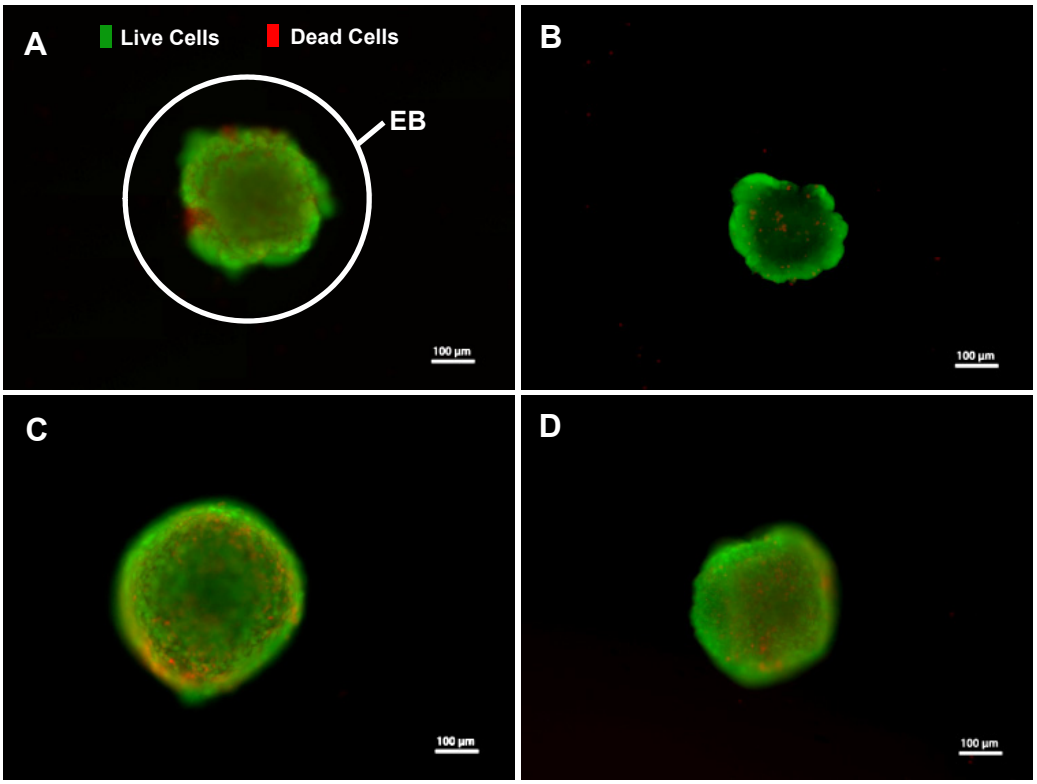

Figure 6 Qualitative viability assessment of iPSC- and ESC-derived 2-/4+ and 4-/4+ EBs at completion of EB formation Fluorescent LIVE/DEAD® images for (A) iPSC-derived 4-/4+ EB, (B) iPSC-derived 2-/4+ EB, (C) ESC-derived 4-/4+ EB, and (D) ESC-derived 2-/4+ EB at completion of the EB formation protocols and prior to seeding in fibrin scaffolds. Green indicates live cells and red indicates dead cells. Scale bars are 100 µm.

Cells viability remains high after 7 and 14 days of culture inside 3D fibrin scaffolds. EBs generated from both differentiation protocols in both cell lines survive and give rise to viable cells after culture inside 3D fibrin scaffolds after 7 and 14 days. As shown in

Figure 7 and Figure 8, no qualitative differences in viability were observed between differentiation protocols or cell lines based on LIVE/DEAD® images at day 7 or day 14. As shown in Figure 9, no quantitative differences in viability between differentiation protocols or cell lines were measured based on ViaCount flow cytometry-based viability analysis at day 14. Furthermore, no quantitative change in viability was measured over the 14 day culture period.

Positive and negative controls were performed for the Viacount assay and the LIVE/DEAD® assay at the outset of the experimental study using live cells directly from routine culture and dead cells from routine culture which were treated with 70% ethanol to induce cell death.

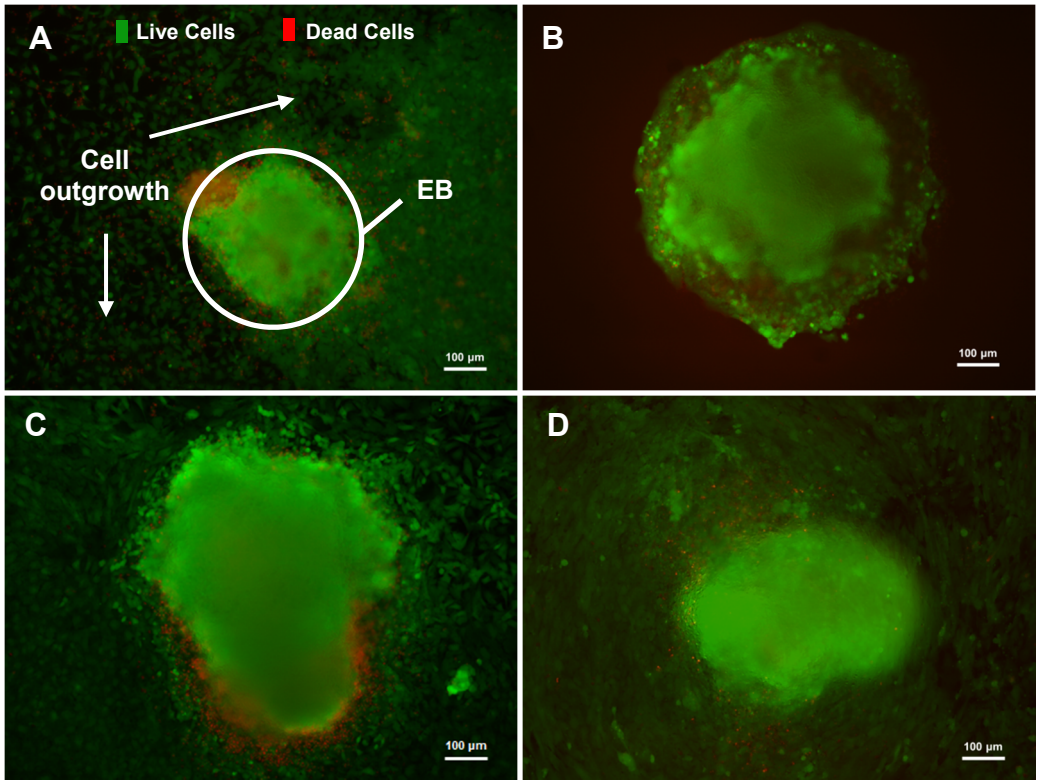

Figure 7 Qualitative viability assessment of iPSC- and ESC-derived 2-/4+ and 4-/4+ EBs after 7 days of culture in fibrin scaffolds Fluorescent LIVE/DEAD® images for (A) iPSC-derived 4-/4+ EB, (B) iPSC-derived 2-/4+ EB, (C) ESC-derived 4-/4+ EB, and (D) ESC-derived 2-/4+ EB after 14 days of culture in fibrin scaffolds. Green indicates live cells and red indicates dead cells. Scale bars are 100 µm.

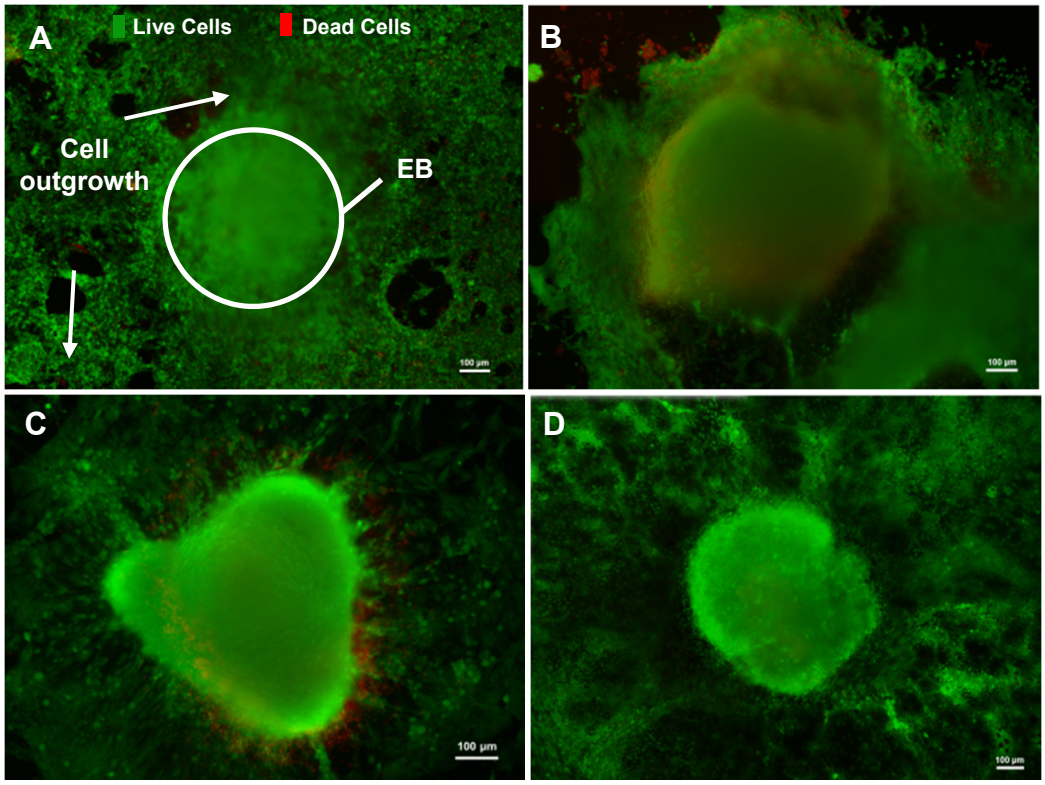

Figure 8 Qualitative viability assessment of iPSC- and ESC-derived 2-/4+ and 4-/4+ EBs after 14 days of culture in fibrin scaffolds Fluorescent LIVE/DEAD® images for (A) iPSC-derived 4-/4+ EB, (B) iPSC-derived 2-/4+ EB, (C) ESC-derived 4-/4+ EB, and (D) ESC-derived 2-/4+ EB after 14 days of culture in fibrin scaffolds. Green indicates live cells and red indicates dead cells. Scale bars are 100 µm.

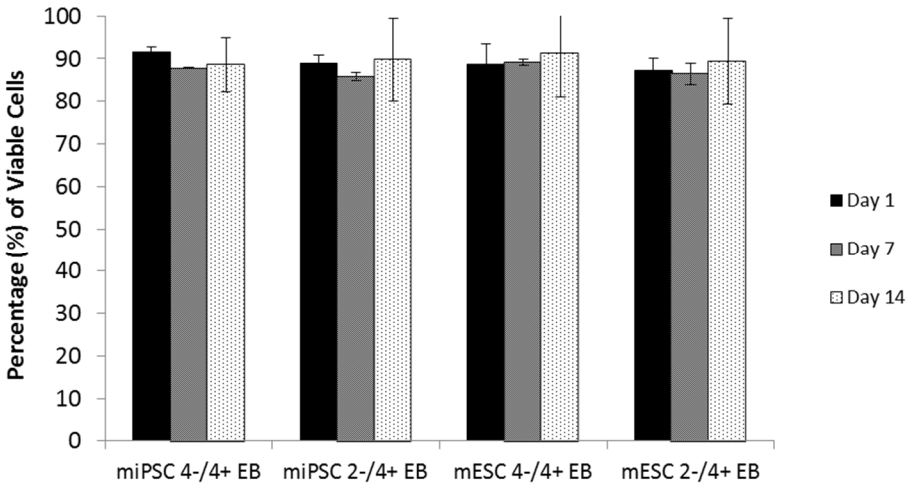

Figure 9 Cell viability at day 1, day 7, and day 14 of seeding inside 3D fibrin scaffolds Viability for iPSC 4-/4+ EBs was 92%±1% at day 0, 88%±1% at day 7, and 89%±7% at day 14.Viability for iPSC 2-/4+ EBs was 89%±2% at day 0, 86%±1% at day 7, and 90%±10% at day 14. Viability for ESC 4-/4+ EBs was 89%±5% at day 0, 89%±1% at day 7, and 91%±10% at day 14. Viability for ESC 2-/4+ EBs was 87%±3% at day 0, 86%±3% at day 7, and 89%±10% at day 14. Error bars show SEM. Sample size n = 2.

Efficiency of Neuronal Differentiation

Expression of early neuronal marker TUJ1

The percentage of TUJ1-positive immature neuron cells generated from the 2-/4+ protocol was determined to be significantly higher than those generated from the 4-/4+ protocol for both iPSC- and ESC-derived EBs, as determined by flow cytometry shown in Figure 10A. After 14 days, TUJ1 expression for miPSC 2-/4+ cells was 23% (SD=4) while expression for miPSC 4-/4+ cells was 17% (SD=1). The TUJ1 expression for mESC 2-/4+ cells was 36% (SD=5) while expression for mESC 4-/4+ cells was 20% (SD=1). The proportion of TUJ1-positive early neuronal cells generated from the 4-/4+ EB formation protocol were consistent with previously reported values, including studies by Willerth et al. [86 88] which show between 10% to 20% TUJ1-positive cells from 4-/4+ ESC-derived EBs after 2 weeks of culture in fibrin scaffolds with no neurotrophic factor exposure.

Both iPSC- and ESC-derived EBs generated from 2-/4+ and 4-/4+ differentiation protocols show a significant increase in TUJ1 expression between day 7 and day 14, as shown quantitatively in Figure 11 and qualitatively by the TUJ1-positive stained cells in Figure 10. For miPSCs, EBs generated from the 2-/4+ had 11% (SD=6) of cells expressing TUJ1 at day 7, increasing to 23% (SD=4) by day 14, while those generated from the 4-/4+ protocol had 8%(SD=2) of cells expressing TUJ1 at day 7, increasing to 17% (SD=1) by day 14. For mESCs, the EBs generated from the 2-/4+ protocol had 13% (SD=6) cells expressing TUJ1 at day 7, increasing to 36% (SD=5) by day 14, while the EBs from the 4-/4+ protocol had 10% (SD=3) cells expressing TUJ1 by day 7, increasing to 20% (SD=1) by day 14. These results also confirm that the 14 day culture period, previously reported for murine ESC-derived 4-/4+ EBs [72 86 88] and based on the length of time that

fibrin persists before degradation by cell-secreted proteases, is an appropriate time period for evaluating neuronal differentiation when using EBs generated from the 2-/4+ protocol as well as EBs derived from iPSCs.

Expression of neural progenitor marker nestin

The percentage of nestin-positive cells generated from the 2-/4+ protocol was determined to be significantly higher compared to those generated from the 4-/4+ protocol for both types of cells. At day 14, nestin expression for miPSC 2-/4+ cells was 13% (SD=6) while expression for miPSC 4-/4+ cells was only 9% (SD=2). Similarly, for ESC-derived EBs, the percentage of nestin-positive cells generated from the 2-/4+ protocol was 17% (SD=5) and only 10% (SD=4) for the 4-/4+ protocol. These results, summarized in Figure 10B, provide further evidence for the ability of the 2-/4+ protocol to generate a greater proportion of neurons compared to the 4-/4+ protocol given the potential for nestin-positive NPCs to differentiate into neuronal lineages. In other words, a population of nestin-positive cells can be used to forecast a future population of TUJ1-postive cells, although it should not be relied upon as a robust forecast as these progenitor cells are not restricted to neurons and may differentiate into other cells such as astrocytes or oligodendrocytes at this stage.

Comparing the expression of neural markers between miPSCs and mESCs

After 14 days, comparisons within each differentiation protocol show that the percentage of TUJ1-positive cells to be higher in ESC-derived EBs compared to iPSC-derived EBs, which is consistent with previous studies reporting lower differentiation efficiency for iPSCs [129]. These previous studies propose that epigenetic factors, such as levels of histone modification, may be playing a role in the reduced ability of iPSCs to

differentiate compared to ESCs. Indeed, histone modifications are an extremely important consideration with iPSCs and have been shown to block iPSC reprogramming, as demonstrated by Rais et al.[31] in their study achieving nearly 100% reprogramming efficiency (discussed in literature review). The results of the present study suggests that while the small molecule Shh agonist purmorphamine has the ability to increase the proportion of neurons generated from the 2-/4+ EBs compared to the 4-/4+ EBs, there remains a shortfall in the neuronal differentiation efficiency of iPSCs relative to ECSs. Given what is currently known about the differences between iPSCs and ESCs, it is likely that this shortfall is due to the overall reduced differentiation efficiency of iPSCs as a result of epigenetic factors.

For the iPSC-derived EBs, the increase in TUJ1 expression from day 7 to day 14 is accompanied by a significant decrease in the expression of neural progenitor marker nestin as well as pluripotency marker SOX2, shown in Figure 10A, Figure 10B, and Figure 10C, respectively. This is consistent with the expectation that the transient expression of the non-specific intermediate filament protein nestin decreases [130] and that the overall proportion of undifferentiated cells expressing SOX2 [131] decreases as the cells specialize down neuronal lineages. For the ESC-derived EBs, however, the decreasing trends of nestin and SOX2 were not determined to be significant. Given comparatively lower expression of TUJ1 for iPSC-derived EBs compared to ESC-derived EBs at these time points, the significant decrease in nestin and SOX2 expression from day 7 to day 14 cannot be said to correlate with an increase in differentiation. A further difference between iPSC- and ESC-derived EBs is also seen in the nestin expression, with a significant difference between the 2-/4+ and 4-/4+ protocols which is shown by the ESC-

derived NPCs at day 7 and day 14 but does not emerge for iPSC-derived NPCs until day 14. In addition, when comparing between cell types within each differentiation protocol, the SOX2 expression is significantly different between iPSC- and ESC-derived NPCs at day 7 but this is diminished by day 14. These results may suggest differences in the specific cell lines as iPSCs and ESCs have been shown to have temporally consistent neural differentiation programs, although high variability in differentiation efficiency is known to be exhibited between different cell lines [29 63 129].

Given that SOX2 is one of the induced factors used in the generation of the miPSC line, it is not generally considered to be the most robust marker for pluripotency. This is because the measured levels of SOX2 may include residual expression and not necessarily reflect the changes in expression that may be occurring due to cellular processes. Thus, the expression of surface antigen SSEA1 was explored as an alternative to SOX2, as summarized in Table 1. While only a single replicate is available for each trial, these results confirm that another pluripotency marker indeed decreases as the cells differentiate into neurons. Interestingly, the pluripotency marker SSEA1 is lower in the miPSCs than the mESCs, indicating that the SOX2 expression may not be a reliable indicator of pluripotency in this experiment. Regardless of whether SOX2 or SSEA1 expression is considered, the results in Figure 10 and Table 1 identify a population of undifferentiated cells that persist after 14 days of culture inside 3D fibrin scaffolds.

It should also be noted that the TUJ1-, nestin-, and SOX2-positive cells reported in Figure 10 do not represent mutually exclusive populations and, furthermore, these cells do not account 100% of the total cell population. Making up the balance of cells unaccounted for must therefore be cells differentiating into non-neural cell types. This

remains problematic for stem-cell based clinical applications where a high quality population of one desired cell type (or even multiple desired cell types) is needed. As discussed in the literature review, *in vivo* studies in a rat spinal cord injury model by Johnson et al.[97] showed that fibrin scaffolds containing neurotrophic factors increased the proliferation of transplanted mESC-derived EBs (which had been generated from the 8-day retinoic acid-based 4-/4+ protocol). When the fibrin scaffolds were functionalized with an affinity-based drug delivery system for the neurotrophic factors, even more proliferation was achieved. Unfortunately, the increased proliferation also applied to the non-NPC population – estimated to be approximately 30% of the implanted cells – and this proliferation of non-neural cells ultimately led to reduced functional recovery in the affected animals. The Johnson et al. study underscores the importance of achieving a pure population of NPCs for stem-cell based therapies for spinal cord injury repair.

Considering the present study, that a significant degree of heterogeneity in the population persists even in the presence of improved differentiation approaches – i.e. the 2-/4+ protocol – suggests that there is further optimization of neuronal differentiation protocols required for murine iPSCs.

Table 2 SSEA1 expression in miPSC- and mESC-derived EBS from Day 1 to Day 14 in fibrin

Cell Type	SSEA1 Day 1 EB	SSEA1 Day 7 EB	Fold Change Day 1 : Day 7	SSEA1 Day 14 EB	Fold Change Day 1 : Day 14
miPSC 4-/4+	34 %	11%	3	3%	11
miPSC 2-/4+	56%	11%	5	9%	6
mESC 4-/4+	53%	33%	2	12%	4
mESC 2-/4+	56%	35%	2	18%	3

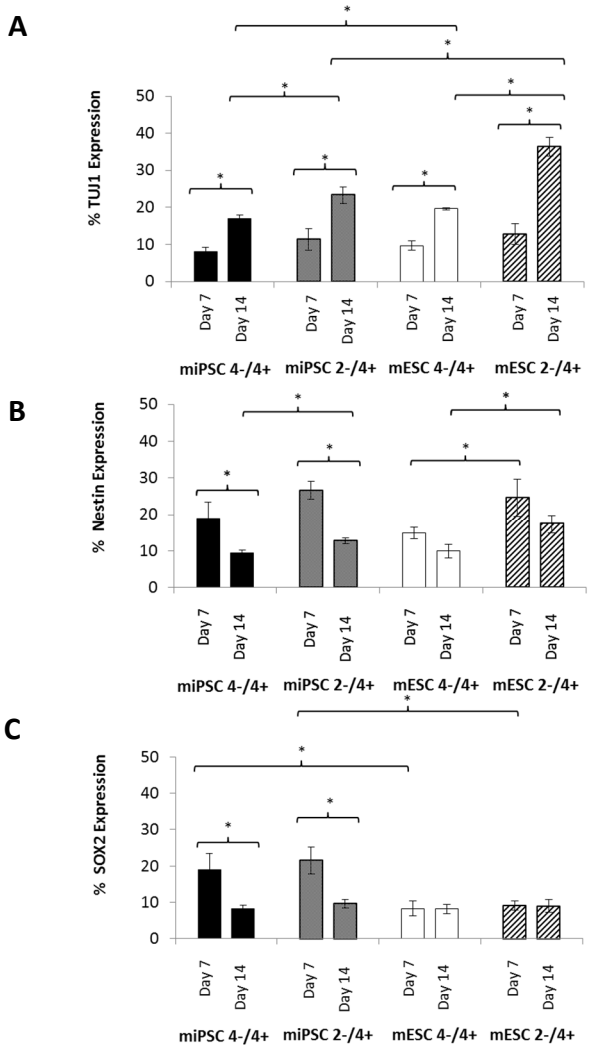

Figure 10 Quantitative expression of early neuronal marker TUJ1, neural progenitor marker nestin, and pluripotency marker SOX2 after 7 days and 14 days of culture in fibrin as determined by flow cytometry **(A)** Early neuronal marker TUJ1 expression for miPSC 4-/4+ is 8% (SD=2) after 7 days and 17% (SD=1) after 14 days; for miPSC 2-/4+ is 11% (SD=6) after 7 days and 23% (SD=4) after 14 days; for mESC 4-/4+ is 10% (SD=3) after 7 days and 20% (SD=1) after 14 days; for mESC 2-/4+ is 13% (SD = 6) after 7 days and 36% (SD=5) after 14 days. **(B)** Neural progenitor cell marker nestin expression for miPSC 4-/4+ is 19% (SD=9) after 7 days and 9% (SD=2) after 14 days; for miPS 2-/4+ cells is 27% (SD=5) after 7 days and 13% (SD=2) after 14 days; for mESC 4-/4+ is 15% (SD=3) after 7 days and 10% (SD=4) after 14 days; for mESC 2-/4+ is 25% (SD = 10) after 7 days and 17% (SD=5) after 14 days. **(C)** Pluripotency marker SOX2 expression for miPSC 4-/4+ is 19% (SD=9) after 7 days and 8% (SD=2) after 14 days; for miPSC 2-/4+ is 22% (SD=7) after 7 days and 10% (SD=2) after 14 days; for mESC 4-/4+ is 8% (SD=3) after 7 days and 8% (SD=3) after 14 days; for mESC 2-/4+ is 10% (SD = 3) after 7 days and 9% (SD=4) after 14 days. Error bars show SEM. Sample size n = 4. * indicates $p < 0.05$

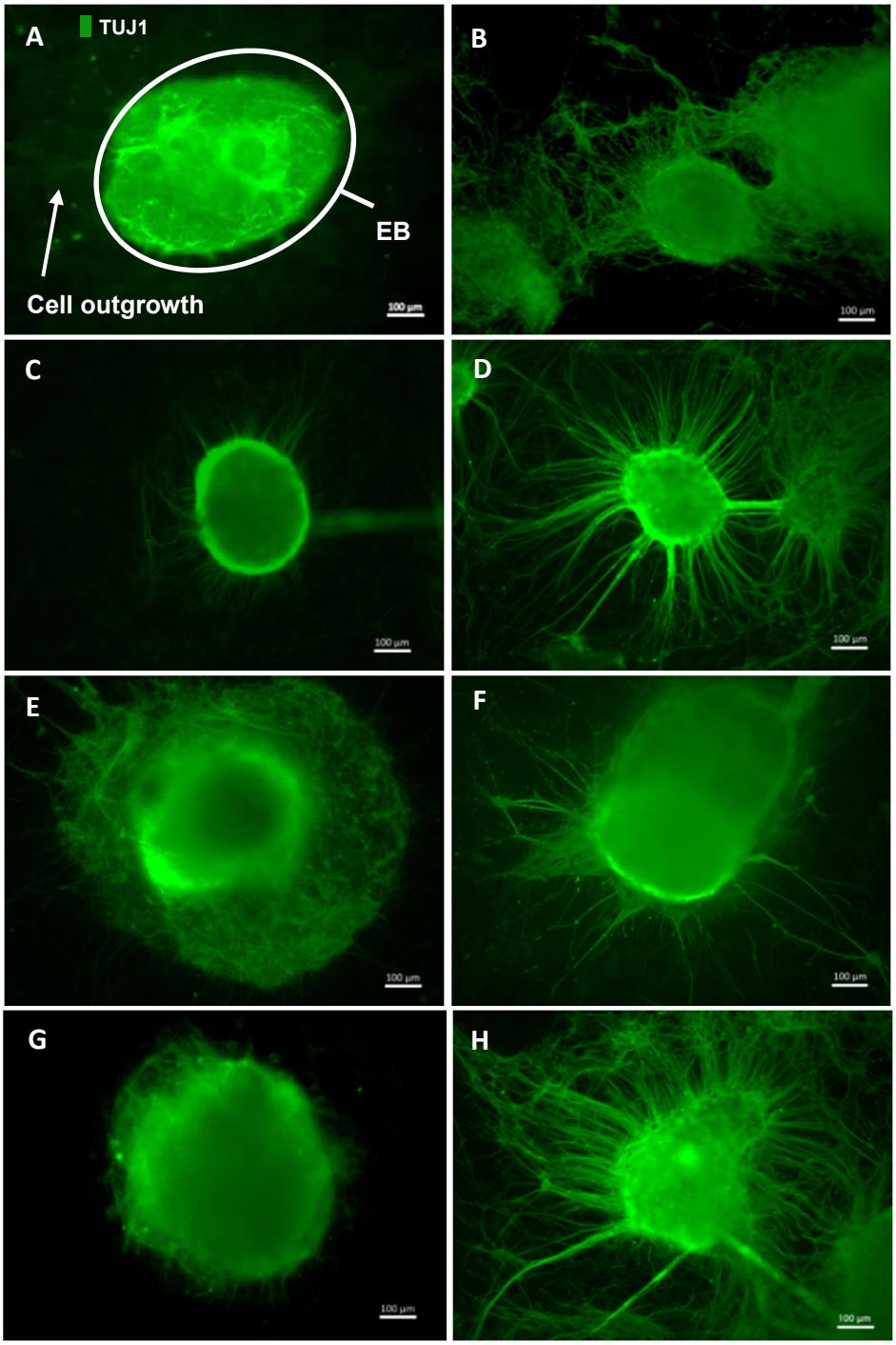

Figure 11 Early neuronal marker TUJ1 positive cells after (A,C,E,G) 7 days and (B,D,F,H) 14 days of culture in fibrin Cell outgrowth stained positive for early neuronal marker β-III-tubulin (TUJ1) for iPSC-derived 4-/4+ EBs at day 7 (A) and day 14 (B), iPSC-derived 2-/4+ EBs at day 7 (C) and day 14 (D), ECS-derived 4-/4+ EBs at day 7 (E) and day 14 (F), and ESC-derived 2-/4+ EBs at day 7 (G) and day 14 (H). Scale bars are 100 µm.

Chapter 6 Experimental Methods – Aim 2

Cell culture protocols

Maintenance of pluripotent cells

All reagents were supplied by STEMCELL Technologies unless otherwise stated. Human iPSCs (iPS Foreskin 1-DL-01)[28] and ESCs (H9) (WiCell) were cultured as adherent colonies on tissue culture plates coated with recombinant vitronectin protein, Vitronectin-XF, in the presence of TeSR-E8 defined low-protein stem cell culture media. Full media changes were performed daily. Cultures were monitored for spontaneous differentiation based on morphological assessment and any areas of differentiation were manually scraped away immediately prior to passaging. Colonies were passaged approximately every 5 to 7 days at a ratio of 1:12 using exposure to Gentle Cell Dissociation Reagent at room temperature for 3 minutes to dislodge cells from the plate surface. Cultures were maintained at 37˚C and 5% CO_2 throughout routine culture and differentiation protocols.

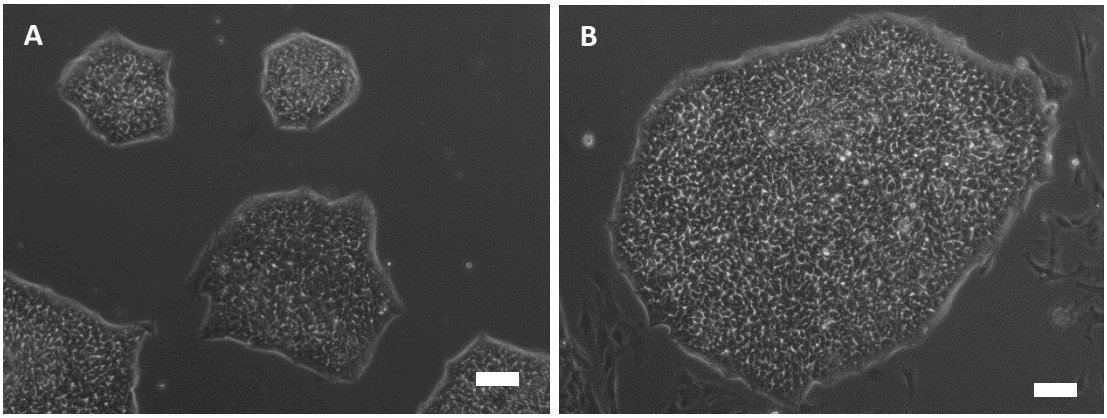

Figure 12 Human induced pluripotent stem cell (hiPSC) colonies maintained in conditions free of animal components Cells were plated on Vitronectin-XF and cultured in TeSR-E8 media. **(A)** Several hiPSC colonies 2 days after plating. **(B)** A single hiPSC colony 6 days after plating and 1 day prior to passaging and neural aggregate formation. Scale bars are 100 μm.

Differentiation protocols: neural aggregates

Adherent colonies were dissociated into single cell suspensions by exposure to marine-origin enzyme Accutase (Life Technologies) for 5 minutes at room temperature and resuspended in Neural Induction Media (NIM). Approximately 2 x 10^6 cells/mL were added to a single well of an AggreWell-800 microwell plate and centrifuged at low speed to collect cells in the microwells and initiate the formation neural aggregates. A ¾ media change was performed every day for 5 days. On the fifth day, neural aggregates were harvested from the AggreWell plate, passed through a 37 μm reversible strainer to remove any unincorporated single cells, and retained for seeding.

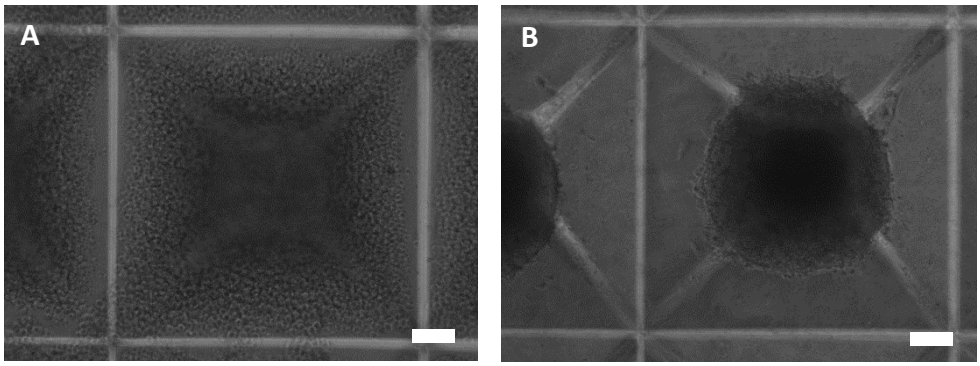

Figure 13 Formation of hiPSC-derived neural aggregates in AggreWell microwell plates. (A) Pluripotent hiPSCs (single cells) collected in a microwell. **(B)** Neural aggregates formed after 5 days. Note that the majority of single cells have been incorporated into a single spherical aggregate. Cells maintained in Neural Induction Media (NIM). Scale bars are 100 μm.

Seeding inside 3D fibrin scaffolds: neural aggregates

Fibrinogen solutions were prepared from lyophilized protein as described in Aim 1. For seeding in fibrin matrices of varying concentrations, neural aggregates were harvested on the fifth day of induction. A series of fibrinogen solutions were prepared yielding 4 mg/mL, 8 mg/mL, 12 mg/mL, and 16 mg/mL fibrin gels. Solutions were polymerized into fibrin in the presence of 40 U/mL thrombin and 50 mM $CaCl_2$ in the wells of a 24-well polystyrene cell culture plate; single neural aggregates were seeded on the surface of

a 300 µL fibrin gel with another 100 µL fibrin gel subsequently polymerized on top. Cell-seeded fibrin gels were incubated for 1 hour before the addition of 1 mL of NIM to each well. Neural aggregates were maintained for 2 weeks before harvesting for flow cytometric analysis or fixed for immunocytochemistry.

Differentiation protocols: neural rosettes and neural progenitor cells

Neural aggregates were harvested from a single well of the AggreWell plate, passed through a 37 µm reversible strainer to remove any unincorporated single cells, and plated in single well of a poly-L-ornithine(PLO)/laminin(Sigma)-coated 6-well tissue culture plate and maintained in NIM for an additional 7 days, for a cumulative 12 days of induction to form neural rosettes, shown in Figure 14C. Daily media changes were performed. On day 12, the rosettes were harvested selectively from the surrounding outgrowth of neural crest cells by exposure to the Neural Rosette Selection Agent (NRSA) and re-plated on PLO/laminin plates in Neural Progenitor Media (NPM). NPCs were then maintained in culture, with passaging approximately every 5 to 7 days at a ratio of 1:12, shown in Figure 15. The timeline of neural induction is shown in

Figure 16.

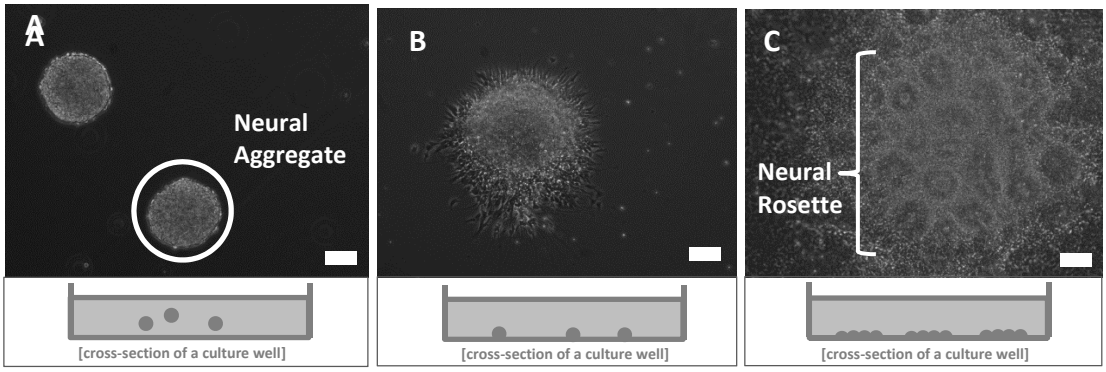

Figure 14 Representative formation of neural rosettes from neural aggregates. (A) Neural aggregates derived from human pluripotent stem cells immediately after harvesting from the AggreWell plate. **(B)** Neural aggregate beginning to spread out 24 hours after seeding on a 2D laminin surface. **(C)** Neural rosette formed after 7 days. Cells maintained in Neural Induction Media (NIM). Scale bars are 100 µm.

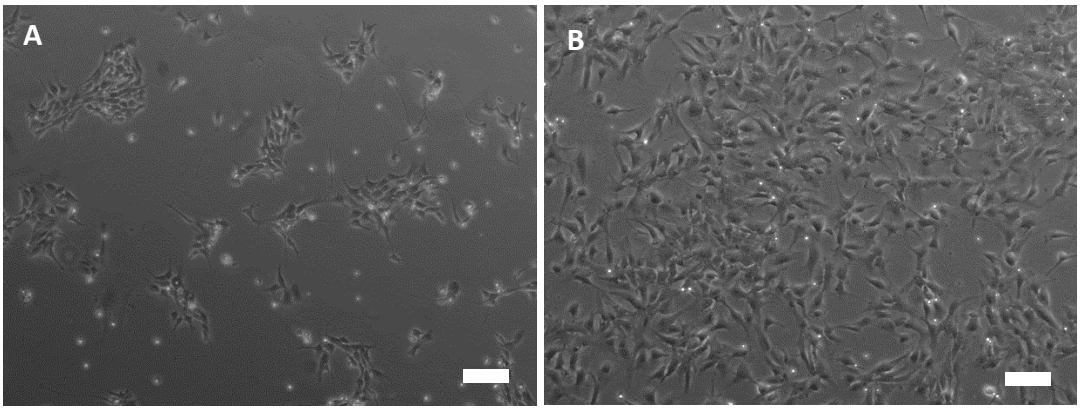

Figure 15 Neural progenitor cells cultured on 2D laminin surface. Neural progenitor cells (NPCs) were harvested from neural rosettes and re-plated on 2D laminin surface and maintained in Neural Progenitor Media (NPM). **(A)** NPCs 1 day after re-plating from neural rosettes. **(B)** NPCs 5 days after re-plating from neural rosettes. Scale bars are 100 μm.

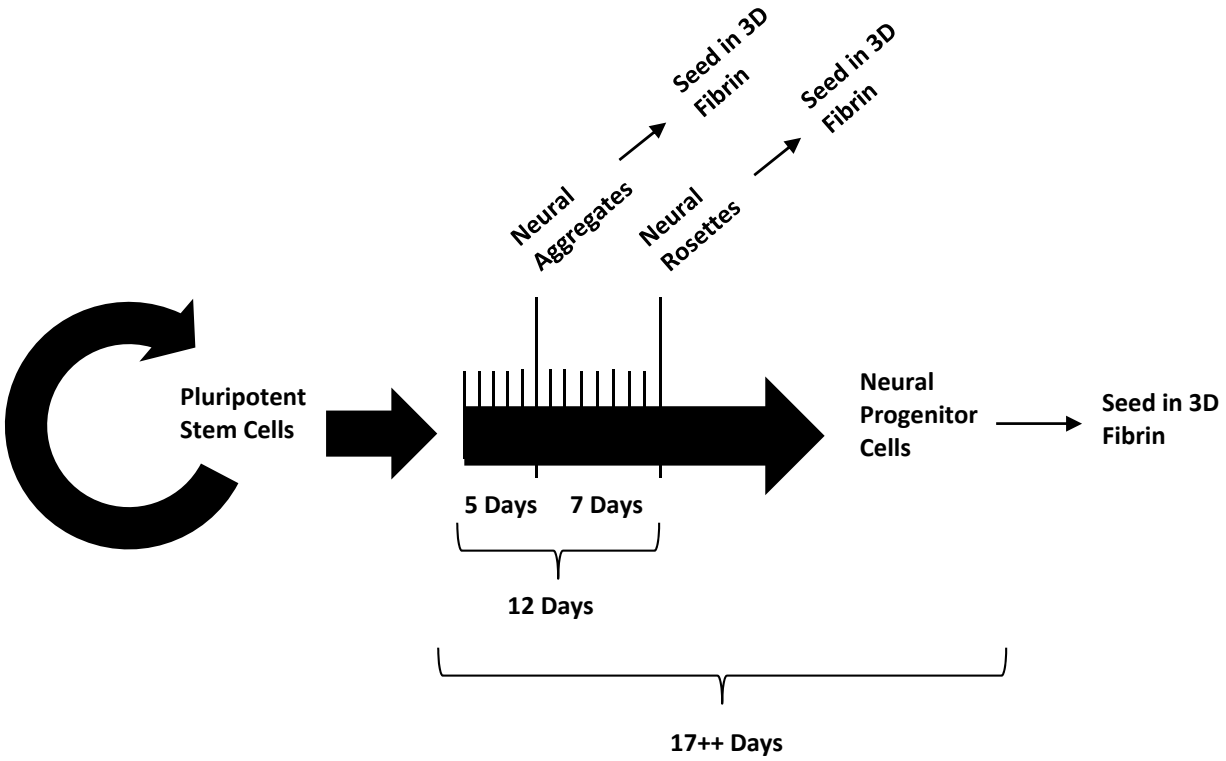

Figure 16 Typical timeline of neural induction oh human pluripotent stem cells. Pluripotent stem cells are maintained at the highest possible level of pluripotency until commencement of differentiation. The differentiation program begins with neural aggregate formation for 5 days followed by 7 more days of adherent neural rosette formation. Neural progenitor cells are derived from re-plated rosettes and maintained as progenitor cells in culture.

Seeding inside 3D fibrin scaffolds: neural rosettes and neural progenitor cells

For seeding in fibrin matrices at different time points in the differentiation program, neural rosettes were harvested on the twelfth overall day of neural induction, and NPCs were harvested after at least one passage after re-plating.

For neural rosettes, a fibrinogen solution was prepared to yield a 10 mg/mL fibrin gel. Fibrinogen was polymerized into fibrin in the presence of 40 U/mL thrombin and 50 mM $CaCl_2$ in the wells of a 24-well polystyrene cell culture plate. Single neural rosettes were seeded on the surface of a 300 μL fibrin gel with another 100 μL fibrin gel subsequently polymerized on top.

NPCs isolated from neural rosettes were seeded as single cells. Single cell suspensions in TBS were combined with the fibrinogen solution to achieve a 10 mg/mL fibrin gel containing approximately 1 x 10^5 cells/mL. The fibrinogen/cell mixture was polymerized into fibrin in the presence of 40 U/mL thrombin and 50 mM $CaCl_2$ in the wells of a 24-well polystyrene cell culture plate.

Fibrin gels containing neural rosettes or NPCs were incubated for 1 hour at 37 ˚C to allow for full polymerization prior to the addition of 1 mL of NIM to each well. Neural aggregates and neural progenitor cells were maintained for 2 weeks before harvesting for analysis. Media was not changed during the culture period.

Chapter 7 Results and Discussion – Aim 2

Viability assessment

Neural aggregates

Neural aggregates derived from hiPSCs after 5 days of neural induction (prior to neural rosette formation) and seeded inside fibrin scaffolds showed high viability after 7 days in all fibrin concentrations, with no qualitative differences in viability evident between the different concentrations, based on LIVE/DEAD® images as shown in Figure 17. This high cell viability is further sustained after 14 days in all fibrin concentrations, with no qualitative differences in viability evident between the different concentrations, based on LIVE/DEAD® images as shown in Figure 18. As shown in Figure 19, no quantitative differences in viability between differentiation protocols or cell lines were measured based on ViaCount flow cytometry-based viability analysis.

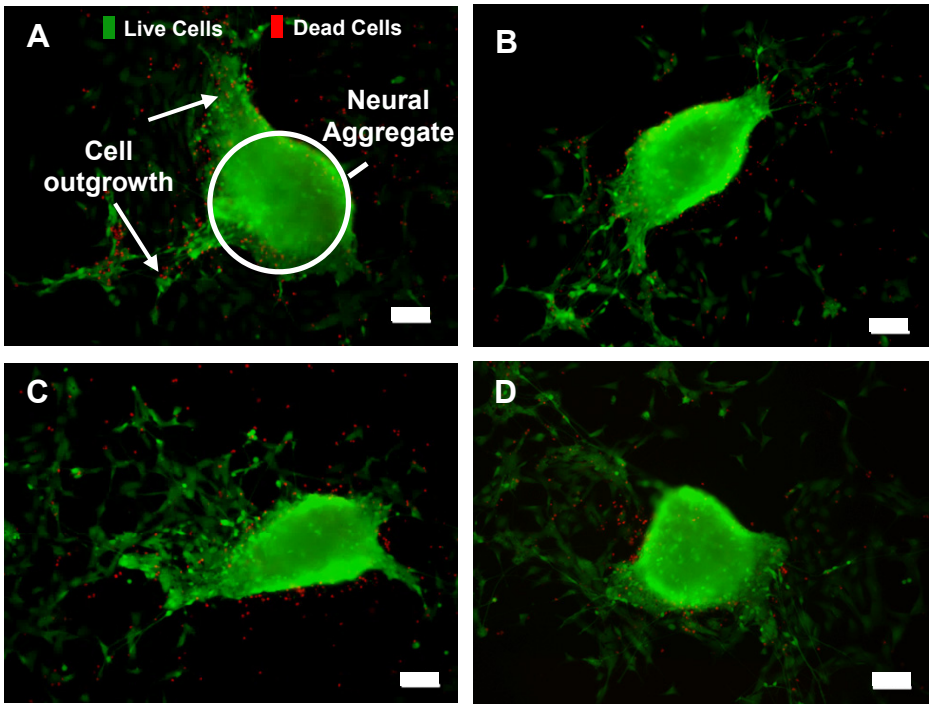

Figure 17 Viability of hiPSC-derived neural aggregates seeded in fibrin after 7 days. Fibrin gels of different concentrations are shown: (A) 16 mg/mL (B) 12 mg/mL (C) 8 mg/mL and (D) 4 mg/mL. Green indicates live cells, red indicates dead cells. Scale bars are 100 μm.

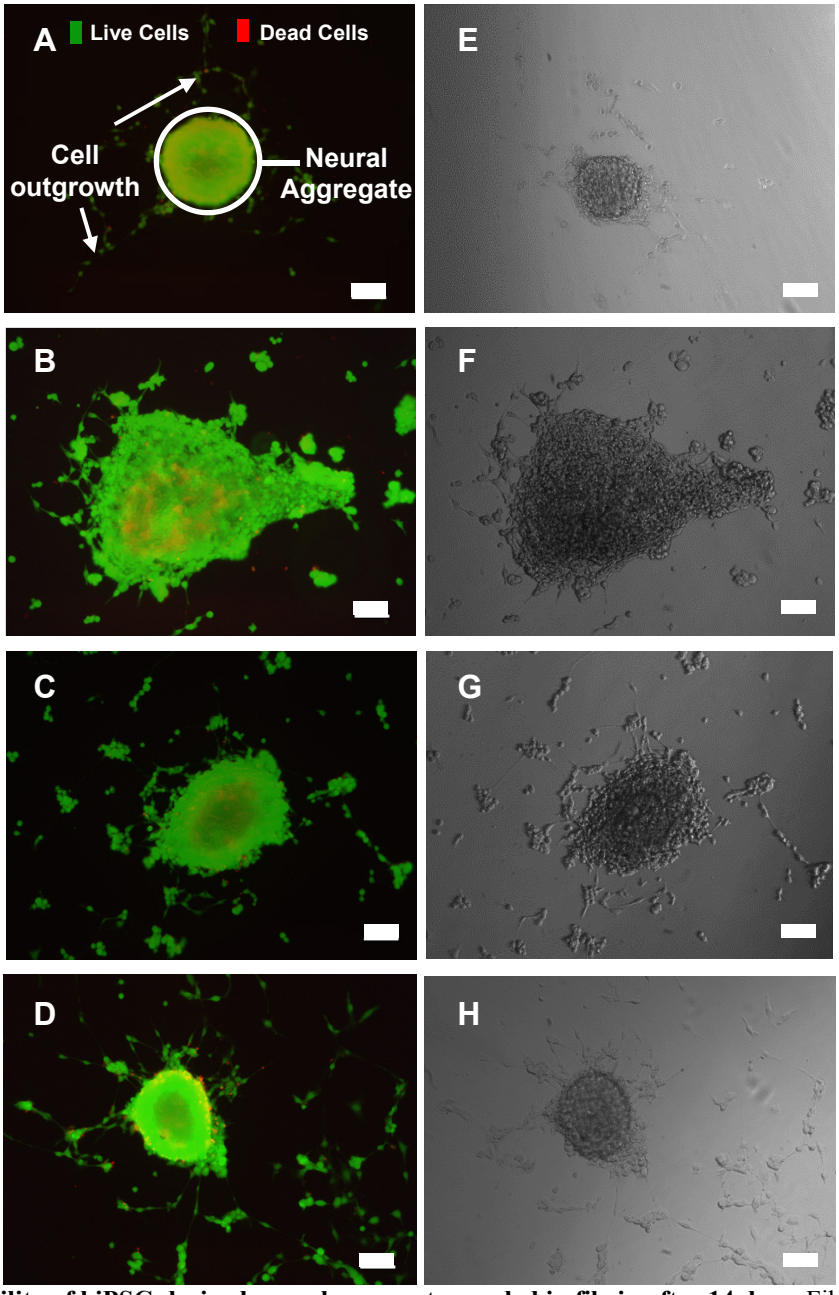

Figure 18 Viability of hiPSC-derived neural aggregates seeded in fibrin after 14 days. Fibrin gels of different concentrations are shown: (A) 16 mg/mL (B) 12 mg/mL (C) 8 mg/mL and (D) 4 mg/mL. Green indicates live cells, red indicates dead cells. Corresponding phase contrast images are shown in (E),(F),(G) and (H) to show neurite extensions which are not as visible in fluorescence. Scale bars are 100 μm.

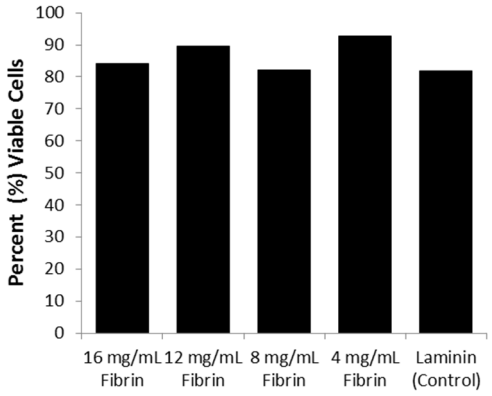

Figure 19 Cell viability at day 14 of seeding inside 3D fibrin scaffolds The percentages of viable cells after 14 days of culture in the four different concentrations fibrin were measured to be greater than 80%. Approximately 1000 events were collected for each sample condition. Sample size n = 1.

Neural rosettes

Neural rosettes seeded inside 10 mg/mL fibrin scaffolds showed high viability after 14 days, based on LIVE/DEAD® images as shown in Figure 20. Morphological assessment revealed that the seeded neural rosettes remained aggregated with little to no cell spreading. This behaviour differs from previously reported behaviour for seeding neural rosettes on 2D laminin surfaces for the expansion of NPCs[59 63 132] but appears similar to suspension culture of neurospheres[59 62 133] or as neural rosettes in suspension[134].

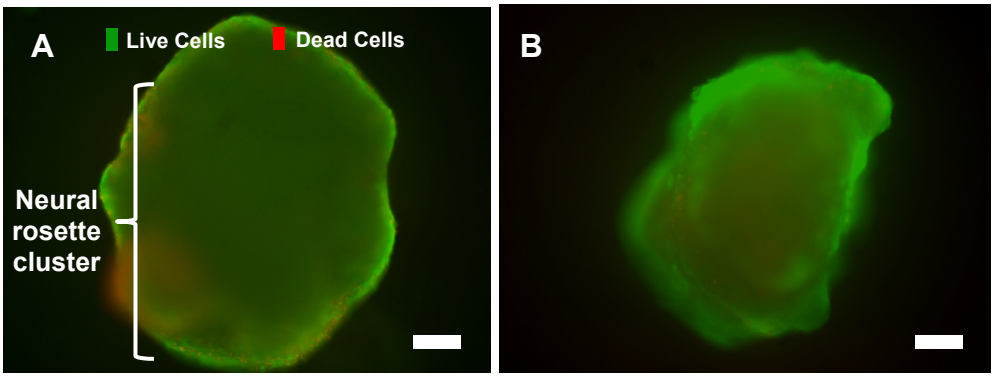

Figure 20 Viability of hiPSC-derived neural rosettes seeded inside 3D fibrin scaffolds for 14 days. Each of (A), (B), (C), and (D) show an hiPSC-derived neural rosette after seeding in fibrin for 14 days. While highly viable, no cell outgrowth was observed from the neural rosettes. Green indicates live cells, red indicates dead cells. Scale bars are 100 µm.

Neural progenitor cells

Neural progenitor cells seeded as single cells inside 10 mg/mL fibrin scaffolds showed high viability after 14 days, based on LIVE/DEAD® images as shown in Figure 21. Similar to the fibrin-seeded neural rosettes, morphological assessment revealed that the seeded NPCs tended to aggregate together with little to no cell spreading. This is in contrast to previous studies of NPCs seeded on 2D laminin[60] or fibronectin[132] surfaces for expansion but appears similar to suspension culture of neurospheres[59 62 133] or as neural rosettes in suspension[134]

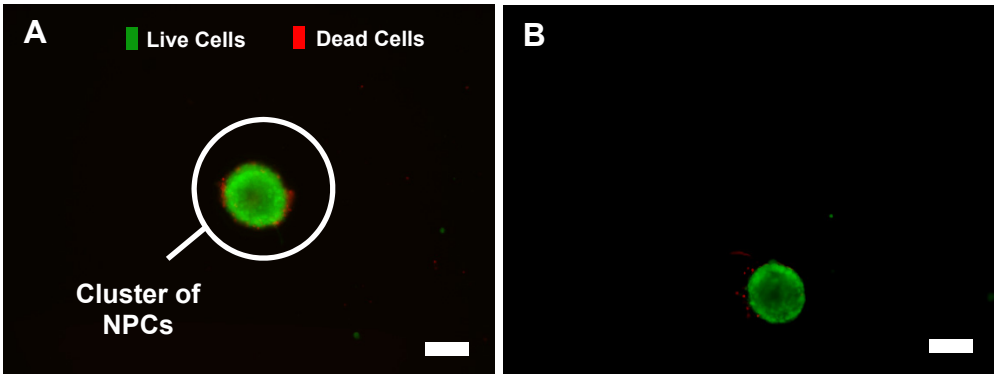

Figure 21 Viability of hiPSC-derived neural progenitor cells (NPCs) seeded inside 3D fibrin scaffolds for 14 days. Both (A), and (B) show a cluster of hiPSC-derived NPCs after seeding in fibrin for 14 days. While highly viable, NPCs, tended to aggregate together with little to no cell outgrowth observed. Green indicates live cells, red indicates dead cells. Scale bars are 100 μm.

Based on the different behaviour exhibited by neural aggregates (5 days induction), neural rosettes (12 days induction), and NPCs (17+ days induction) when seeded in fibrin, there is a need to further investigate the optimal cell seeding time with respect to the human pluripotent stem cell neuronal differentiation program in order to achieve outgrowth of highly viable cells in 3D biomaterial matrices. Given the morphological similarity of fibrin-seeded neural rosettes and NPCs to neurospheres or suspended neural rosette culture, it may be instructive to develop comparisons against these conditions.

Neuronal differentiation assessment

Neural aggregates

Neural aggregates derived from hiPSCs seeded inside 3D fibrin scaffolds after 5 days of neural induction (prior to neural rosette formation) were able to differentiate into neurons, as seen qualitatively in Figure 22 by the cells stained positively for early neuronal marker TUJ1, and quantitatively in Figure 23 by the TUJ1-positive population of cells measured by flow cytometry. These new proof-of-concept results, which indicate that the amount of neurons generated may vary with fibrin concentration, provide confirmation that 3D fibrin scaffolds are a permissible and supportive biomaterial matrix for the differentiation of neurons from hiPSCs. These results must still be strengthened by completing additional replicate trials. At this preliminary stage, however, there is an indication that fibrin matrices may be further tailored for hiPSC applications, similar to previous efforts to optimize these scaffolds for murine stem cells.[72]

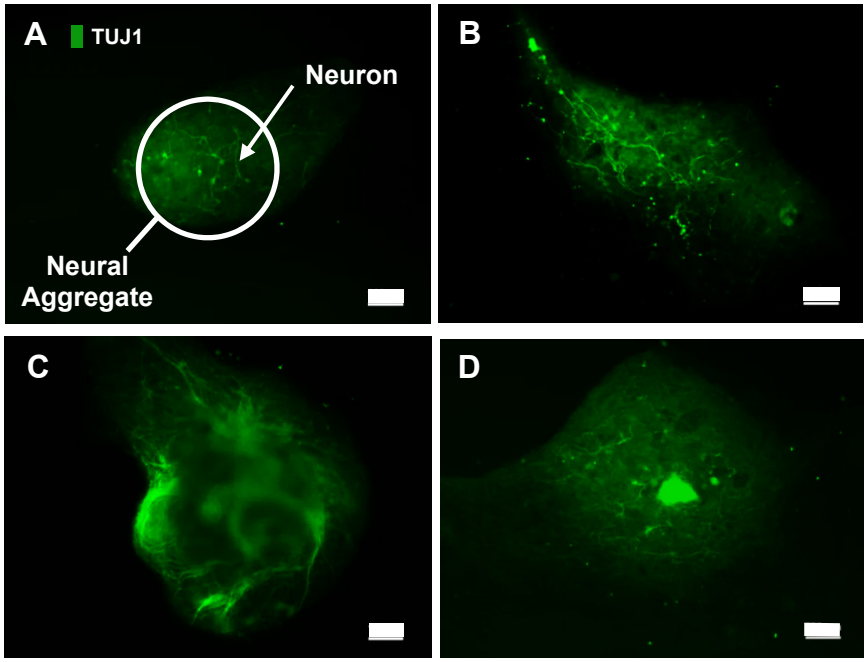

Figure 22 Fluorescent microscopy images showing cells positively stained for early neuronal marker TUJ1 after 14 days of culture in different fibrin concentrations. Fibrin gels of different concentrations are shown: (A) 16 mg/mL (B) 12 mg/mL (C) 8 mg/mL and (D) 4 mg/mL. Scale bars are 100 μm.

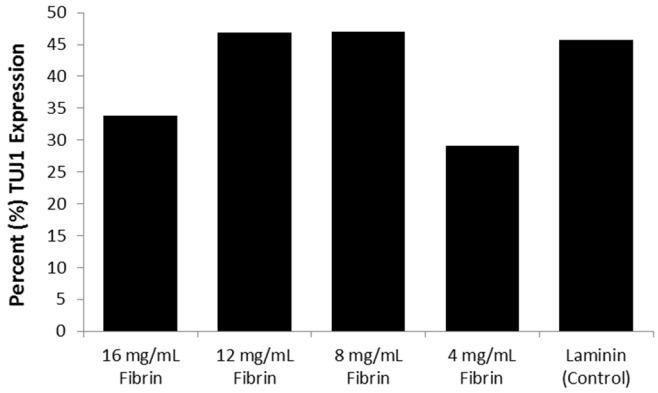

Figure 23 Early neuronal marker TUJ1 expression after 14 days of seeding inside 3D fibrin scaffolds with different fibrin concentrations. Fibrin hydrogels at 16 mg/mL, 12 mg/mL, 8 mg/mL, and 4 mg/mL were seeded with neural aggregates produced by 5 days of neural induction. A 2D laminin-coated surface was used as a control representing previously reported seeding conditions. Approximately 5000 events were collected for each experimental condition in the sample set. Sample size n = 1.

Neural rosettes and neural progenitor cells

Neural rosettes and NPCs derived from hiPSCs seeded inside 3D fibrin scaffolds did not demonstrate a strong ability to differentiate into neurons, as seen qualitatively in Figure 24A and Figure 24B by the cells stained positively for early neuronal marker TUJ1. Although some TUJ1-positive cells are visible, the generation of neuronal phenotypes takes on a different characteristics compared to the typically reported 2D method of NPC expansion which is shown for comparison in Figure 24C. Together with the viability data, these results represent a first exploration of seeding hiPSCs in fibrin at different time points along the neural induction program. Although the neuronal differentiation shown by neural rosettes and neural progenitor cells appears limited in this first assay, it does not necessarily mean that these cells are unable to efficiently yield neurons when seeded in 3D fibrin scaffolds; rather, it suggests that more appropriate conditions for seeding should be pursued, as parameters such as seeding density and fibrin concentration[72] have been shown to influence the differentiation of pluripotent cells.

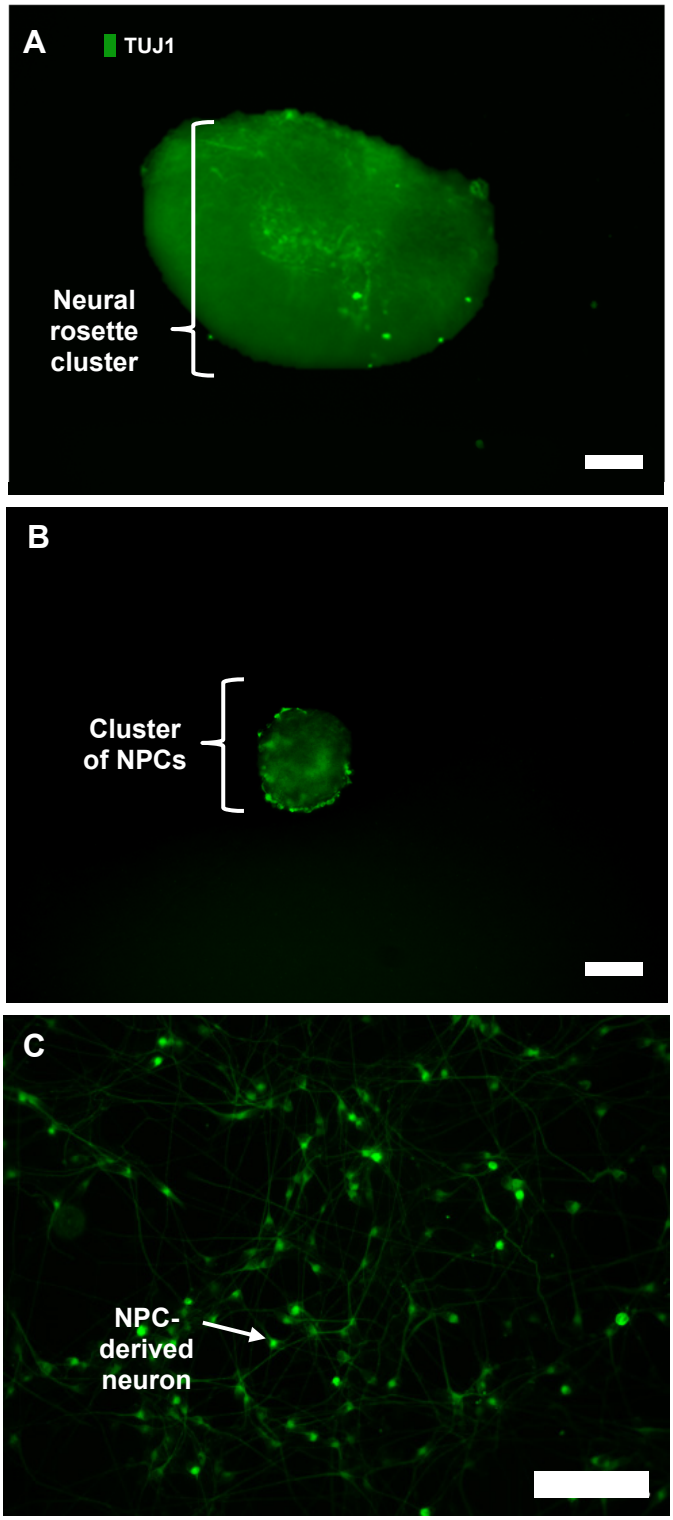

Figure 24 Fluorescent microscopy images of cells positive for early neuronal marker TUJ1 for hiPSC-derived neural rosettes and NPCs seeded in fibrin for 14 days. (A) hiPSC-derived neural rosette seeded in fibrin **(B)** hiPSC-derived NPCs seeded in fibrin. For comparison to 2D protocols, the image in **(C)** shows the same hiPSC-derived NPCs from (B) except when seeded on laminin for 14 days. Scale bars are 100 µm. Note that (A) and (B) are taken at 10X magnification; (C) is taken at 40X magnification.

Chapter 8 Experimental Methods – Aim 3

HSP70 equilibrium release study

Preparation of fibrin gels

Fibrinogen solution was prepared from lyophilized protein as described in Aim 1. The strategically selected peptide, amino acid sequence NQEQVSPKAAKVKGDGTISAITE based on transglutaminase fibrin-binding domain[119] and a sequence with HSP70 binding affinity reported by Grossman et al.,[123] was obtained from a commercial supplier. Prior to preparation of the gels, a 24-well tissue culture plate was incubated at 37 ˚C with 1% bovine serum albumin (BSA; Sigma) solution overnight to block any undesired binding to the plate surface. Fibrin gels were polymerized in 400 μL volumes in the wells of the BSA-blocked 24-well tissue culture plate. Two sets of gels were prepared according to the protocol previously described by Willerth et al.[85]. One set of gels contained 100 ng/mL concentration HSP70 (rat, Enzo) (hereafter referred to as the *HPS70 Only*) and one set contained100 ng/mL concentration peptide and 100 ng/mL concentration HSP70 (hereafter referred to as the *HSP70 +Peptide*) in addition to the base fibrin hydrogel, both polymerized from 10 mg/mL fibrinogen, 40 U/ml thrombin (Sigma), and 50 mM $CaCl_2$. After 1 hour incubation at 37 ˚C to complete polymerization, 400 μL TBS wash was added on top of the gels. The samples were then incubated at 37 ˚C for 48 hours.

Sample collection

Samples were collected as previously described by Willerth et al.[85]. Washes were collected and stored at 2 to 8 ˚C prior to the ELISA. A heparin-based extraction buffer was used to release the HSP70 from the fibrin gels; the buffer was prepared in TBS using 5 % heparin (Sigma), 5% BSA, and 1% Triton-X (Sigma). The fibrin was first physically degraded using a blade to cut each gel into approximately 2 mm by 2 mm pieces.

Degraded gels were then placed in 4 mL of the extraction buffer (1:10 dilution) and incubated at 2 to 8 ˚C for 48 hours while agitated on a plate shaker.

HSP70 ELISA

An ELISA was performed to measure HSP70 concentration in the washes and gel extractions using an R&D Systems DuoSet HSP70 ELISA kit. Briefly, a 96-well ELISA plate was prepared with capture antibody and incubated at room temperature overnight. Any plate surface not covered by capture antibody was then then blocked by incubating with 1% BSA solution at room temperature for 2 hours. Samples and standards were then added and incubated at room temperature for 2 hours. In addition to the standard provided in the ELISA kit (Standard 1), a separate standard was prepared from the same HSP70 solution used to prepare the fibrin gels in order to more precisely match the detection for the specific HSP70 in the equilibrium study (Standard 2). Serial dilutions of the two standards were performed in the extraction buffer. Gel extractions, already diluted 1:10, were added to the plate without further dilution. Washes were diluted 1:10 in extraction buffer immediately prior to sample addition. All samples and standards were prepared in triplicate. The detection antibody was then added and incubated at room temperature for 2 hours. Washes between each step were performed three times with decanting at the end of the third wash. New plate sealer was applied for the incubations between each step. At the final detection stage, substrate solution (H_2O_2 and tetramethylbenzidine) was added and incubated at room temperature for 20 minutes, protected from light. Colour development was halted with stop solution (H_2SO_4) and the optical density of plate was determined using an optical plate reader at 450 nm. A second reading at 540 nm was also taken to account for the plate background.

Determining HSP70 concentration

The sample population included two independent trials, each with 4 samples run in triplicate for the different experimental conditions. Background subtracted optical densities were used. Two standard curves were prepared for each independent trial. Standard 1 was prepared from the standard provided in the ELISA kit and was considered as a control to validate that the ELISA was completed successfully. Standard 2 was prepared from a known concentration of the same HSP70 used in the fibrin gels and was used to determine the relationship between optical density and HSP70 concentration based on the equation of a 5-point linear best fit line.

Statistical analysis

Sample sets for statistical analysis represented the 4 experimental conditions: *HSP70 Only* gel, *HSP70 Only* wash, *HSP70+Peptide* gel, and *HSP70+Peptide* wash. There were 8 samples for each experimental condition, 4 of which were obtained from one independent trial and 4 of which were obtained from another independent trial. Each sample represented the mean value of 3 replicates assayed in the ELISA. In order to determine the applicable statistical tools to be used, sample sets were first tested for normality using the one sample Kolmogorov-Smirnov (K-S) test. Results were determined to a 5% significance level. Sample sets were not found to be normally distributed and therefore significant differences between sample sets were tested using the two sample K-S test and the Kruskal-Wallis (K-W) one-way analysis of variance test, both of which are applicable to data sets which do not have an underlying distribution. Results were determined to a 5% significance level for both tests. Standard deviation (SD) and standard error of the mean (SEM) are reported. All p-values are reported in Supplementary Table 19.

Chapter 9 Results and Discussion – Aim 3

HSP70 concentration

Preparation of standard curve

Preliminary results indicated that the detection of the standard provided in the DuoSet ELISA kit (R&D) was not equivalent to the detection of a standard prepared with the HSP70 (Enzo) used in the equilibrium study. Two standards were therefore prepared for each trial. Standard 1, prepared from a known concentration of the DuoSet ELISA kit standard, was used to verify that the assay was completed successfully while Standard 2, prepared from a known concentration of the HSP70 used in the equilibrium study, was used to create the standard curve for interpolating HSP70 concentration from measured optical densities. Only ELISA trials that produced standard curves with a strong linear relationship ($r^2 > 0.99$) were used for analysis. Standard curves for a typical trial are shown in Figure 25. Figures showing typical colour development and plate layout are provided in Supplementary Table 18.

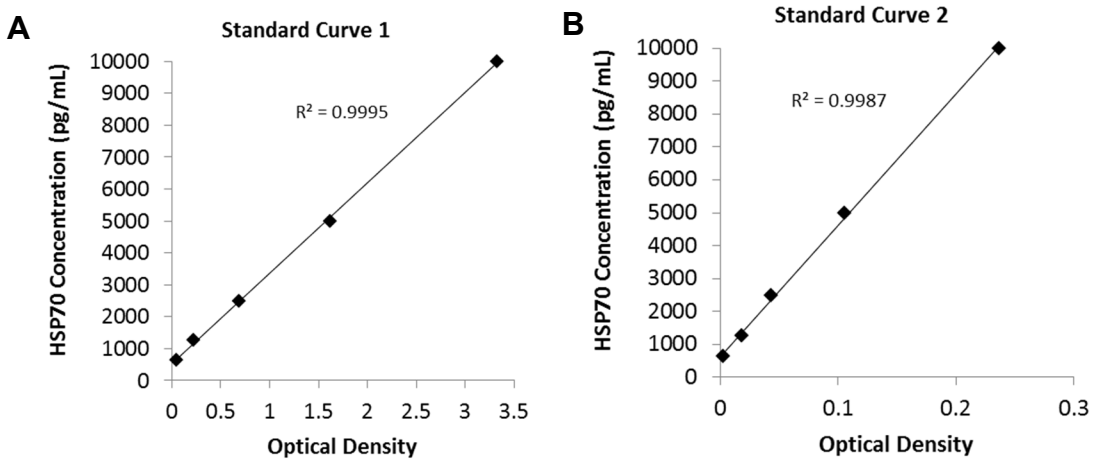

Figure 25 Standard curves prepared for Standard 1 and Standard 2. (A) Standard Curve 1 was prepared from the DuoSet ELISA kit standard. (B) Standard Curve 2 was prepared from the same HSP70 that was used in the equilibrium study. Note the difference in optical density corresponding to HSP70 concentration between the two standard curves. In general, optical density readings over 1 are not reliable.

Equilibrium HSP70 concentrations

The percentage of HSP70 in retained by each gel was calculated by dividing the amount of HSP70 present in the gel and dividing by the amount of HSP70 in both gel and corresponding wash. The *HSP70+Peptide* fibrin gels accounted for 63% ±SD=1% of the measured HSP70 with corresponding *HSP70+Peptide* washes accounting 37%±SD=1%. This difference was determined to be statistically significant ($p<0.01$), providing evidence for the ability of strategically selected peptides to sequester HSP70 in fibrin gels. These results contrast the results for the *HSP70 Only* gels and washes, which showed 49%±SD=2% and 51%±SD=2% respectively, and between which no statistically significant difference was found. Furthermore, the *HSP70+Peptide* gels were determined to have retained significantly more HSP70 than *HSP70 Only* gels. These results are summarized in Figure 26 below.

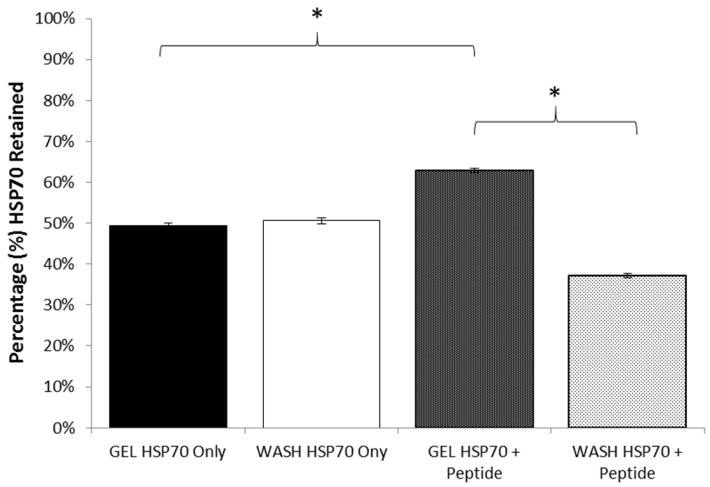

Figure 26 HSP70 retained by fibrin gels with and without the HSP70-binding peptide. HSP70 was incorporated into fibrin gels with and without a strategically selected peptide. The gels (GEL *HSP70 Only* and GEL *HSP70+Peptide*) were covered in an equal volume of saline wash (WASH *HSP70 Only* and WASH *HSP70+Peptide*) and incubated at 37˚C for 48 hours in order for the HSP70 to diffuse by concentration gradient towards equilibrium. The GEL *HSP70+Peptide* (dark grey) accounted for a larger proportion of the total HSP70 compared to the corresponding WASH *HSP70+Peptide* (light grey). The GEL *HSP70+Peptide* also retained a greater proportion of the HSP70 at equilibrium compared to the GEL *HSP70 Only* (black). * indicates $p<0.01$. Sample size n = 8.

Retention of 63% HSP70 in the *HSP70+Peptide* gels is comparable to previous affinity-based drug delivery systems in fibrin using rationally-designed peptides. It was previously shown that NGF-binding peptides cross-linked into fibrin matrices were able to sequester NGF up to 65% in the most effective case.[85] As demonstrated in the NGF study, the equilibrium results forecast the development of an effective drug delivery system, including characterization of a controlled release profile and positive *in vitro* bioactivity. Such studies will be the logical next phase for the investigation of the *HSP70+Peptide* gels. Furthermore, while the peptide sequence AKVKGDGTISAITE has shown an ability to interact with HSP70, other sequences with identified HSP70 binding affinities[121-123] remain to be explored for comparison. Overall, the results of this equilibrium study support the further development of an affinity-based drug delivery system for HSP70 from fibrin using strategically selected fibrin-binding peptides.

Chapter 10 Conclusion

Addressing the problem statement

The broad problem statement framing the development of tissue engineered strategies for spinal cord injury repair is the need to optimize the choice of cells, biomaterial matrix, and delivery systems for neurotrophic factors. The research presented here addresses this problem statement in three specific ways:

Restatement of problem and research aim 1

There are multiple differentiation protocols reported for the generation of neurons from mESCs. These protocols had not yet been compared in terms of their capacity to generate neurons and, furthermore, the capacity to generate neurons has been shown to vary between types of stem cells. As such, it was proposed that the protocols developed and optimized for murine embryonic stem cells be evaluated in applications using murine induced pluripotent stem cells.

As a specific aim, this research sought to evaluate the differentiation efficiency of the 6-day 2-/4+ neural differentiation protocol using retinoic acid and purmorphamine compared to the traditional 8-day 4-/4+ retinoic acid-based protocol using murine induced pluripotent stem cells. Differentiation efficiency was defined as the quantity of neurons generated – specifically, those cells expressing neuronal marker β-III-tubulin (TUJ1) – as a proportion of the total cell population.

It was hypothesized that the 2-/4+ differentiation protocol would have the ability to produce neurons from murine induced pluripotent stem cells with higher efficiency than the 4-/4+ protocol when seeded inside 3D fibrin matrices for 14 days.

Conclusion of problem and research aim 1

The comparison was based on the cell viability as well as the proportion of neurons after 14 days of culture inside 3D fibrin matrices. The results of cell viability analysis revealed no significant differences in the proportion of viable cells between the two differentiation protocols and no significant differences between murine embryonic stem cells and induced pluripotent stem cells. The results of the analysis of neural differentiation revealed that the 2-/4+ protocol was able to generate a higher proportion of neurons than the 4-/4+ protocol in both murine ESCs and iPSCs. For both protocols, it was noted that miPSCs generated a lower proportion of neurons compared to ESCs. These results substantiate the hypothesis of specific aim 1 and support the use of the 2-/4+ protocol as an effective method of generating neurons from miPSCs going forward.

Restatement of problem and research aim 2

Of the biomaterial matrices for tissue engineering, naturally-derived protein-based fibrin matrices have been extensively characterized for neural differentiation using murine embryonic stem cells. However, to increase the clinical relevance of this approach, the existing fibrin-based cell delivery tools should be adapted for human cells, in particular, human induced pluripotent stem cells.

As a specific aim, this research sought to evaluate the ability of fibrin-based matrices to provide functional support of neural progenitor cells derived from human induced pluripotent stem cells in terms of viability and differentiation efficiency. Viability was defined as the proportion of viable cells out of the total cell population. Differentiation efficiency was defined as the proportion of neurons generated – specifically, cells expressing neuronal marker β-III-tubulin (TUJ1) – as a proportion of the total cell population.

It was hypothesized that neural progenitor cells derived from human induced pluripotent stem cells would exhibit high levels of viability when seeded inside 3D fibrin scaffolds for 14 days. It was also hypothesized that neural progenitor cells derived from human induced pluripotent stem cells would differentiate into neurons when seeded inside 3D fibrin scaffolds for 14 days.

Conclusion of problem and research aim 2

The investigation involved seeding of hiPSC-derived neural progenitor cells inside fibrin matrices of varying concentrations and at different time points in the differentiation program. Cell viability was found to be similar for all fibrin gel concentrations, and generally at levels of greater than 80%. It was also found that higher proportion on neurons were generated from aggregates seeded in gels of 8 mg/mL and 12 mg/mL fibrin compared to those seeded in lower concentration at 4 mg/mL and the higher concentration at 16 mg/mL. These results substantiate both hypotheses of specific aim 2 and provide justification for the further investigation of neuronal differentiation of hiPSCs in 3D fibrin matrices.

Restatement of problem and research aim 3

Drug-releasing fibrin matrices have been developed with various therapeutic factors using affinity-based drug delivery systems; however, this had not yet been investigated for heat shock proteins. Heat shock proteins have been shown to play an important role in the regeneration of neurons after spinal cord injury and the exogenous application of heat shock proteins have been shown to have a neuroprotective effect on neural cells in culture. Given the emerging evidence supporting heat shock proteins as a promising

spinal cord injury therapeutic, a new affinity-based drug delivery system for the controlled release of these proteins from fibrin matrices was investigated.

As a specific aim, this research sought to develop an affinity-based drug delivery system for the controlled release of HSP70 from fibrin matrices. In this work, the ability of fibrin matrices modified with HSP70-binding peptide to sequester HSP70 was compared to unmodified fibrin matrices.

It was hypothesized that under equilibrium conditions, fibrin matrices modified with a covalently bound HSP70-affinity peptide would retain more of the loaded HSP70 than unmodified fibrin matrices.

Conclusion of problem and research aim 3

The ability of fibrin matrices with covalently incorporated HSP70-binding peptide to sequester HSP70 was compared to unmodified fibrin matrices. Equilibrium studies revealed that fibrin gels containing a peptide with established affinity for HSP70 were able to retain more HSP70 than unmodified fibrin gels. These results substantiate the hypothesis of specific aim 3 and provide a basis for further developing an affinity-based delivery system of HSP70 from fibrin matrices.

Overall conclusion and future work

This work is representative of an important transition in the field of tissue engineering from the traditional embryonic stem cells to the more recently discovered induced pluripotent stem cells. It contributes to a broad body of existing work across many disciplines that together continues to elucidate many of the underlying mechanisms – both physical and chemical – that regulate stem cell behaviour.

In order to advance toward clinically relevant therapies for spinal cord injury repair, a continued effort must be made to optimize the combination of cells, materials, and drug delivery systems in tissue engineering applications. There are several promising avenues of future research that build upon the proof-of-concept work presented.

One such avenue is the continued investigation of the behaviour of iPSCs with reference to the behaviour previously reported for ESCs in terms of differentiation efficiency. Furthermore, an increased focus on human cell lines, such as investigating the role of retinoic acid and purmorphamine in the development of motor neuron differentiation protocols for hiPSCs,[51 135] will further support the clinical relevance of this work.

Optimization of 3D fibrin scaffolds for the culture of neurons from hiPSC-derived neural precursor and progenitor cells at different stages of development remains an important next step in uncovering the potential of this biomaterial as a delivery tool for human cells. Factors to further investigate include stage of neural differentiation for seeded cells, cell seeding density, and fibrin concentration.

Lastly, continued characterization of affinity-based drug delivery systems in 3D fibrin scaffolds incorporating fibrin-binding peptides with affinity for HSP70 is required. Immediate objectives should include generating a controlled release profile as well as confirming bioactivity of the released protein *in vitro* and *in vivo*. Additional investigation of peptide sequences with demonstrated HSP70 affinity is also recommended to fully explore the range of release characteristics that may be possible for this system.

Bibliography

1. Farry A, Baxter D. Incidence and Prevalence of Spinal Cord Injury in Canada: Overview and estimates based on current evidence. Vancouver: Rick Hansen Institute and Urban Futures Institute, 2010.
2. Norenberg MD, Smith J, Marcillo A. The pathology of human spinal cord injury: Defining the problems. *Journal of neurotrauma* 2004;21(4):429-40.
3. Webb AA, Ngan S, Fowler JD. Spinal cord injury I: A synopsis of the basic science. *The Canadian Veterinary Journal* 2010;51(5):485.
4. Willerth SM, Sakiyama-Elbert SE. Cell therapy for spinal cord regeneration. *Advanced Drug Delivery Reviews* 2008;60(2):263-76.
5. Madigan NN, McMahon S, O'Brien T, Yaszemski MJ, Windebank AJ. Current tissue engineering and novel therapeutic approaches to axonal regeneration following spinal cord injury using polymer scaffolds. *Respiratory Physiology & Neurobiology* 2009;169(2):183-99.
6. Tetzlaff W, Okon EB, Karimi-Abdolrezaee S, Hill CE, Sparling JS, Plemel JR, et al. A Systematic Review of Cellular Transplantation Therapies for Spinal Cord Injury. *Journal of Neurotrauma* 2011;28(8):1611-82.
7. Kubinová Š, Syková E. Biomaterials combined with cell therapy for treatment of spinal cord injury. *Regenerative Medicine* 2012;7(2):207-24.
8. Nakamura M, Tsuji O, Nori S, Toyama Y, Okano H. Cell transplantation for spinal cord injury focusing on iPSCs. *Expert Opinions in Biological Therapy* 2012.
9. Fitch MT, Silver J. CNS injury, glial scars, and inflammation: Inhibitory extracellular matrices and regeneration failure. *Experimental neurology* 2008;209(2):294-301.
10. Morgenstern DA, Asher RA, Fawcett JW. Chondroitin sulphate proteoglycans in the CNS injury response. *Progress in brain research* 2002;137:313-32.
11. Alper J. Geron gets green light for human trial of ES cell-derived product. *Nat Biotech* 2009;27(3):213-14.
12. Keirstead HS, Nistor G, Bernal G, Totoiu M, Cloutier F, Sharp K, et al. Human Embryonic Stem Cell-Derived Oligodendrocyte Progenitor Cell Transplants Remyelinate and Restore Locomotion after Spinal Cord Injury. *The Journal of Neuroscience* 2005;25(19):4694-705.
13. Baker M. Stem-cell pioneer bows out. *Nature* 2011;479(7374):459.
14. Martin GR. Isolation of a pluripotent cell line from early mouse embryos cultured in medium conditioned by teratocarcinoma stem cells. *Proceedings of the National Academy of Sciences* 1981;78(12):7634-38.
15. Evans MJ, Kaufman MH. Establishment in culture of pluripotential cells from mouse embryos. *Nature* 1981;292(5819):154-56.
16. Cole MF, Johnstone SE, Newman JJ, Kagey MH, Young RA. Tcf3 is an integral component of the core regulatory circuitry of embryonic stem cells. *Genes & Development* 2008;22(6):746-55.
17. Chen X, Vega VB, Ng H-H. Transcriptional Regulatory Networks in Embryonic Stem Cells. *Cold Spring Harbor Symposia on Quantitative Biology* 2008;73:203-09.

18. Bongso A, Richards M. History and perspective of stem cell research. *Best Practice & Research Clinical Obstetrics and Gynaecology* 2004;18(6):827-42.
19. Bieberich E, Wang G. Molecular Mechanisms Underlying Pluripotency. 2013.
20. Till JE, McCulloch EA. A direct measurement of the radiation sensitivity of normal mouse bone marrow cells. *Radiation Research Society* 2011;175:145-49.
21. Becker AJ, McCulloch EA, Till JE. Cytological demonstration of the clonal nature of spleen colonies derived from transplanted mouse marrow cells. *Nature (London)* 1963;197:452-4.
22. Evans M. Discovering pluripotency: 30 years of mouse embryonic stem cells. *Nat Rev Mol Cell Biol* 2011;12(10):680-86.
23. Martin GR, Evans MJ. Differentiation of clonal lines of teratocarcinoma cells: formation of embryoid bodies in vitro. *Proceedings of the National Academy of Sciences* 1975;72(4):1441-45.
24. Andrews PW. From teratocarcinomas to embryonic stem cells. *Philosophical Transactions of the Royal Society of London. Series B: Biological Sciences* 2002;357(1420):405-17.
25. Thomson JA, Itskovitz-Eldor J, Shapiro SS, Waknitz MA, Swiergiel JJ, Marshall VS, et al. Embryonic stem cell lines derived from human blastocysts. *Science* 1998;282(5391):1145-7.
26. Takahashi K, Yamanaka S. Induction of pluripotent stem cells from mouse embryonic and adult fibroblast cultures by defined factors. *Cell* 2006;126(4):663-76.
27. Takahashi K, Tanabe K, Ohnuki M, Narita M, Ichisaka T, Tomoda K, et al. Induction of pluripotent stem cells from adult human fibroblasts by defined factors. *Cell* 2007;131(5):861-72.
28. Yu J, Vodyanik MA, Smuga-Otto K, Antosiewicz-Bourget J, Frane JL, Tian S, et al. Induced pluripotent stem cell lines derived from human somatic cells. *Science* 2007;Scienceexpress Report:1-4.
29. Yamanaka S. Induced pluripotent stem cells: past, present, and future. *Cell Stem Cell* 2012;10:678-84.
30. Kim K, Doi A, Wen B, Ng K, Zhao R, Cahan P, et al. Epigenetic memory in induced pluripotent stem cells. *Nature* 2010;467(7313):285-90.
31. Rais Y, Zviran A, Geula S, Gafni O, Chomsky E, Viukov S, et al. Deterministic direct reprogramming of somatic cells to pluripotency. *Nature* 2013;502(7469):65-70.
32. Downing TL, Soto J, Morez C, Houssin T, Fritz A, Yuan F, et al. Biophysical regulation of epigenetic state and cell reprogramming. *Nat Mater* 2013;12(12):1154-62.
33. Okita K, Nakagawa M, Hyenjong H, Ichisaka T, Yamanaka S. Generation of Mouse Induced Pluripotent Stem Cells Without Viral Vectors. *Science* 2008;322(5903):949-53.
34. Miura K, Okada Y, Aoi T, Okada A, Takahashi K, Okita K, et al. Variation in the safety of induced pluripotent stem cell lines. *Nat Biotech* 2009;27(8):743-45.
35. Tsuji O, Miura K, Okada Y, Fujiyoshi K, Mukaino M, Nagoshi N, et al. Therapeutic potentiall of appropriately evaluate safe-induved pluripotent stem cells for spinal cord injury. *Proceedings of the National Academy of Science* 2010;107(28):12704-09.

36. Temple S. Division and differentiation of isolated CNS blast cells in microculture. *Nature* 1989;340(6233):471-3.
37. Reynolds BA, Weiss S. Generation of neurons and astrocytes from isolated cells of the adult mammalian central nervous system. *Science* 1992;255(5052):1707-10.
38. Weiss S, Dunne C, Hewson J, Wohl C, Wheatley M, Peterson AC, et al. Multipotent CNS Stem Cells Are Present in the Adult Mammalian Spinal Cord and Ventricular Neuroaxis. *The Journal of Neuroscience* 1996;16(23):7599-609.
39. Tachibana M, Amato P, Sparman M, Gutierrez Nuria M, Tippner-Hedges R, Ma H, et al. Human Embryonic Stem Cells Derived by Somatic Cell Nuclear Transfer. *Cell* 2013;153(6):1228-38.
40. Cao Q, Xu X-M, DeVries WH, Enzmann GU, Ping P, Tsoulfas P, et al. Functional Recovery in Traumatic Spinal Cord Injury after Transplantation of Multineurotrophin-Expressing Glial-Restricted Precursor Cells. *The Journal of Neuroscience* 2005;25(30):6947-57.
41. Faulkner JR, Herrmann JE, Woo MJ, Tansey KE, Doan NB, Sofroniew MV. Reactive astrocytes protect tissue and preserve function after spinal cord injury. *The Journal of Neuroscience* 2004;24(9):2143-55.
42. Wosnick JH, Baumann MD, Shoichet MS. 73 - Tissue Therapy: Central Nervous System. *Principles of Regenerative Medicine*. San Diego: Academic Press, 2008:1248-69.
43. Bain G, Kitchens D, Yao M, Huettner JE, Gottlieb DI. Embryonic stem cells express neuronal properties in vitro. *Developmental Biology* 1995;168(2):11307-12.
44. Rhinn M, Dollé P. Retinoic acid signalling during development. *Development* 2012;139(5):843-58.
45. Maden M. Retinoic acid in the development, regeneration and maintenance of the nervous system. *Nature Reviews Neuroscience* 2007;8:755-65.
46. Briscoe J, Ericson J. The specification of neuronal identity by graded sonic hedgehog signalling. *Seminars in Cell & Developmental Biology* 1999;10(3):353-62.
47. Jessell TM. Neuronal specification in the spinal cord: inductive signals and transcriptional codes. *Nature Reviews Genetics* 2000;1(1):20-29.
48. Ericson J, Rashbass P, Schedl A, Brenner-Morton S, Kawakami A, van Heyningen V, et al. Pax6 Controls Progenitor Cell Identity and Neuronal Fate in Response to Graded Shh Signaling. *Cell* 1997;90(1):169-80.
49. Crompton T, Outram SV, Hager-Theodorides AL. Sonic hedgehog signalling in T-cell development and activation. *Nat Rev Immunol* 2007;7(9):726-35.
50. Wichterle H, Lieberam I, Porter JA, Jessel TM. Directed differentiation of embryonic stem cells into motor neurons. *Cell* 2002;110:385-97.
51. Li X-J, Hu B-Y, Jones SA, Zhang Y-S, Vaute TL, Du Z-W, et al. Directed differentiation of ventral spinal progenitors and motor neurons from human embryonic stem cells by small molecules. *Stem Cells* 2008;26:886-93.
52. Briscoe J. Agonizing hedgehog. *Nature Chemical Biology* 2006;2(1):10-11.
53. El-Akabawy G, Medina LM, Jeffries A, Price J, Modo M. Purmorphamine increases DARPP-32 differentiation in human striatal neural stem cells through the hedgehog pathway. *Stem Cells and Development* 2011;20(1):1873-87.
54. Pellet S, Du Z-w, Pier CL, Tepp WH, Zhang S-c, Eric A J. Sensitive and quantitative detection of botulinum neurotoxin in neurons derviced from mouse embryonic

stem cells. *Biochemical and Biophysical Research Communications* 2011;404(1):388-92.
55. McCreedy DA, Rieger CR, Gottlieb DI, Sakiyama-Elbert SE. Transgenic enrichment of mouse embryonic stem cell-derived progenitor motor neurons. *Stem Cell Research* 2012;8:368-78.
56. Itskovitz-Eldor J, Schuldiner M, Karsenti D, Eden A, Yanuka O, Amit M, et al. Differentiation of human embryonic stem cells into embryoid bodies comprising the three embryonic germ layers. *MOLECULAR MEDICINE-CAMBRIDGE MA THEN NEW YORK-* 2000;6(2):88-95.
57. Höpfl G, Gassmann M, Desbaillets I. Differentiating embryonic stem cells into embryoid bodies. *Germ Cell Protocols*: Springer, 2004:79-98.
58. Trounson A. The production and directed differentiation of human embryonic stem cells. *Endocrine reviews* 2006;27(2):208-19.
59. Wilson P, Stice S. Development and differentiation of neural rosettes derived from human embryonic stem cells. *Stem Cell Rev* 2006;2(1):67-77.
60. Elkabetz Y, Panagiotakos G, Al Shamy G, Socci ND, Tabar V, Studer L. Human ES cell-derived neural rosettes reveal a functionally distinct early neural stem cell stage. *Genes & Development* 2008;22(2):152-65.
61. Conti L, Cattaneo E. Neural stem cell systems: physiological players or in vitro entities? *Nature Reviews Neuroscience* 2010;11(3):176-87.
62. Zhang S-C, Wernig M, Duncan ID, Brüstle O, Thomson JA. In vitro differentiation of transplantable neural precursors from human embryonic stem cells. *Nature biotechnology* 2001;19(12):1129-33.
63. Schwartz PH, Brick DJ, Stover AE, Loring JF, Müller F-J. Differentiation of neural lineage cells from human pluripotent stem cells. *Methods* 2008;45(2):142-58.
64. Luckenbill-Edds L. Laminin and the mechanism of neuronal outgrowth. *Brain Research Reviews* 1997;23(1–2):1-27.
65. Reilly GC, Engler AJ. Intrinsic extracellular matrix properties regulate stem cell differentiation. *Journal of Biomechanics* 2010;43(1):55-62.
66. Murry CE, Keller G. Differentiation of Embryonic Stem Cells to Clinically Relevant Populations: Lessons from Embryonic Development. *Cell* 2008;132(4):661-80.
67. Doolittle RF. Fibrinogen and Fibrin. *eLS*: John Wiley & Sons, Ltd, 2001.
68. Ahmed TA, Dare EV, Hincke M. Fibrin: a versatile scaffold for tissue engineering applications. *Tissue Engineering Part B: Reviews* 2008;14(2):199-215.
69. King VR, Alovskaya A, Wei DY, Brown RA, Priestley JV. The use of injectable forms of fibrin and fibronectin to support axonal ingrowth after spinal cord injury. *Biomaterials* 2010;31(15):4447-56.
70. Pettersson J, Kalbermatten D, McGrath A, Novikova LN. Biodegradable fibrin conduit promotes long-term regeneration after peripheral nerve injury in adult rats. *Journal of Plastic, Reconstructive & Aesthetic Surgery* 2010;63(11):1893-99.
71. Pettersson J, McGrath A, Kalbermatten DF, Novikova LN, Wiberg M, Kingham PJ, et al. Muscle recovery after repair of short and long peripheral nerve gaps using fibrin conduits. *Neuroscience Letters* 2011;500(1):41-46.
72. Willerth SM, Arendas KJ, Gottlieb DI, Sakiyama-Elbert SE. Optimization of fibrin scaffolds for differentiation of murine embryonic stem cells into neural lineage cells. *Biomaterials* 2006;27(36):5990-6003.

73. Kolehmainen K, Willerth SM. Preparation of 3D fibrin scaffolds for stem cell culture applications. *J Vis Exp* 2012;2(61).
74. Mahoney MJ, Saltzman WM. Controlled release of proteins to tissue transplants for the treatment of neurodegenerative disorders. *J Pharm Sci* 1996;85(12):1276-81.
75. Cao XD, Shoichet MS. Delivering neuroactive molecules from biodegradable microspheres for application in central nervous system disorders. *Biomaterials* 1999;20(4):329-39.
76. Chen FM, An Y, Zhang R, Zhang M. New insights into and novel applications of release technology for periodontal reconstructive therapies. *J Control Release* 2011;149(2):92-110.
77. Anand P. Neurotrophic factors and their receptors in human sensory neuropathies. 2004;146:477-92.
78. Bensadoun J-C, Pereira de Almeida L, Fine EG, Tseng JL, Déglon N, Aebischer P. Comparative study of GDNF delivery systems for the CNS: polymer rods, encapsulated cells, and lentiviral vectors. *Journal of Controlled Release* 2003;87(1-3):107-15.
79. Johnson PJ, Parker SR, Sakiyama-Elbert SE. Controlled release of neurotrophin-3 from fibrin-based tissue engineering scaffolds enhances neural fiber sprouting following subacute spinal cord injury. *Biotechnol Bioeng* 2009;104(6):1207-14.
80. Johnson PJ, Tatara A, Shiu A, Sakiyama-Elbert SE. Controlled release of neurotrophin-3 and platelet-derived growth factor from fibrin scaffolds containing neural progenitor cells enhances survival and differentiation into neurons in a subacute model of SCI. *Cell Transplant* 2010;19(1):89-101.
81. Maxwell DJ, Hicks BC, Parsons S, Sakiyama-Elbert SE. Development of rationally designed affinity-based drug delivery systems. *Acta Biomater* 2005;1(1):101-13.
82. Sakiyama-Elbert SE, Hubbell JA. Controlled release of nerve growth factor from a heparin-containing fibrin-based cell ingrowth matrix. *Journal of Controlled Release* 2000;69(1):149-58.
83. Taylor SJ, McDonald JW, 3rd, Sakiyama-Elbert SE. Controlled release of neurotrophin-3 from fibrin gels for spinal cord injury. *J Control Release* 2004;98(2):281-94.
84. Taylor SJ, Sakiyama-Elbert SE. Effect of controlled delivery of neurotrophin-3 from fibrin on spinal cord injury in a long term model. *J Control Release* 2006;116(2):204-10.
85. Willerth SM, Johnson PJ, Maxwell DJ, Parsons SR, Doukas ME, Sakiyama-Elbert SE. Rationally designed peptides for controlled release of nerve growth factor from fibrin matrices. *Journal of Biomedical Materials Research Part A* 2007;80A(1):13-23.
86. Willerth SM, Rader A, Sakiyama-Elbert SE. The effect of controlled growth factor delivery on embryonic stem cell differentiation inside fibrin scaffolds. *Stem Cell Res* 2008;1(3):205-18.
87. Wood MD, Borschel GH, Sakiyama-Elbert SE. Controlled release of glial-derived neurotrophic factor from fibrin matrices containing an affinity-based delivery system. *Journal of Biomedical Materials Research Part A* 2009;89A(4):909-18.

88. Willerth SM, Faxel TE, Gottlieb DI, Sakiyama-Elbert SE. The effects of soluble growth factors on embryonic stem cell differentiation inside of fibrin scaffolds. *Stem Cells* 2007;25(9):2235-44.
89. Edelman ER, Mathiowitz E, Langer R, Klagsbrun M. Controlled and Modulated Release of Basic Fibroblast Growth-Factor. *Biomaterials* 1991;12(7):619-26.
90. Shimoke K, Chiba H. Nerve growth factor prevents 1-methyl-4-phenyl-1,2,3,6-tetrahydropyridine-induced cell death via the Akt pathway by suppressing caspase-3-like activity using PC12 cells: Relevance to therapeutical application for Parkinson's disease. *Journal of Neuroscience Research* 2001;63(5):402-09.
91. Kerkhoff H, Jennekens FGI. Peripheral-Nerve Lesions - the Neuropharmacological Outlook. *Clinical Neurology and Neurosurgery* 1993;95:S103-S08.
92. Moore AM, Wood MD, Chenard K, Hunter DA, Mackinnon SE, Sakiyama-Elbert SE, et al. Controlled delivery of glial cell line-derived neurotrophic factor enhances motor nerve regeneration. *J Hand Surg Am* 2010;35(12):2008-17.
93. Grondin R, Gash DM. Glial cell line-derived neurotrophic factor (GDNF): a drug candidate for the treatment of Parkinson's disease. *Journal of Neurology* 1998;245:P35-P42.
94. Lee AC, Yu VM, Lowe JB, 3rd, Brenner MJ, Hunter DA, Mackinnon SE, et al. Controlled release of nerve growth factor enhances sciatic nerve regeneration. *Exp Neurol* 2003;184(1):295-303.
95. Zeng L, Worseg A, Redl H, Schlag G. Peripheral nerve repair with nerve growth factor and fibrin matrix. *European journal of plastic surgery* 1994;17(5).
96. Chunzheng G, Shengzhong M, Yinglian J, Ji-e W, Jianmin L. Siatic nerve regeneration in rats stimulated by fibrin glue containing nerve growth factor: An experimental study. *Injury* 2008;39(12):1414-20.
97. Johnson PJ, Tatara A, McCreedy DA, Shiu A, Sakiyama-Elbert SE. Tissue-engineered fibrin scaffolds containing neural progenitors enhance functional recovery in a subacute model of SCI. *Soft Matter* 2010;6(20):5127-37.
98. Lu P, Wang Y, Graham L, McHale K, Gao M, Wu D, et al. Long-distance growth and connectivity of neural stem cells after severe spinal cord injury. *Cell* 2012;150(6):1264-73.
99. Macario AJ, Macario ECd. Sick chaperones, cellular stress, and disease. *New England Journal of Medicine* 2005;353(14):485-501.
100. Richter K, Haslbeck M, Buchner J. The heat shock response: life on the verge of death. *Mol Cell* 2010;40(2):253-66.
101. Henderson B. Integrating the cell stress response: a new view of molecular chaperones as immunological and physiological homeostatic regulators. *Cell Biochem Funct* 2010;28(1):1-14.
102. Van Roon J, van Eden W, Van Roy J, Lafeber F, Bijlsma J. Stimulation of suppressive T cell responses by human but not bacterial 60-kD heat-shock protein in synovial fluid of patients with rheumatoid arthritis. *Journal of Clinical Investigation* 1997;100(2):459.
103. Vanags D, Williams B, Johnson B, Hall S, Nash P, Taylor A, et al. Therapeutic efficacy and safety of chaperonin 10 in patients with rheumatoid arthritis: a double-blind randomised trial. *The Lancet* 2006;368(9538):855-63.

104. Tytell M. Release of heat shock proteins (Hsps) and the effects of extracellular Hsps on neural cells and tissues. *International journal of hyperthermia* 2005;21(5):445-55.
105. Tidwell JL, Houenou LJ, Tytell M. Administration of Hsp70 in vivo inhibits motor and sensory neuron degeneration. *Cell stress & chaperones* 2004;9(1):88.
106. Franklin T, Krueger-Naug A, Clarke D, Arrigo A-P, Currie R. The role of heat shock proteins Hsp70 and Hsp27 in cellular protection of the central nervous system. *International journal of hyperthermia* 2005;21(5):379-92.
107. Sõti C, Nagy E, Giricz Z, Vígh L, Csermely P, Ferdinandy P. Heat shock proteins as emerging therapeutic targets. *British journal of pharmacology* 2005;146(6):769-80.
108. Korochkin L, Revishchin A, Okhotin V. Neural stem cells and their role in recovery processes in the nervous system. *Neuroscience and behavioral physiology* 2006;36(5):499-512.
109. Reddy SJ, La Marca F, Park P. The role of heat shock proteins in spinal cord injury: Review article. *Neurosurgical focus* 2008;25(5):E4.
110. Robinson MB, Tidwell JL, Gould T, Taylor AR, Newbern JM, Graves J, et al. Extracellular heat shock protein 70: a critical component for motoneuron survival. *The Journal of Neuroscience* 2005;25(42):9735-45.
111. Lai Y, Du L, Dunsmore KE, Jenkins LW, Wong HR, Clark RS. Selectively increasing inducible heat shock protein 70 via TAT-protein transduction protects neurons from nitrosative stress and excitotoxicity. *Journal of Neurochemistry* 2005;94(2):360-66.
112. Prinsloo E, Setati MM, Longshaw VM, Blatch GL. Chaperoning stem cells: a role for heat shock proteins in the modulation of stem cell self-renewal and differentiation? *Bioessays* 2009;31(4):370-77.
113. Frebel K, Wiese S. Signalling molecules essential for neuronal survival and differentiation. *Biochemical Society Transactions* 2006;34(6):1287-90.
114. Kurosawa S, Hashimoto E, Ukai W, Toki S, Saito S, Saito T. Olanzapine potentiates neuronal survival and neural stem cell differentiation: regulation of endoplasmic reticulum stress response proteins. *Journal of neural transmission* 2007;114(9):1121-28.
115. Walsh D, Li Z, Wu Y, Nagata K. Heat shock and the role of the HSPs during neural plate induction in early mammalian CNS and brain development. *Cellular and Molecular Life Sciences CMLS* 1997;53(2):198-211.
116. Yang J, Oza J, Bridges K, Chen KY, Liu AY-C. Neural differentiation and the attenuated heat shock response. *Brain research* 2008;1203:39-50.
117. Luna E, Postol E, Caldas C, Benvenuti L, Rodrigues J, Lima K, et al. Treatment with encapsulated Hsp60 peptide (p277) prolongs skin graft survival in a murine model of minor antigen disparity. *Scandinavian journal of immunology* 2007;66(1):62-70.
118. Lee J, Tan CY, Lee S-K, Kim Y-H, Lee KY. Controlled delivery of heat shock protein using an injectable microsphere/hydrogel combination system for the treatment of myocardial infarction. *Journal of Controlled Release* 2009;137(3):196-202.

119. Schense JC, Hubbell JA. Cross-linking exogenous bifunctional peptides into fibrin gels with factor XIIIa. *Bioconjugate Chemistry* 1999;10(1):75-81.
120. Flynn GC, Pohl J, M.T. F, J.E. R. Peptide-binding specificity of the molecular chaperone BiP. *Nature* 1991;353(6346):726-30.
121. Lam KT, Calderwood SK. hsp70 binds specifically to a peptide derived from the highly conserved domain (I) region of p53. *Biochemical and Biophysical Research Communications* 1992;184(1):167-74.
122. Becker T, Hartl F-U, Wieland F. CD40, an extracellular receptor for binding and uptake of Hsp70–peptide complexes. *The Journal of cell biology* 2002;158(7):1277-85.
123. Grossmann ME, Madden BJ, Gao F, Pang Y-P, Carpenter JE, McCormick D, et al. Proteomics shows Hsp70 does not bind peptide sequences indiscriminately in vivo. *Experimental Cell Research* 2004;297(1):108-17.
124. Hubbell JA. Biomaterials in Tissue Engineering. *Nat Biotech* 1995;13(6):565-76.
125. Dawson E, Mapili G, Erickson K, Taqvi S, Roy K. Biomaterials for stem cell differentiation. *Advanced Drug Delivery Reviews* 2008;60(2):215-28.
126. Mohtaram NK, Montgomery A, Willerth SM. Biomaterial-based drug delivery systems for the controlled release of neurotrophic factors. *Biomedical Materials* 2013;8(2):022001.
127. Nagy A, Rossant J, Nagy R, Abramow-Newerly W, Roder JC. Derivation of completely cell culture-derived mice from early-passage embryonic stem cells. *Proceedings of the National Academy of Science* 1993;90:8424-28.
128. Kolemainen K, Willerth SM. Preparation of 3D fibrin scaffolds for stem cell culture applications. *Journal of Visualized Experiments* 2012;61:e3641.
129. Hu B-Y, Weick JP, Yu J, Ma L-X, Zhang X-Q, Thomson JA, et al. Neural differentiation of human induced pluripotent stem cells follows developmental principles but with variable potency. *Proceedings of the National Academy of Sciences* 2010;107(9):4335-40.
130. Dahlstrand J, Lardelli M, Lendahl U. Nestin mRNA expression correlates with the central nervous system progenitor cell state in many, but not all, regions of developing central nervous system. *Developmental Brain Research* 1995;84(1):109-29.
131. Wegner M, Stolt CC. From stem cells to neurons and glia: a Soxist's view of neural development. *Trends in Neurosciences* 2005;28(11):583-88.
132. Carpenter MK, Inokuma MS, Denham J, Mujtaba T, Chiu C-P, Rao MS. Enrichment of Neurons and Neural Precursors from Human Embryonic Stem Cells. *Experimental neurology* 2001;172(2):383-97.
133. Reubinoff BE, Itsykson P, Turetsky T, Pera MF, Reinhartz E, Itzik A, et al. Neural progenitors from human embryonic stem cells. *Nat Biotech* 2001;19(12):1134-40.
134. Bajpai R, Coppola G, Kaul M, Talantova M, Cimadamore F, Nilbratt M, et al. Molecular stages of rapid and uniform neuralization of human embryonic stem cells. *Cell Death Differ* 2009;16(6):807-25.
135. Karumbayaram S, Novitch BG, Patterson M, Umbach JA, Richter L, Lindgren A, et al. Directed Differentiation of Human-Induced Pluripotent Stem Cells Generates Active Motor Neurons. *Stem Cells* 2009;27(4):806-11.

Supplementary Data

Supplementary Table 3

Summary of quantitative viability data at Day 1, Day 7, and Day 14 of seeding inside fibrin scaffolds.

	Day 1		Day 7		Day 14	
	Mean (%)	**SD (%)**	**Mean (%)**	**SD (%)**	**Mean (%)**	**SD (%)**
miPSC 4-/4+	92	1	88	1	89	7
miPSC 2-/4+	89	2	86	1	90	10
mESC 4-/4+	89	5	89	1	91	10
mESC 2-/4+	87	3	86	3	89	10

Supplementary Table 4

Results from significance test comparing cell viability between differentiation protocols and cell types.

Comparison			K-S p-value
miPSC 2-/4+	vs	miPSC 4-/4+	0.3180
mESC 2-/4+	vs	mESC 4-/4+	1.0000
miPSC 4-/4+	vs	mESC 4-/4+	0.8096
miPSC 2-/4+	vs	mESC 2-/4+	1.0000

Supplementary Table 5

Results from significance test comparing cell viability between differentiation protocols and cell types.

Comparison			K-S p-value
miPSC 4-/4+			
Day 1	vs	Day 7	0.0970
Day 1	vs	Day 14	0.8438
Day 7	vs	Day 14	0.8438
miPSC 2-/4+			
Day 1	vs	Day 7	0.0970
Day 1	vs	Day 14	0.8438
Day 7	vs	Day 14	0.8438
mESC 4-/4+			
Day 1	vs	Day 7	0.8438
Day 1	vs	Day 14	0.8438
Day 7	vs	Day 14	0.8438
mESC 2-/4+			
Day 1	vs	Day 7	0.8438
Day 1	vs	Day 14	0.8438
Day 7	vs	Day 14	0.8438

Supplementary Table 6

Summary of percent (%) TUJ1, Nestin, and SOX2 expression at day 7 and day 14

		Day 7		Day 14	
		Mean (%)	**SD (%)**	**Mean (%)**	**SD (%)**
TUJ1	**miPSC 4-/4+**	8	2	17	2
	miPSC 2-/4+	11	6	23	5
	mESC 4-/4+	10	3	20	1
	mESC 2-/4+	13	6	36	5
Nestin	**miPSC 4-/4+**	27	5	13	2
	miPSC 2-/4+	27	5	13	2
	mESC 4-/4+	15	3	10	4
	mESC 2-/4+	25	10	17	5
SOX2	**miPSC 4-/4+**	18	9	8	2
	miPSC 2-/4+	22	7	10	2
	mESC 4-/4+	8	4	8	3
	mESC 2-/4+	9	3	9	4

Supplementary Table 7

Results from significance tests comparing marker expression between differentiation protocols and cell types after 7 days of culture in fibrin. Bolded values indicates significance at $p<0.05$.

Comparison			**K-S p-value**	**K-W p-value**
TUJ1				
miPSC 2-/4+	vs	miPSC 4-/4+	0.5344	0.0650
mESC 2-/4+	vs	mESC 4-/4+	0.5344	0.1391
miPSC 4-/4+	vs	mESC 4-/4+	0.5344	0.1804
miPSC 2-/4+	vs	mESC 2-/4+	0.5344	0.4624
Nestin				
miPSC 2-/4+	vs	miPSC 4-/4+	0.1075	0.1081
mESC 2-/4+	vs	mESC 4-/4+	**0.0111**	**0.0202**
miPSC 4-/4+	vs	mESC 4-/4+	0.1075	0.1465
miPSC 2-/4+	vs	mESC 2-/4+	0.5344	0.6612
SOX2				
miPSC 2-/4+	vs	miPSC 4-/4+	0.5344	0.4678
mESC 2-/4+	vs	mESC 4-/4+	0.9969	0.6552
miPSC 4-/4+	vs	mESC 4-/4+	**0.0111**	**0.0209**
miPSC 2-/4+	vs	mESC 2-/4+	**0.0111**	**0.0202**

Supplementary Table 8

Results from significance tests comparing marker expression between differentiation protocols and cell types after 14 days of culture in fibrin. Bolded values indicates significance at $p<0.05$.

Comparison			K-S p-value	K-W p-value
TUJ1				
miPSC 2-/4+	vs	miPSC 4-/4+	**0.0111**	**0.0172**
mESC 2-/4+	vs	mESC 4-/4+	**0.0111**	**0.0194**
miPSC 4-/4+	vs	mESC 4-/4+	**0.0111**	**0.0165**
miPSC 2-/4+	vs	mESC 2-/4+	**0.0111**	**0.0187**
Nestin				
miPSC 2-/4+	vs	miPSC 4-/4+	**0.0111**	**0.0194**
mESC 2-/4+	vs	mESC 4-/4+	0.1075	**0.0284**
miPSC 4-/4+	vs	mESC 4-/4+	0.9969	0.8817
miPSC 2-/4+	vs	mESC 2-/4+	0.1075	0.0560
SOX2				
miPSC 2-/4+	vs	miPSC 4-/4+	0.1075	0.1059
mESC 2-/4+	vs	mESC 4-/4+	0.5344	0.5516
miPSC 4-/4+	vs	mESC 4-/4+	0.9969	1.0000
miPSC 2-/4+	vs	mESC 2-/4+	0.5344	0.4388

Supplementary Table 9

Results from significance tests comparing marker expression between day 7 and day 14 of culture in fibrin for each differentiation protocol. Bolded values indicates significance at $p<0.05$.

Comparison				K-S p-value	K-W p-value
TUJ1					
miPSC 4-/4+	Day 1	vs	Day 7	**0.0111**	**0.0194**
miPSC 2-/4+	Day 1	vs	Day 7	**0.0111**	**0.0194**
mESC 4-/4+	Day 1	vs	Day 7	**0.0111**	**0.0194**
mESC 2-/4+	Day 1	vs	Day 7	**0.0111**	**0.0172**
Nestin					
miPSC 4-/4+	Day 1	vs	Day 7	**0.0111**	**0.0194**
miPSC 2-/4+	Day 1	vs	Day 7	0.1075	**0.0421**
mESC 4-/4+	Day 1	vs	Day 7	0.1075	0.1081
mESC 2-/4+	Day 1	vs	Day 7	**0.0111**	**0.0202**
SOX2					
miPSC 4-/4+	Day 1	vs	Day 7	**0.0111**	**0.0202**
miPSC 2-/4+	Day 1	vs	Day 7	0.9969	0.9939
mESC 4-/4+	Day 1	vs	Day 7	0.9969	0.7409
mESC 2-/4+	Day 1	vs	Day 7	**0.0111**	**0.0202**

Supplementary Table 10

Histograms show expression of TUJ1, Nestin, and SOX2 for EBs seeded in fibrin after 7 days. Data represents flow cytometry analysis based on one sample set (1 of 4), with approximately 5000 events collected for each sample.

	TUJ1	Nestin	SOX2
miPSC 4-/4+	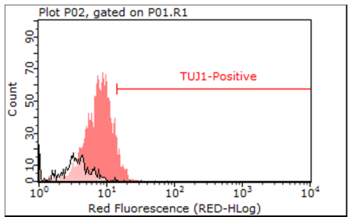	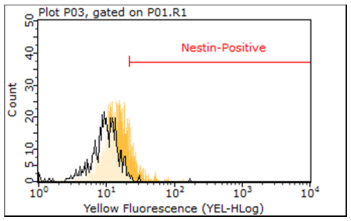	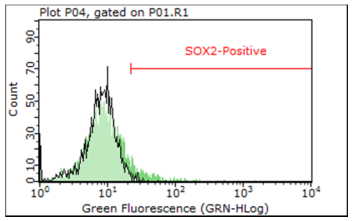
miPSC 2-/4+	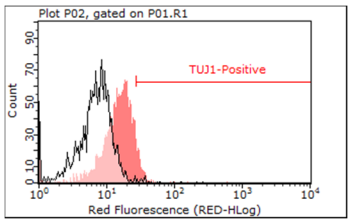	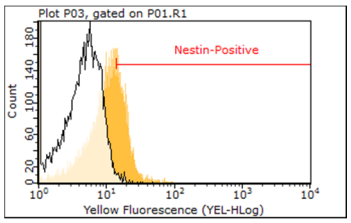	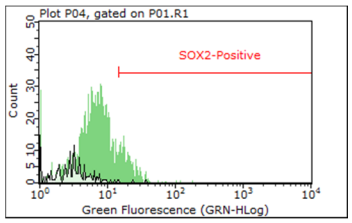
mESC 4-/4+	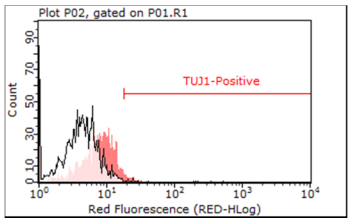	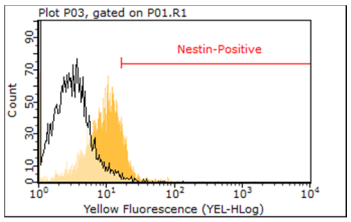	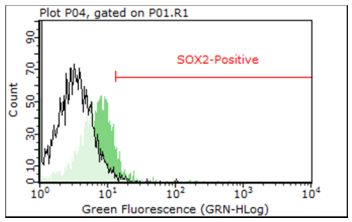
mESC 2-/4+	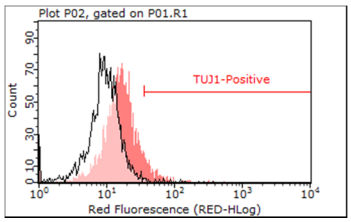	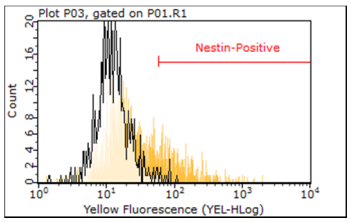	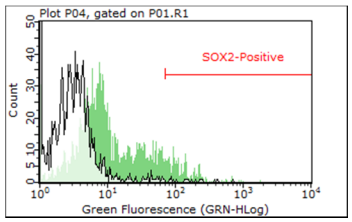

Supplementary Table 11

Histograms show expression of TUJ1, Nestin, and SOX2 for EBs seeded in fibrin after 7 days. Data represents flow cytometry analysis based on one sample set (2 of 4), with approximately 5000 events collected for each sample.

	TUJ1	Nestin	SOX2
miPSC 4-/4+	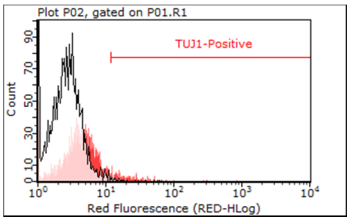	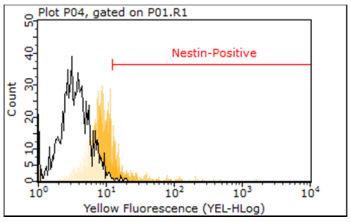	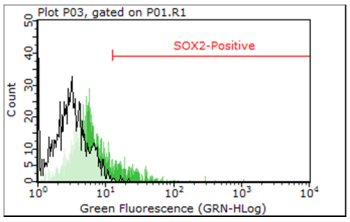
miPSC 2-/4+	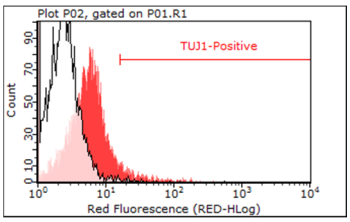	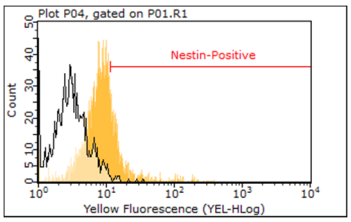	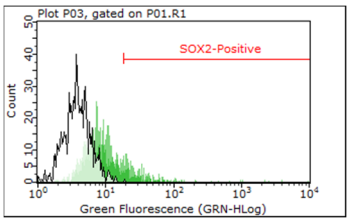
mESC 4-/4+	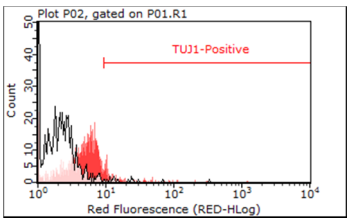	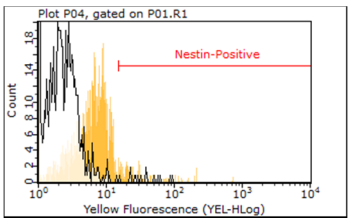	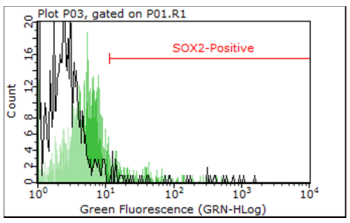
mESC 2-/4+	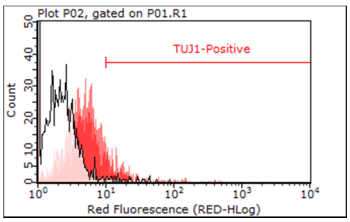	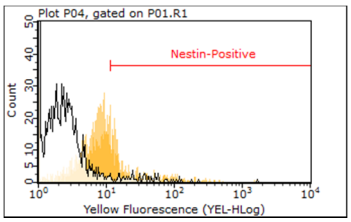	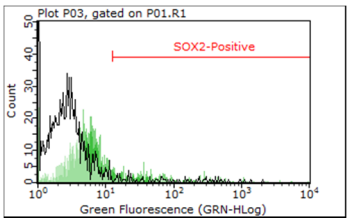

Supplementary Table 12

Histograms show expression of TUJ1, Nestin, and SOX2 for EBs seeded in fibrin after 7 days. Data represents flow cytometry analysis based on one sample set (3 of 4), with approximately 5000 events collected for each sample.

	TUJ1	Nestin	SOX2
miPSC 4-/4+	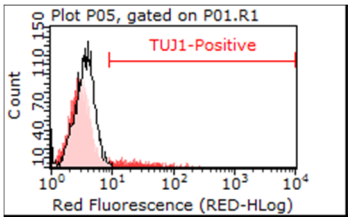	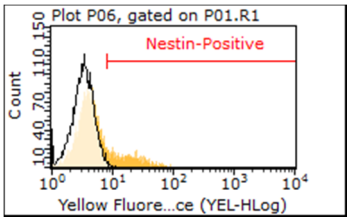	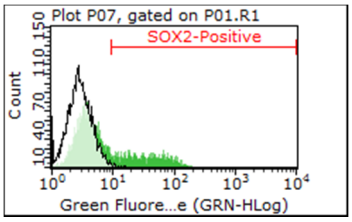
miPSC 2-/4+	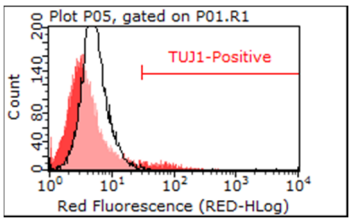	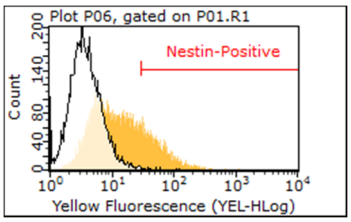	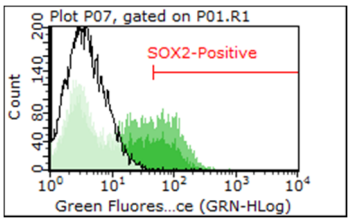
mESC 4-/4+	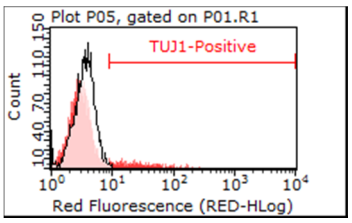	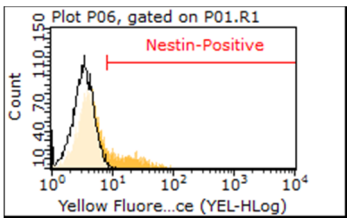	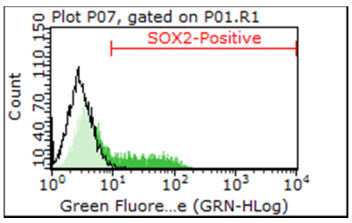
mESC 2-/4+	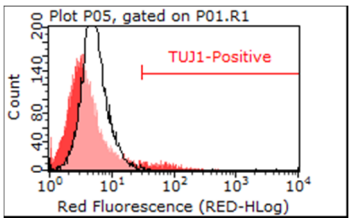	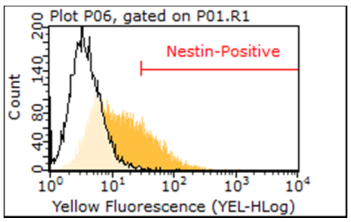	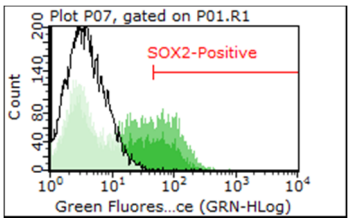

Supplementary Table 13

Histograms show expression of TUJ1, Nestin, and SOX2 for EBs seeded in fibrin after 7 days. Data represents flow cytometry analysis based on one sample set (4 of 4), with approximately 5000 events collected for each sample.

	TUJ1	Nestin	SOX2
miPSC 4-/4+	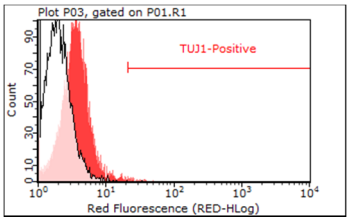	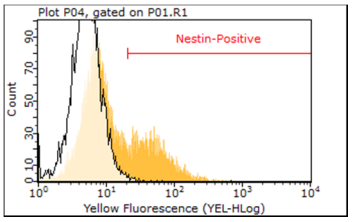	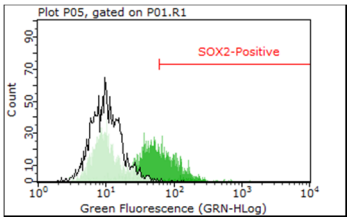
miPSC 2-/4+	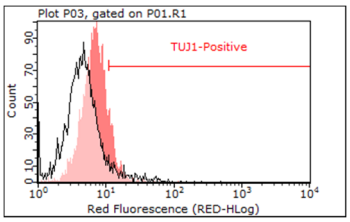	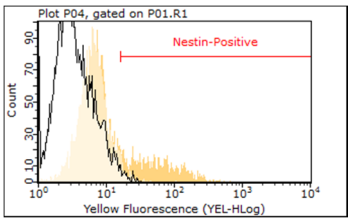	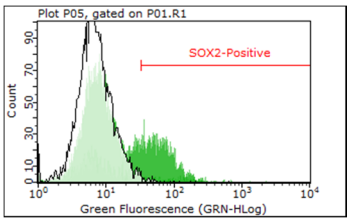
mESC 4-/4+	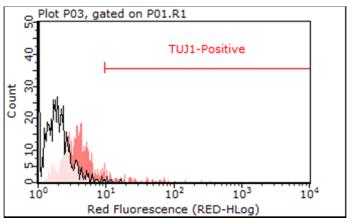	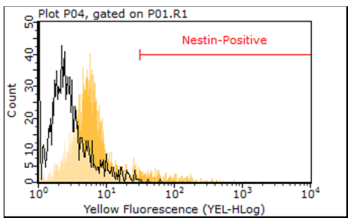	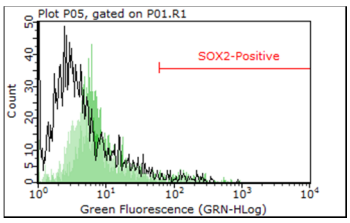
mESC 2-/4+	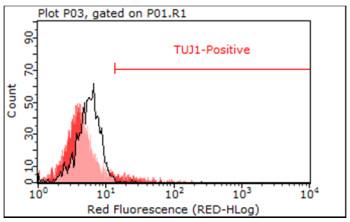	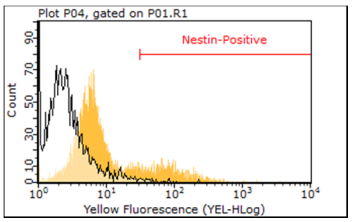	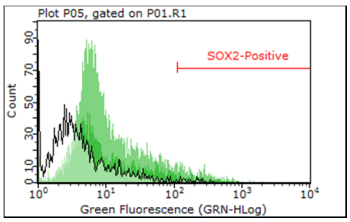

Supplementary Table 14

Histograms show expression of TUJ1, Nestin, and SOX2 for EBs seeded in fibrin after 14 days. Data represents flow cytometry analysis based on one sample set (1 of 4), with approximately 5000 events collected for each sample.

	TUJ1	Nestin	SOX2
miPSC 4-/4+	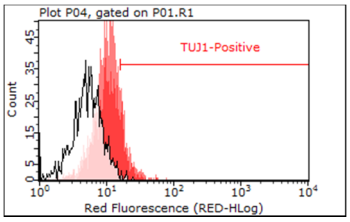	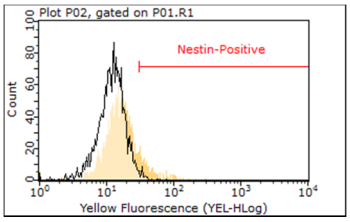	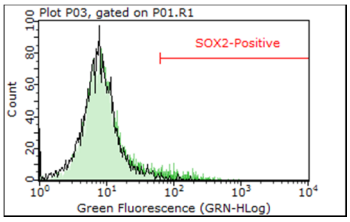
miPSC 2-/4+	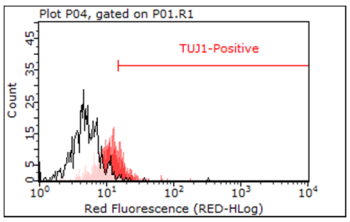	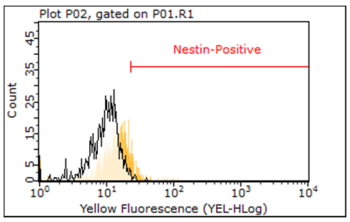	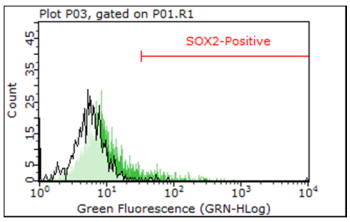
mESC 4-/4+	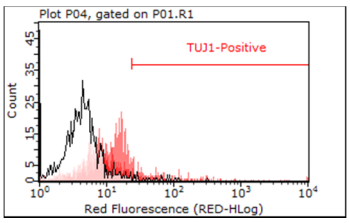	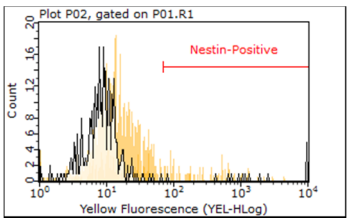	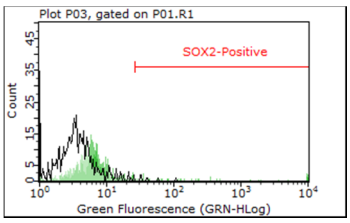
mESC 2-/4+	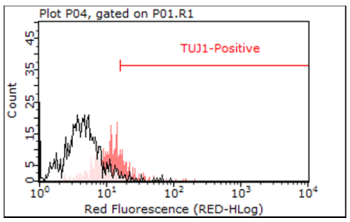	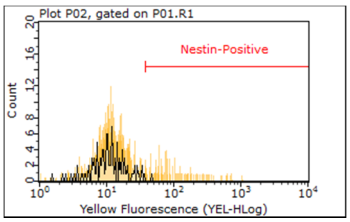	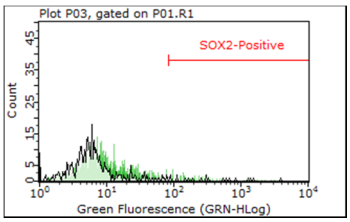

Supplementary Table 15

Histograms show expression of TUJ1, Nestin, and SOX2 for EBs seeded in fibrin after 14 days. Data represents flow cytometry analysis based on one sample set (2 of 4), with approximately 5000 events collected for each sample.

	TUJ1	Nestin	SOX2
miPSC 4-/4+	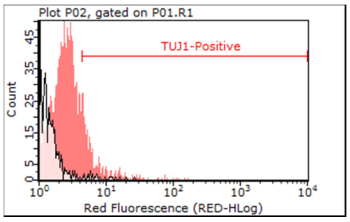	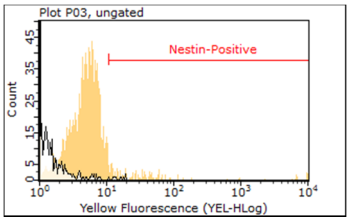	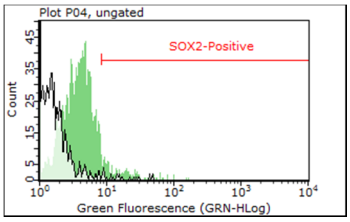
miPSC 2-/4+	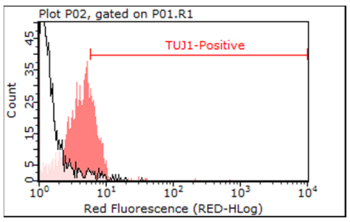	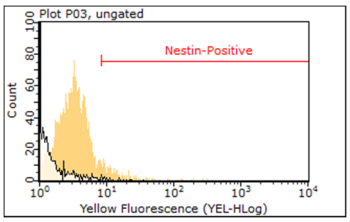	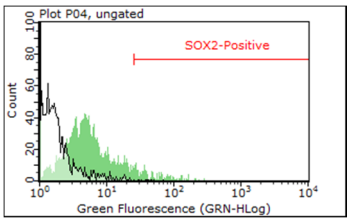
mESC 4-/4+	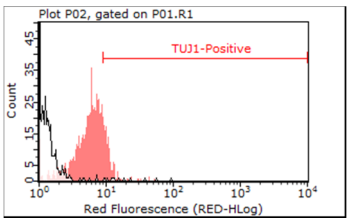	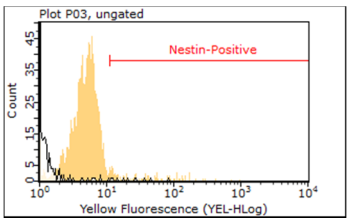	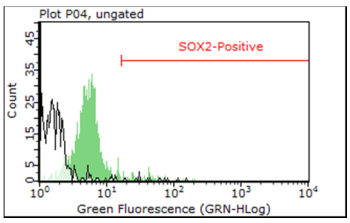
mESC 2-/4+	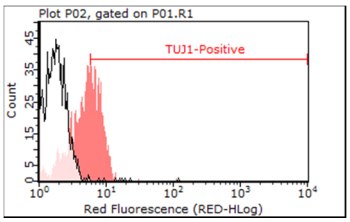	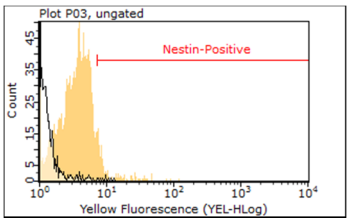	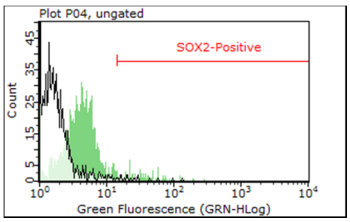

Supplementary Table 16

Histograms show expression of TUJ1, Nestin, and SOX2 for EBs seeded in fibrin after 14 days. Data represents flow cytometry analysis based on one sample set (3 of 4), with approximately 5000 events collected for each sample.

	TUJ1	Nestin	SOX2
miPSC 4-/4+	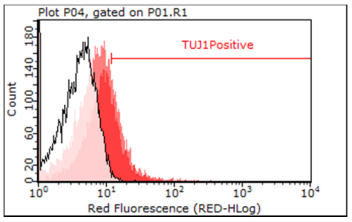	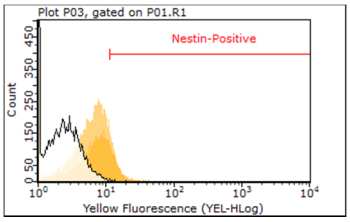	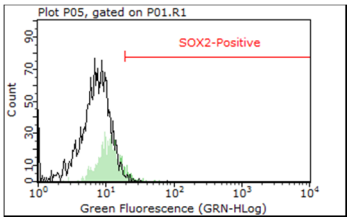
miPSC 2-/4+	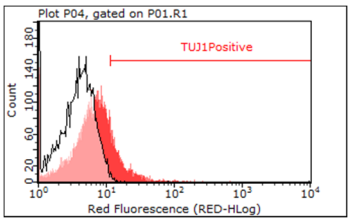	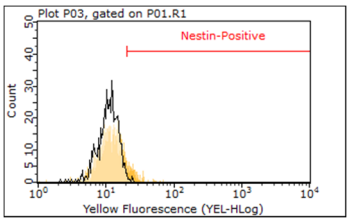	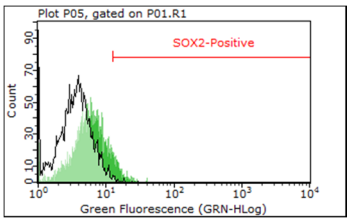
mESC 4-/4+	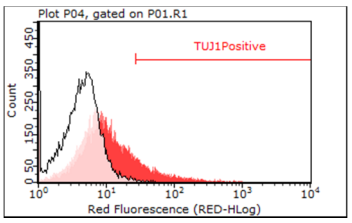	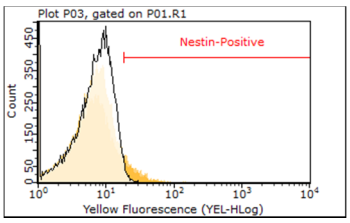	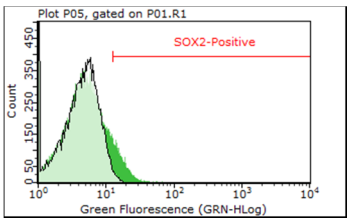
mESC 2-/4+	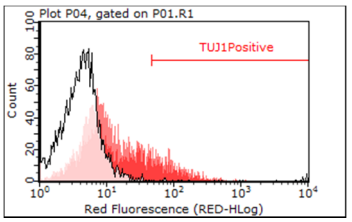	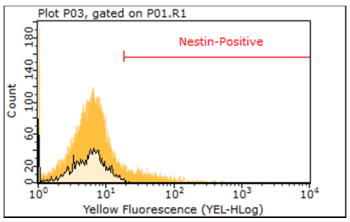	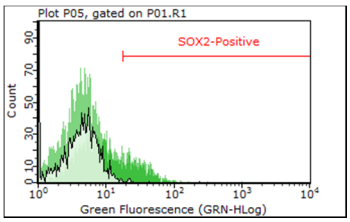

Supplementary Table 17

Histograms show expression of TUJ1, Nestin, and SOX2 for EBs seeded in fibrin after 14 days. Data represents flow cytometry analysis based on one sample set (4 of 4), with approximately 5000 events collected for each sample.

	TUJ1	Nestin	SOX2
miPSC 4-/4+	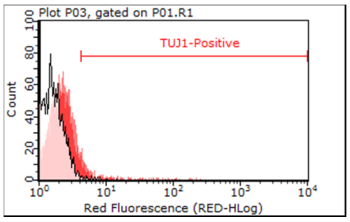	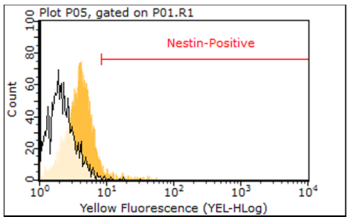	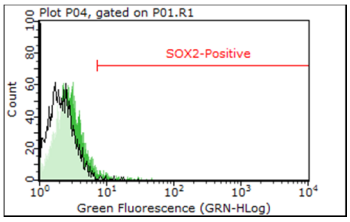
miPSC 2-/4+	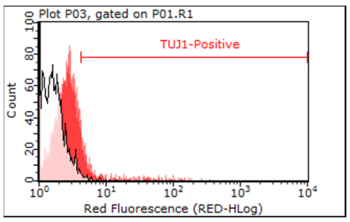	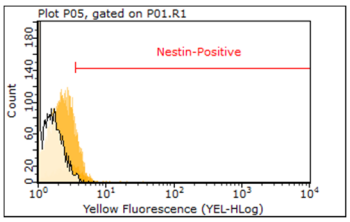	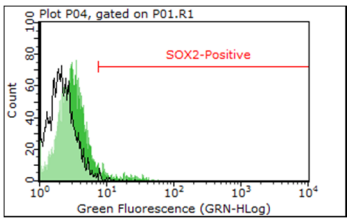
mESC 4-/4+	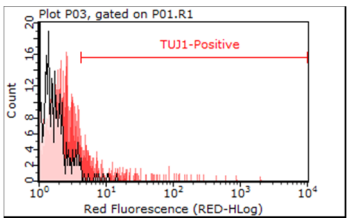	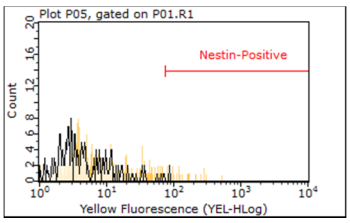	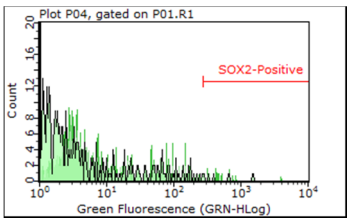
mESC 2-/4+	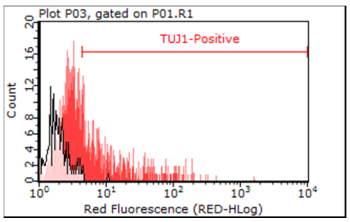	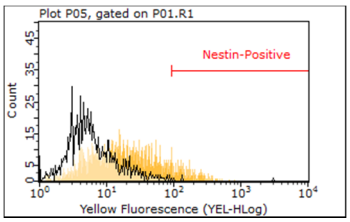	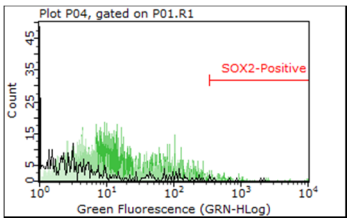

Supplementary Table 18

Histograms show expression of SSEA1 for EBs seeded in fibrin after 1, 7 & 14 days. Data represents flow cytometry analysis based on one sample set (1 of 1), with approximately 5000 events collected for each sample.

	SSEA1 - Day 1	SSEA1 - Day 7	SSEA1 – Day 14
miPSC 4-/4+	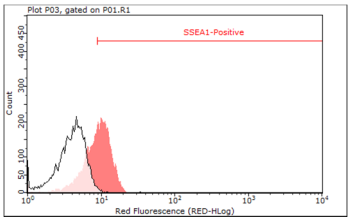	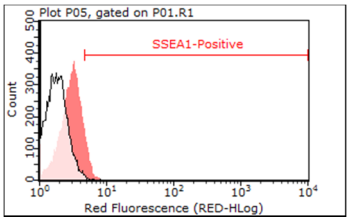	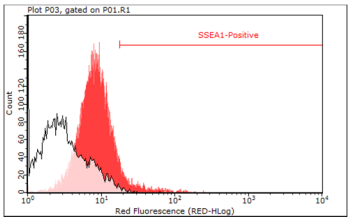
miPSC 2-/4+	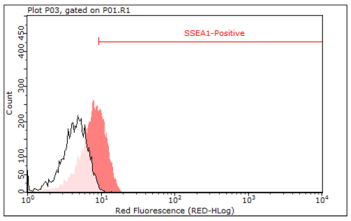	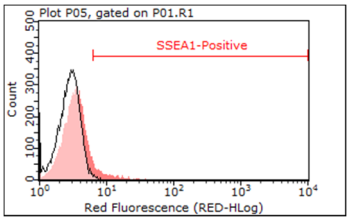	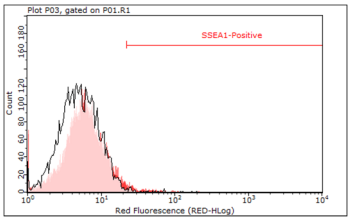
mESC 4-/4+	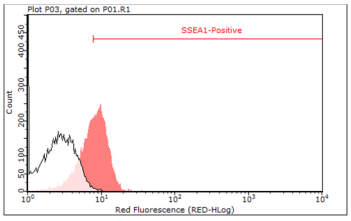	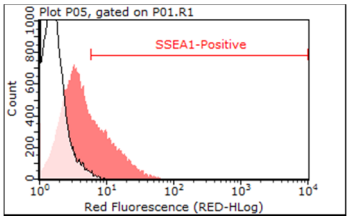	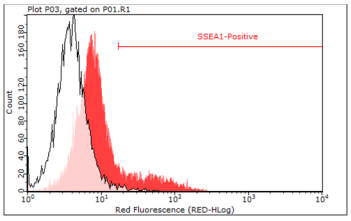
mESC 2-/4+	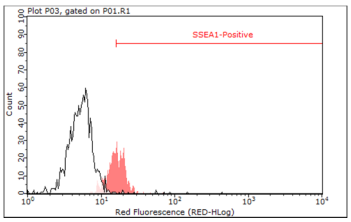	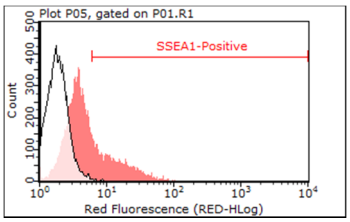	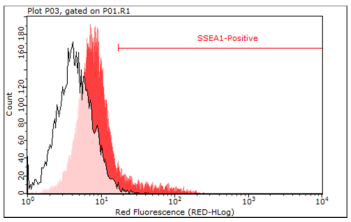

Supplementary Table 19

Histograms with expression of TUJ1 for neural aggregates seeded in fibrin for 14 days at different fibrin concentrations. Data represents flow cytometry analysis based on one sample set (1 of 1), with approximately 5000 events collected for each sample.

	Histogram	TUJ1 Expression (%)
4 g/mL Fibrin	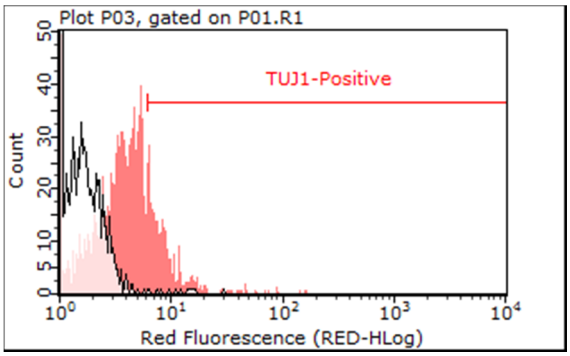	34%
8 mg/mL Fibrin	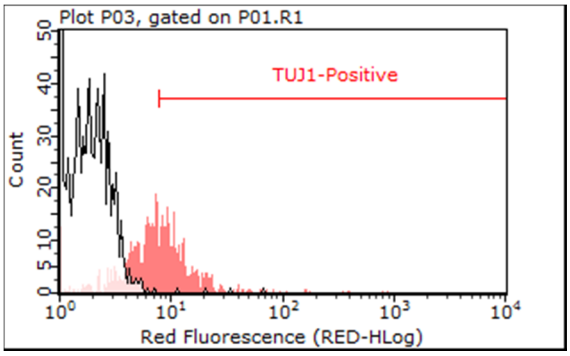	47%
12 mg/mL Fibrin	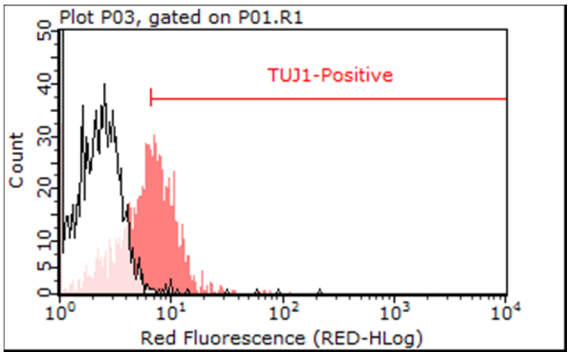	47%
16 mg/mL Fibrin	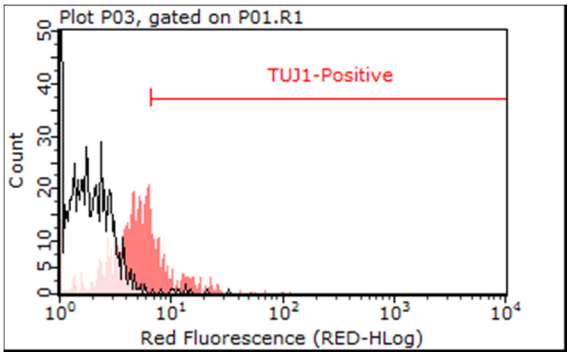	29%

Supplementary Table 20

The image shows colour development after the final stage of the ELISA protocol, with corresponding plate layout. The optical density of each well is proportional to HSP70 concentration and is measured quantitatively by an optical plate reader. Note the higher intensity of Standard 1 in the first 3 columns compared to the intensity of Standard 2 in the next 3 columns, indicating a difference in detection levels for the same concentration.

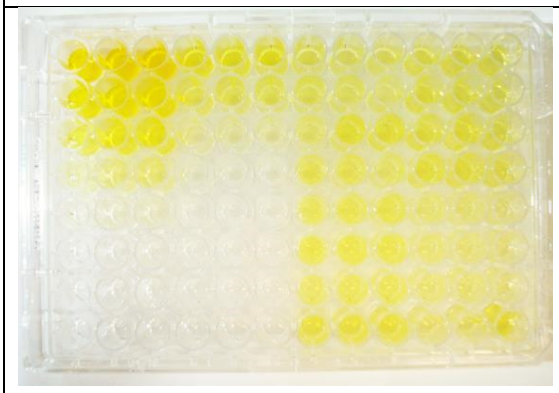

Standard 1	Standard 2	Gels	Washes
10,000 pg/mL	10,000 pg/mL	HSP70 Only	HSP70 Only
5,000 pg/mL	5,000 pg/mL		
2,500 pg/mL	2,500 pg/mL		
1,250 pg/mL	1,250 pg/mL		
625 pg/mL	625 pg/mL	HSP70 + Peptide	HSP70 + Peptide
312.5 pg/mL	312.5 pg/mL		
156.25 pg/mL	156.25 pg/mL		
0 pg/mL	0 pg/mL		

Supplementary Table 21

Results from significance test comparing HSP70 concentration in fibrin gels and washes after reaching equilibrium. Bolded values indicates significance at $p<0.05$.

Comparison			K-S p-value
HSP70 Only Gel	vs	HSP70 Only Wash	**2.4777×10^{-11}**
HSP70 + Peptide Gel	vs	HSP70 + Peptide Wash	0.1094
HSP70 + Peptide Gel	vs	HSP70 Only Gel	**0.0019**